Addis Ababa University

Ethiopian Institute of Water Resources

GROUNDWATER RECHARGE ESTIMATION USING DISTRIBUTED MODEL (WETSPASS): THE CASE OF THE AFA-SELGA WATERSHED, ABBAY BASIN

MSc THESIS

BY

HAYAL DERB ANDARGE

October, 2024

ADDIS ABABA, ETHIOPIA

ADDIS ABABA UNIVERSITY

ETHIOPIAN INSTITUTE OF WATER RESOURCE

GROUNDWATER RECHARGE ESTIMATION USING DISTRIBUTED MODEL (WETSPASS): THE CASE OF AFA-SELGA WATERSHED, ABAY BASIN

HAYAL DERB ANDARGE

GSR/6809/12

ADVISOR: - TAYE ALEMAYEHU (PHD)

A THESIS SUBMITTED TO THE ADDIS ABABA UNIVERSITY,
ETHIOPIAN INSTITUTE OF WATER RESOURCES,
IN PARTIAL FULFILLMENT OF THE REQUIREMENTS FOR THE DEGREE OF MASTER OF SCIENCE IN WATER RESOURCE ENGINEERING AND MANAGEMENT, SPECIALIZATION IN GROUNDWATER MANAGEMENT

July, 2024

ADDIS ABABA UNIVERSITY
ADDIS ABABA, ETHIOPIA

DEDICATION

This thesis manuscript is dedicated to my beloved families, my father and my mother for their unconditional love, effortful sacrifice, support, and endless encouragement throughout my life that helped me to accomplish things with success!

STATEMENT OF THE AUTHOR

First, I declare that this thesis is my genuine work and that all sources of materials used for this thesis have been duly acknowledged. This thesis has been submitted in partial fulfillment of the requirements for the degree of Master of Science in **water resource engineering and management specialization in groundwater management**. It is deposited at the university library to be made available to borrowers under the library's rules. I solemnly declare that this thesis is not submitted to any other institution anywhere for the award of any academic degree, diploma, or certificate.

Brief quotations from this thesis are allowable without special permission provided that accurate acknowledgment of the source is made. Requests for permission for extended quotation from or reproduction of this manuscript in whole or in part may be granted by the head of the major department or the Dean of the School of Graduate Studies when in his or her judgment the proposed use of the material is in the interests of scholarship. In all other instances, however, the author must obtain permission.

Name: Hayal Derb

Date: 09/10/2024

Signature: 

Department: Water Resource Engineering and Management

THESIS APPROVAL SHEET

This is to certify that the thesis presented by Hayal Derb entitled "Groundwater Recharge Estimation Using Distributed Model (WetSpass): The Case of Afa-Selga Watershed, Abbay Basin is submitted in partial fulfillment of the requirements for the degree of Master of Science in Water Resource Engineering and Management with specialization in Groundwater Management to the Graduate Program of Ethiopian Institute of Water Resources, Addis Ababa University complies with the regulations of the University and meets the accepted standards concerning originality and quality.

Signed by the examining committee:

Examiners:

External Examiner: Dr. Sirak Tekleab(PhD) Signature:  Date: 22/10/2024

Internal Examiner: _____ Signature: _____ Date: _____

Advisor: Taye Alemayehu (PhD) Signature:  Date: 09/10/2024

Chairman: _____ Signature _____ Date: _____

Institute Director: _____ Signature: _____ Date: _____

ACKNOWLEDGMENT

First and foremost, God deserves glory and thanks for enabling me to complete this thesis and being by my side throughout my life. My greatest gratitude to my advisor, Dr. Taye Alemayehu, for his excellent guidance, comments, suggestions, support, and patience throughout this study. I want to extend my deepest appreciation and thanks to the Ethiopian Institute of Agricultural Research (EIAR), and Assosa Agricultural Research Center for offering the study opportunity and full financial support.

In addition, I would like to thank the Ethiopian Geological Institute, the Ministry of Water and Energy, Assosa Town Supply and Sewerage Enterprise, B/G/R/S Water Works and Construction Enterprise, Ethiopian Meteorological Institute and EGII (Ethiopian Geospatial Information Institute) for their kindness in providing the data and information needed to complete this study.

My diction is too poor to translate my deep sense of gratitude into words to my friends and all my family for their moral support, encouragement and love in every aspect during my study. Finally, I would like to thank all the people who helped me directly or indirectly during my investigation.

TABLE OF CONTENTS

ACRONYMS AND ABBREVIATIONS

AD	Afar Depression
AET	Actual Evapotranspiration
ASF	Alaska Satellite Facility
BFI	Base Flow Index
BGRS	Benishangul-Gumuz Regional State
DBF	Data Base File
DHB	Distributed Hydrological Budget
GPS	Global Positioning System
DRF	Digital Recursive Filter
EGII	Ethiopian Geospatial Information Institute
ET	Evapotranspiration
EM	Expectation Maximization
FDM	Finite Difference Method
GMS	Groundwater Modeling System
EGI	Ethiopian Geological Institute
EGII	Ethiopian Geospatial Information Institute
HB	Hydrological Budget
HDR	Distributed Hydrological Budget
IDW	Inverse Distance Weighting
MJJAS	May, June, July, August, September
LMM	Local Minimum Method
LULC	Land Use Land Cover

MAR	Missing at Random
MCAR	Missing Completely at Random
MER	Main Ethiopian Rift
MoWE	Ministry of Water and Energy
NMAR	Not Missing Completely at Random
NSE	Nash-Sutcliffe efficiency
EMI	Ethiopian Meteorological Institute
OPM	One-Parameter digital filter method
PET	Potential Evapotranspiration
RS	Remote Sensing
SPI	Standard Precipitation Index
SWAT	Soil and Water Assessment Tool
TDR	Time Domain Reflectometry
TOPMODEL	Topographic Hydrologic Model
USGS	United States Geological Survey
WHAT	Web-Based Hydrograph Analysis Application
WetSpass	Water and Energy Transfer between Soil, Plants, and Atmosphere
WTF	Water Table Fluctuation

LIST OF FIGURES

LIST OF TABLES

LIST OF APPENDICES

ABSTRACT

Understanding the spatial variability of groundwater recharge is crucial for managing and evaluating groundwater resources. In the Afa-Selga watershed Population growth necessitates increased groundwater resources, while water scarcity hinders sustainable development, especially for domestic and agricultural use. Historical rainfall, temperature and wind speed data is crucial for climate studies, water resource processes, and hydrological modeling. Four absolute homogeneity tests were used to investigate the homogeneity of annual rainfall data sets in five meteorological stations in the Afa-Selga watershed, revealing usefulness at a 95% significance level. By preparing inputs in the form of digital maps using remote sensing, GIS tools and processing of meteorological and hydrological observations, that were designed for estimation of the annual and seasonal groundwater recharge, surface runoff, and evapotranspiration amount in the Afa-Selga watershed using WetSpass modeling method, the model spatial and temporal characteristics allow spatially distributed quantification of water balance components. The primary objective of utilizing The WetSpass model was used to estimate annual and seasonal groundwater recharge, evapotranspiration, and surface runoff in the Afa-Selga watershed. Long-term hydro-meteorological and watershed bio-physical data were used for model input. The long-term average annual rainfall of 1246.6 mm was divided into 117.41 mm (9.42%) recharge which is equivalent to 68,039,095 m^3/yr. (579.5 km2), 948.9 mm (80.5%) evapotranspiration, and 125.87 mm (10.08%) surface runoff The hydrological water balance components for the Afa-Selga watershed are accurately simulated by the model. The model performed well, as shown by good statistical values for the correlation coefficient (R^2 = 0.89) and Nash-Sutcliffe (NSE =0.84).

Keywords: Afa-Selga watershed, Groundwater recharge, water balance, WetSpass model

1. INTRODUCTION

1.1 Backgrounds

Water is the most essential component of life which is needed in sufficient quantity and acceptable quality to meet the ever-increasing human demand used for different purposes (Ndambuki and Rwanga, 2017; Rwanga, 2013 and Yenehun et al., 2017). Its availability and distribution are limited in time and space, in which 97.5% of the global water is saline and exists in the oceans. Only 2.5% of it is considered freshwater. 68.7% is fresh water locked up in glaciers while 30.1% and 0.9% represent groundwater, surface water, and other fresh waters respectively (Bate et al., 2004).

Even though the demand for fresh water is rising globally as the world population is expanding, it is a limited but essential and multipurpose natural resource that is sporadically found. This makes series period data necessary for proper planning and management of such resources in terms of distribution, management, utilization, and environmental functions to maximize resource use sustainably (Karimi and Bastiaanssen, 2015).

Water moves downward from surface water to groundwater during a hydrologic process called groundwater recharge. Recharge happens both naturally (via the water cycle) and artificially (i.e., artificial groundwater recharge), where rainwater and/or recovered water are sent to the subsurface (Pandian, et al., 2014).

Ethiopia is blessed with abundant surface and subsurface water resource potential that is subject to both temporal and spatial fluctuations. There are twelve river basins and nine lakes spread throughout the nation. Additionally, Ethiopia has a potential for groundwater of 2.6 to 2.65 billion m^3 and an estimated 122 billion m^3 of yearly runoff water (Awulachew et al., 2007). However,

people only use around 5% of the capacity for surface water, and the groundwater resource is untapped but potentially valuable (Tesfamichael et al., 2013).

Estimation of groundwater recharge is of great importance in water resources management, especially for areas where groundwater is vital for the local water supply. Irrigation could play a critical role in fulfilling basic human food needs at short and long-time scales, and generate further benefits by producing market-oriented crops during the dry season. The exact estimation of regional groundwater recharge requires a good understanding of the hydrological processes in the area, which could be greatly altered by global change and human activities. (Belete, 2018)

Understanding seasonal and annual variations of the water resources, especially runoff, evapotranspiration, and recharge, is necessary for efficient and sustainable management of groundwater (Obuobie, et al., 2008). Since groundwater resources are sensitive functions of climatic factors, geological formation, topography, soil properties, and land-use types (Dragoni & Sukhija, 2013), a detailed understanding of watershed physical and biological characteristics is important.

Identification of the hydrological and biophysical parameters of the watershed is necessary for accurate groundwater resource quantification. Since regional groundwater models are frequently steady state and require input from long-term average recharge, they are frequently used to analyze groundwater systems (infiltration-discharge). Regional groundwater models should take into account the spatial variance in recharge caused by distributed land use, soil type, slope, etc., as this variation might be substantial.

WetSpass was created as a physically-based methodology for the estimation of the three main components of the water balance, surface runoff, actual evapotranspiration, and groundwater

recharge which are spatially variable on an average over a long period. (Belete, 2018). Because it is better protected from surface pollutants and has less of an impact on seasonal changes than surface water, groundwater is a crucial natural resource for water around the world (Zektser and Everett, 2006). The recharge process, which is defined as the rainfall portion that enters the aquifer and participates in its renewal, is what primarily determines the availability of groundwater resources (Tilahun and Merkel, 2009).

The geographic, climatic, hydrological, and hydrogeological aspects of the environment, as well as other factors, affect how quickly the water table recharges. Numerical models that are helpful for spatial analysis use big and complicated groundwater recharge analyses for reliability and accuracy (Jaturon and Srilert 2013).

The Afa-Selga River is one of the major tributaries of the Dabus River. Agriculture is the main economic activity and source of livelihood. Moreover, Climate variability and water shortages are huge threats to the farmers in the Watershed. Therefore, estimating groundwater recharge rates in the water is essential for both the resource's sustainable use and its conservation from pollution and depletion.

In this work, the WetSpass model was used to calculate seasonal and yearly averages of long-term (2004–2020) spatial surface runoff, actual evapotranspiration, and groundwater recharge. WetSpass has been utilized globally since its development (Rwanga S. S., 2013). In addition to the Gaza Strip in Palestine (Aish, 2014), the Geba catchment in Ethiopia (Tesfamichael et al., 2010), and the Nile Delta aquifer (Armanuos, 2016), it has also been effectively used in Belgium (Batelaan & De Smedt, 2001). Thus, the Afa-Selga Watershed's long-term seasonal and annual runoff, actual evapotranspiration, groundwater recharge, and associated water balance components were all simulated using the WetSpass model.

1.2 Problem Statement

Groundwater is currently highly reliable as a source of water. It is preferred over surface water because of its widespread dispersion and low risk of pollution. As a crucial tool for gathering various aquifer databases, groundwater modeling has recently come into its own. Because of this, groundwater modeling has made it possible to better understand hydrological and biophysical components, how aquifers work, and how water demand for domestic and agricultural purposes is always increasing. As a result, it is crucial to manage groundwater resources as best as possible. (Pande and Khadri, 2016).

The Afa-Selga watershed is mainly found in the Dabus sub-catchment of the Abbay River basin. It is very close to the Ethiopia-Sudan border as well as the Ethiopian Grand hydroelectric dam project. Most rural households in the watershed rely mostly on agriculture for their income. The population is constantly expanding, which is increasing the need for groundwater resources for d aily use. Water scarcity is also the key issue impeding sustainable development in the watershed, particularly for sustainable domestic use and agricultural output. (Ibrahim and Gebremarim, 2020)

Moreover, the occurrence, origin, movement, and chemical components of the groundwater regime are all influenced by the geology (lithology), geomorphology (landforms), drainage density, rainfall, geological structures (lineaments), slope, land use/land cover, and soil. According to (Gadisa, 2017) the Study area is located beneath the hard rocks environment (basement area). a huge problem for hard rock is also to know, where the recharge takes place and groundwater occurrence.

Additionally, in the watershed, it has been observed that most of the boreholes are nonfunctional due to over-pumping and low success rate of drilling productive wells. (Gadisa, 2017). Those challenges put groundwater resources under tremendous strain.

There are several previous studies regarding aquifer characterization, geology and hydrogeology of the study area. But the groundwater recharge of the study is not estimated yet. Therefore, quantification of the rate and seasonal changes of groundwater recharge is very essential. This study was conducted using a distributed model (WetSpass) to better understand the hydrological and biophysical components of the watershed with spatial and temporal variation for effective groundwater management, watershed management, wise utilization, future planning, and sustainable resource utilization taking into account sustainable development.

1.3 Objectives of the Study

1.3.1 General Objective

The main objective of the study is to estimate the groundwater recharge of the Afa-Selga Watershed using the distributed Model WetSpass.

1.3.2 Specific Objectives

1. To estimate the water balance components of the watershed;
2. To estimate the spatial and temporal variability of groundwater recharge of the Watershed

1.4 Research Question

1. What are the water balance components of the Watershed?
2. How much groundwater is recharged in the Watershed?
3. Is there a change in groundwater recharge spatially and temporarily?

1.5 Significance of Study

In this research, the groundwater recharge of the Afa-Selga watershed was estimated and determined by a distributed model. Quantifying the amount of groundwater recharge helps to manage the water resource. The research is significant to manage water resources effectively, making the best use of available water enhancing water sources and minimizing the impact of water shortage problems. Be helpful to planners in the development and management of groundwater, watershed management practice and groundwater-related works in the study area. Furthermore, the findings of this research will also serve as a baseline information and reference for those who want to conduct further research on the area.

1.6 Limitation

This study is done Groundwater recharge of this study was constructed using available hydrological, hydrogeological, hydro-meteorological, and physiographic data of the study area. To produce a Groundwater level grid map, static water level data which are taken at different seasons are required. In this regard well-completion report could have been helpful, but is lacking for most parts of the study area. In addition, available groundwater level data are not well organized.

2. LITERATURE REVIEW

2.1 Groundwater Recharge

Groundwater recharge is the process of water that enters the saturated zone of water made available at the water table surface and flows away from the water table in the saturated zone in response (Freeze et al., 1979, Pandian, et al., 2014). Rainfall and snowmelt that permeate through the ground surface and move to the water table are the primary sources of natural groundwater recharge.

Understanding rainfall-runoff connections is essential for quantifying recharge from precipitation. After deducting what is lost to evapotranspiration and runoff from the total amount of precipitation, the first step is to calculate the percentage of precipitation that is available for groundwater recharging. The land cover, soil type, and prior moisture status are all crucial factors in the rainfall-runoff interaction. In general, soils that are well-drained have high effective porosities and high hydraulic conductivities, whereas poorly-drained soils have higher total porosities and lower hydraulic conductivities. Together with the initial moisture content, these physical features help influence the ability of terrestrial soils to infiltrate water. (Belete, 2018).

Rainfall serves as the primary source of recharging the groundwater system. Paved, impervious surfaces prevent any water from penetrating the soil column, while open, densely vegetated fields encourage infiltration. No matter the soil type, prior wetness, or kind of land cover, the sequence of events leading up to a storm event is the same (Xu, 2002).

Recharge procedures differ from one location to another, and there is no consensus that a technique created and applied in one area would produce trustworthy outcomes when applied in another. Therefore, before choosing a recharge method to use, it is crucial to understand the likely flow mechanisms and the significant elements impacting the recharge in a region (Lerner et al., 1990,

cited in Daniel, 2016). There are three different types of recharge: direct (diffuse), indirect, and localized.

Direct (diffuse) recharge: this can be the water superimposed on the groundwater system is much larger than soil moisture deficits and evapotranspiration by direct infiltration of precipitation and percolation via the unsaturated (vadose) zone (Sanford, 2002; Zdon et al, 2019) The entire vadose zone experiences this kind of replenishment. Because the vadose zone has high water content and little extra storage capacity due to frequent precipitation, direct recharging makes the best contribution to humid climates. The flow of water into the groundwater system through the beds of surface water bodies is an example of indirect or non-diffuse recharge (Scanlon and Cook, 2002).

The most significant and essential recharge in arid regions is indirect recharge, which disperses floodwater over large areas on either side of watercourses (Ali P. and Takashi Oguchi, 2015). (Srinivasa and Jugran, 2003); Senanayake, et al 2016)) describe artificial recharge as a type of controlled recharge where surface water is injected into the ground and then flows to the geological formation to support groundwater supplies.

According to Bhattacharya, (2010), artificial recharge is "the practice of boosting the number of waters entering the undersea reservoirs via artificial means." In groundwater management, particularly in the joint utilization of surface and groundwater resources, the use of artificial recharge is becoming more and more crucial.

Localized recharge is a middle kind of groundwater recharge that occurs when water is concentrated horizontally and close to the surface without flowing through clearly defined channels like small depressions, joints, or rivulets. (Daniel, 2016, cited in Lerner et al., 1990).The

assessment is complicated since the mechanisms mentioned above frequently occur in conjunction rather than independently.

Even though, several variables, including the climate (rainfall, temperature, etc.), topography, drainage, geologic framework, soil type, and land use/land cover, etc., affect an area's recharge and discharge conditions. (Belete, 2018)

2.1.1 Merit and Demerit of Some Groundwater Recharge Estimation Models

Since it cannot be evaluated directly, it is challenging to evaluate groundwater recharge accurately. Groundwater recharge evaluation is essential for effective and long-term groundwater system management. Several techniques can be used to calculate groundwater recharge. (Belete, 2018)

Among the techniques typically employed for groundwater study are hydrologic models. The components of the water balance can be determined using groundwater modeling approaches. Groundwater modeling tools can be used to identify the elements of the water balance based on the biophysical factors of the watershed and climatic time-series data. Applying groundwater modeling methods is crucial for predicting water availability over the long term. (Al Kuisi, et al, 2013).

Beven (2001) states that the dynamics of the hydrological cycle over the entire river basin or just a part of it can be quantified using simplified systems called hydrological models. They are based on a system of related equations that attempt to translate the physical principles that control incredibly complicated natural events.

Moreover, a variety of models can be applied depending on the targeted analysis, the input variables, the database being used, and the considered output. A simple mathematical connection between the input and output variables of the basin can be used to represent the physical processes

that rainfall-runoff models describe, or they can contain a description of the fundamental mechanisms that contribute to runoff formation. Various models have been developed over some time in different parts of the world. These models can be broadly categorized as physically based distributed models, conceptual models, and data-driven models based on the process description. (Beven, 2001)

Klemes (1983) suggested two different modeling strategies: a top-down strategy and a bottom-up approach. Physically-based distributed models are an illustration of a bottom-up modeling strategy (Savenije, 2001; Sivapalan, 2003) that were developed starting in the 1980s concurrently with the development of Remote Sensing Techniques and Geographical Information System Tools and can provide the highest accuracy in the modeling of precipitation-runoff processes (Xu, 2002).

These models are essentially based on the continuity and momentum, mass, and energy conservation laws that govern physical processes. In this modeling approach, the many heterogeneities in the catchment are represented by a large number of model parameters that are expected to be measurable at a plot or micro-catchment scale. In top-down modeling approaches, the equations used to represent the physical processes frequently have (indirect) physical meaning, but parameters are determined through calibration. (Belete, 2018).

In this method, the modeling strategy often begins with a relatively simple model and gradually increases complexity by incorporating process descriptions step-by-step (Sivapalan, 2003; Montanari et al., 2006). Using topography-driven, flexible, conceptual, semi-distributed model frameworks, hydrological process comprehension and modeling have recently advanced (Gharari et al., 2013; Gao et al., 2014).

Data-driven models are based on extracting information that is implicitly included in hydrological data. These models use mathematical equations that don't rely on sensible concepts, such as mass,

momentum, or energy balance equations (Solomatine, 2011). The application of such models requires accurate input/output time series analysis (Bowden et al., 2005).

To simulate and quantify hydrologic responses, several hydrological models have been developed (Poelmans et al. 2010). Distributed hydrologic models with a physical base, such as MIKESHE (System Hydrological European), performed well in ungauged basins, although they need detailed data (Zhang et al. 2015). According to Gumindoga et al. (2014), TOPMODEL (Topographic Hydrologic Model) can be used to investigate runoff areas in mountainous areas.

The SWAT (Soil and Water Assessment Tool) has also been frequently used to forecast how various biophysical basin characteristics, such as soil textures, plant covers, and land use, will affect water production, sediment yield, and non-point source pollution (Singh et al. 2016). The SWAT model is easily available online and enables water managers to model the quantity of surface water and the quality of catchments worldwide. It is a comprehensive model integrating surface land and channel environmental processes. (Glavan and Pintar, 2012)

The major drawback in the model is the non-spatial representation of the HRU inside each sub-catchment. This kept the model simple and supported the application of the model to almost every catchment. Additionally, to run the model, a wide variety of data must be collected, and many parameters must be changed during the calibration process, preventing modelers from using SWAT. However, because the environment is a complex system, inaccurate model outputs and evaluations may result from undervaluing or missing some parameters. Moreover, because the model was initially designed for monocultures, it is not possible to simulate the different plant communities that are available in organic farming, grasslands, and forests. (Glavan and Pintar, 2012)

This is particularly relevant in areas where topography, hydroclimate, and geology exhibit significant variation. According to Hornero et al. (2016), groundwater managers should thus include projections of recharge and the uncertainty associated with them in any management plans. Recharge processes differ greatly between locations, therefore there's no assurance that a method applied successfully in one area will produce acceptable results in another (Obuobie et al., 2012). Various methods of estimating recharge have been developed.

It can be difficult to select appropriate techniques, though. According to Scanlon et al. (2002), major factors to consider while selecting a technique are the study's objective and the space/time scales, range, and reliability of recharge estimations. In limited spaces and times, for example, it is possible to analyze the groundwater resources in a certain area, but flow and contaminant modeling need quantification of recharge amounts at large spatial as well as temporal scales.

The WetSpass model is one of the various recharge estimating techniques utilized because it can calculate recharge by linking surface-subsurface water balances. To understand the dynamics of the hydro ecosystems in the basin, it is also used to model yearly or seasonal averages of groundwater recharge, evapotranspiration, and runoff. The hydrological features of the watershed were also examined using WetSpass (Van Rossum et al., 2001 as cited in Belete, 2018).

WetSpass can quantify the long-term effects of anthropogenic and climatic variability on the groundwater recharge of a watershed by taking into consideration many basin biophysical features, such as terrain, temperature, land use/cover changes, precipitation, and wind speed (Gebreyohannes et al, 2013).

The calibration of the WetSpass water balance components included factors like base flow, total discharge, and surface runoff. The WetSpass calibration was combined with the calibration of the

related groundwater model. The final step was to use mapped areas to confirm the groundwater discharge areas. Additionally, the hydrological properties of the sub-basin were examined using WetSpass (Van Rossum et al., 2001 as cited in Belete, 2018).

2.2 WetSpass model

WetSpass stands for the transfer of water and energy between soil, plants and atmosphere under quasi-steady-state conditions (Batelaan and De Smedt, 2001). It is a physically based model for the estimation of long-term average spatial patterns of groundwater recharge, surface runoff and evapotranspiration employing physical and empirical relationships. WetSpass is a quasi-steady state model developed as a regional groundwater model to simulate infiltration–discharge relations based on long-term average recharge input data.

Based on distributed data, this model simulates the elements of the water balance, surface runoff, actual evapotranspiration, and groundwater recharge. The model was created as a way to calculate dispersed, long-term average water balance components (Batelaan and De Smedt, 2001). This model was developed using the WetSpass time-dependent spatial water balance model (Wang et al. 1996; Batelaan et al., 1996; Batelaan and De Smedt, 2001).

The model was developed and used to investigate the effects of long-term land cover changes on a basin's water regime (Batelaan et al., 2003; De Smedt and Batelaan, 2003). The model simulates the temporal average and spatial information of groundwater recharge, actual evapotranspiration and actual evapotranspiration by using long-term average standard hydro-meteorological parameters as inputs.

At seasonal and annual scales, the model estimates groundwater recharge in space. Regional groundwater models used to analyze recharge-discharge relations are frequently quasi-steady and

require long-term average recharge input that takes into consideration the spatial variability of the recharge. As a result, they can perform their calculations using the recharge output from WetSpass.

WetSpass, which was built on the time-dependent spatially distributed water balance model known as "WetSpa," is particularly well suited for researching the long-term consequences of land-use changes on the water regime in a watershed. (Batelaan et al., 1996; Wang et al., 1997; De Smedt et al., 2000).

Grid maps of land use, groundwater depth, precipitation, potential evapotranspiration, wind speed, temperature, soil, slope, are among the inputs for this model. Land use and soil type tables, for example, are connected to the model as attribute tables of the respective grids. The model splits the precipitation into surface runoff, evapotranspiration, and groundwater recharge using grid GIS technology and digital data. In the model, attribute tables of land use and soil raster maps are connected as parameter tables for land use and soil types, allowing for new definitions of climatic as well as land use and soil types. (Batelaan et al., 2003).

WetSpass was first developed for circumstances in temperate zones, particularly in Europe. To be used globally, WetSpass has been developed (Rwanga S. S., 2013). It has been employed successfully in many places throughout the world. Belgium is where the WetSpass model was first successfully implemented (Batelaan & De Smedt, 2001). The overall water balance for each raster cell in the WetSpass model is split into different water balances for the vegetated, bare soil, open-water, and impermeable areas.

This explains why the land use in each cell is not uniform because it depends on the raster cell's resolution. Each cell's internal functions are built up in a cascading manner. This indicates that an assumption is made regarding the processes' assumed order of occurrence after the precipitation event. It is necessary to define such an order before the processes may be quantified across a

seasonal timescale. The processes are described in terms of a mixture of physical and empirical relationships. Consequently, there are several restrictions on the quantity established for each step. (Batelaan and De Smedt, 2007).

2.3 Previous Work on Groundwater Recharge Estimation Using WetSpass

There are Experimental approaches, empirical methods, distributed hydrological budget (DHB), and water table fluctuation (WTF) are some of the techniques used to evaluate the water balance and groundwater quantities. Experimental techniques utilizing isotope tracers were employed by (Wang et al., 2008) to assess groundwater recharge. By utilizing modified WTF and groundwater hydrographs for the basin of a river in South Korea, (Moon et al., 2004) estimated groundwater recharge. To calculate the annual average groundwater recharge in West Africa, (Martin, 2005) applied WTF. The recharge, he discovered, ranged from 13 to 143 millimeters.

(El-Rawy et al., 2016) estimated the distribution of recharge rate over the Zarqa River Basin, Jordan, using the DHB technique. To calculate the groundwater recharge in the Hemet sub-basin, the United States, Manghi et al., (2005) used the (HB) approach. The presented data show that between 1997 and 2005, the annual long-term average recharge was 12.5 million cubic meters.

Using empirical methods based on WTF and precipitation depths, groundwater recharging was achieved in the Cn-Szaporca oxbow of the Drava floodplain, Hungary. Recently, researchers have examined the transmission of energy and water between plants, soil, and the environment in a quasi-steady state (Salem et al., 2018). The WetSpass model has been extensively used in groundwater recharge assessments (Batelaan and de Smedt, 2001).

The seasonal resolution is scaled down to a monthly scale by (Abdollahi et al., 2017) to create a WetSpass-M model. The WetSpass-Jor model for watersheds was created by (Abu-Saleem, 2010)

by modifying the parameters for Jordanian conditions. It has been proven that the WetSpass model could be used to more accurately describe recharging, including its diversity across global geographies.

The model has been used successfully in different environments, including Belgium (Batelaan and de Smedt, 2001), the Hasa and Jafr basins in Jordan (Abu-Saleem et al, 2010; (Al Kuisi, and El-Naqa, 2017), the Birki watershed, the Werii watershed, and the Geba basin in Ethiopia (Gebremeskel, and Kebede, 2017; Arefaine et al, 2012), (Bitsiet and Dessie, 2019) upper Bilate river catchment the Mashhad basin. Iran (Zarei et al, 2016) Gaza Strip, Palestine (Aish, 2014), Drava Basin in Hungary (Salem et al., 2019), Nile Delta aquifer, Egypt (Armanuos et al, 2016), and WetSpass-MODFLOW perform well in the Takelsa multilayer aquifer in northern Tunisia (Ghouili, 2017).

Therefore there are different types of groundwater modeling. In this research, the spatially distributed WetSpass model was used because of its advantage over other modeling. Groundwater modeling like lumped sum models the whole catchment is considered as a single entity and considers meteorological data as inputs.

But in spatially distributed models like WetSpass, spatial variability of processes, input, boundary conditions, watershed characteristics and outputs are considered at the pixel level and consider the land use, soil and groundwater level in addition to the meteorological data as an input. (Belete, 2018)

3. MATERIALS AND METHODOLOGY

3.1 Description of the Study Area

3.1.1 Location

The Afa-Selga watershed is located in Benishangul Gumuz Regional State (BGRS), which is one of the thirteen regional states comprising the Ethiopian federal structure it lies between 34^{o} 30' 30" and 34^{o} 51' 10" East and between 9^{o} 51' 15" and 10^{o} 6' 15" North, in the Dabus River sub-basin of Abbay River basin. It covers an area of approximately 579.5 km^{2}.

The watershed is located 687 kilometers distance from Addis Ababa and About 90 kilometers from the Ethiopia-Sudan border, making it one of the nation's border areas. Both ground and air transportation are available to get to Assosa town which is a part of the study area. The ground approach is on the way to Ambo-Nekemte-Gimbi-Nejo-Mendi-Bambasi, and then to Assosa town which is a part of the Afa-Selga watershed.

The watershed is mostly covered with savanna and woodland flora. They are a mix of savanna and deciduous forests with numerous acacia species. During the dry season, the majority of the trees lose their leaves because they are deciduous. Even though the watershed has a variety of trees, the mango tree is the most common one. (Gadisa, 2017)

Bamboo is the most widely used plant by humans. is used for construction, flooring, paper, fishing rods, water pipes, musical instruments, and chopsticks. They are also planted as ornamentals and eaten as food. Eucalyptus, Neam, and papaya trees are among the various species of trees that are present in the watershed. The watershed is situated in a hot environment, yet despite this, the good vegetation cover (trees) provides a moderating effect on the temperature, keeping it relatively cool. (Gadisa, 2017)

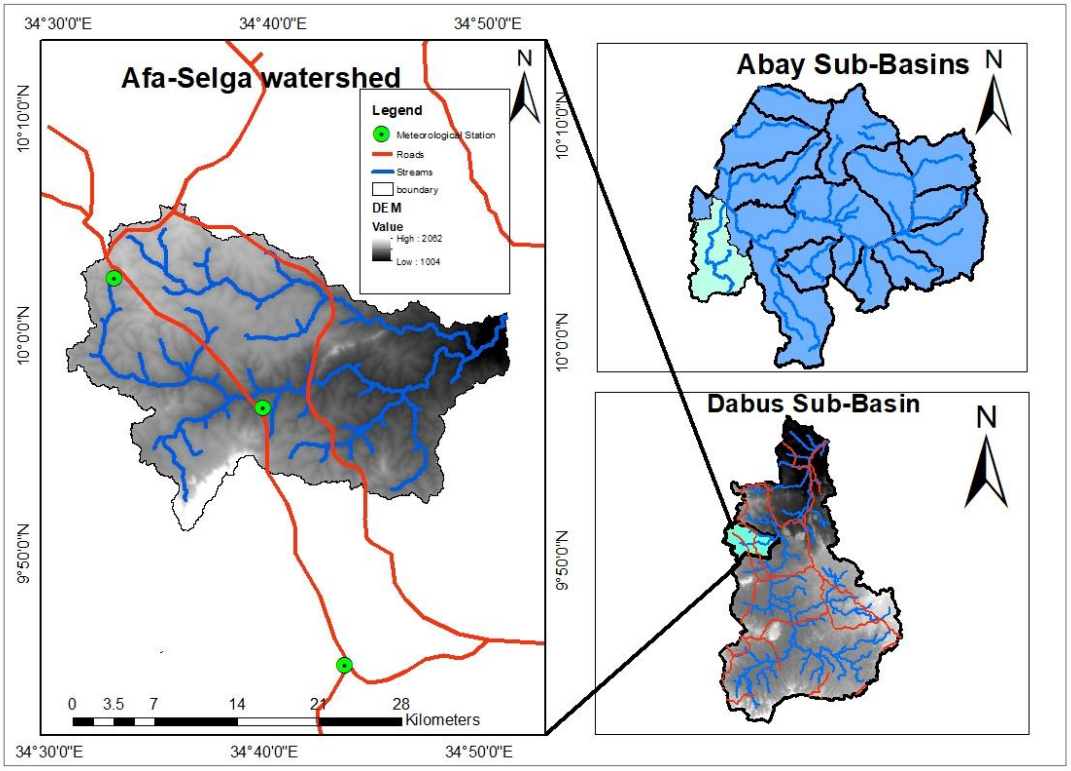

Figure 3.1: Location of Afa-Selga Watershed

3.1.2 Climate

According to EMI, (2001) the Afa-Selga watershed is located in the "Kola" climate zone. The Temperature of the area shows strong altitudinal variations. The Afa-Selga watershed mean maximum temperature ranges from 24.2 °C to 34.8 °C, and its mean minimum temperature is between 12.6 °C and 19.2 °C. The maximum value (34.8 ^{o} c) was recorded in the stations of Sherkole and Bambasi in the month of March, and the lowest value (12.6 ^{o}c) was recorded in the Assosa and Bambasi stations in the month of December.

The area's long-term average mean annual rainfall is estimated to be 1121.8 mm. More than 75% of the annual precipitation falls during the four months from June to September (JJAS), with the remaining 25% falling during the dry season. The Amba16 station recorded the highest mean

annual rainfall with a value of 1324.8 mm, while the Abadi station recorded the lowest mean monthly rainfall with a value of 918.8 mm. *(Figure. 3.2b)*

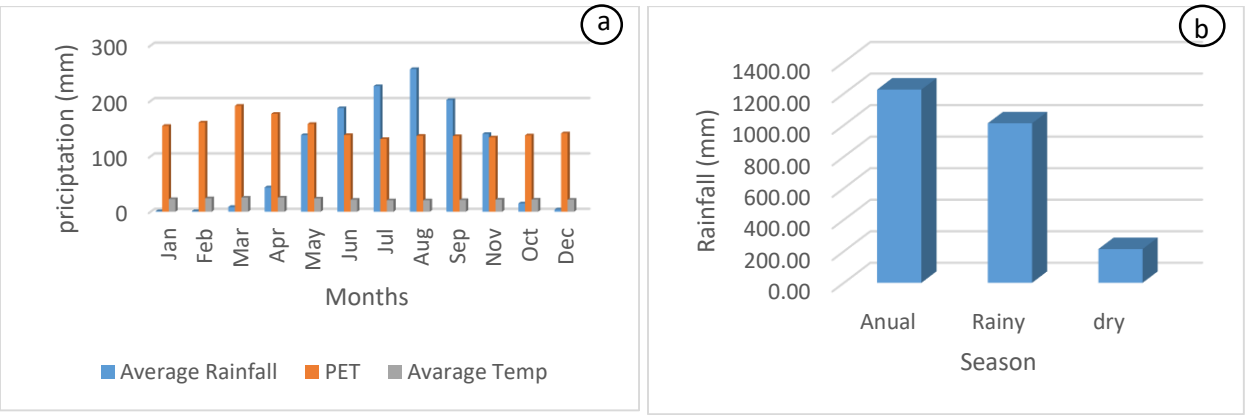

Figure 3.2: (a) Long-term mean monthly precipitation, temperature, and PET (b) Seasonal Precipitation

3.1.3 Topography/Physiography and Drainage

Ethiopia can be divided into four major physiographic regions, widely known as the Western Plateau, the southeastern plateau, the Main Ethiopian Rift (MER) and the Afar Depression (AD). From these four major physiographic regions, the study area is located at the western plateau; its geomorphology is an outcome of repeated tectonic, with associated intrusion and erosion (Gadisa, 2017). According to Gadisa, (2017), the local geological variation and tectonic activity are also partially or completely responsible for the drainage density and pattern.

The drainage density is greater in relatively elevated regions, particularly when the weathered section is thick or when the pattern of structures crossing the rocks is higher. The area is characterized by a fluctuating land escape, narrower flat plains that follow streamlines in some areas, and moderate to hilly slopes that are surrounded by relatively highlands The watershed is located between 1004 and 2062 meters above sea level. The area's major geomorphologic features can be divided into the following categories:

3.1.3.1 The Afa Plain

The Afa Plain is a relatively level plain created by basaltic lava flow. Typically, the lava flows are thin, exposing the foundation rock through tiny gullies formed by erosion. Under some of the basaltic lava flows, extremely thick (>1 m) soil has developed (Gadisa, 2017).

3.1.3.2 Volcanic Plain

Some of the Assosa and its surroundings are composed of flat, rolling plains covered in basalt rocks. The Catchment's trap series was laid unevenly on Precambrian rocks, and the rock type is hard aphanite basalt with occasional plagioclase phenocrysts. Comparatively wider river channels can be found in the lowlands. Afa River and Selga River are two of these rivers, which are

tributaries of the Dabus River. The lowest or flattest parts are created by these river channels and tectonized terrains, and Assosa town is situated on this flat plain landform. (Gadisa, 2017)

3.1.3.3 Ridges and Isolated Hills

The granitoids emerge above the plain at a relatively high relief. This formation is responsible for the majority of the hills and ridges that have developed. The highlands are typically home to narrow gorges that range in depth from deep to shallow. In the area of Inzi Hill, the granitoids provide a reasonably high relief standing among the plain. (Gadisa, 2017)

3.1.3.3 The Anbesa Chaka Massif

The Anbesa Chaka Massif Is a long, elevated area towards NNW, In general, granitic massif makes up this rocky chain. The Asosa-Kurmuk extends northward from there. While the western part of this massif flows into the west and continues to the Sirkole River, the eastern part of this massif drains into Dabus (Gadisa, 2017). But only small portions are a part of the watershed.

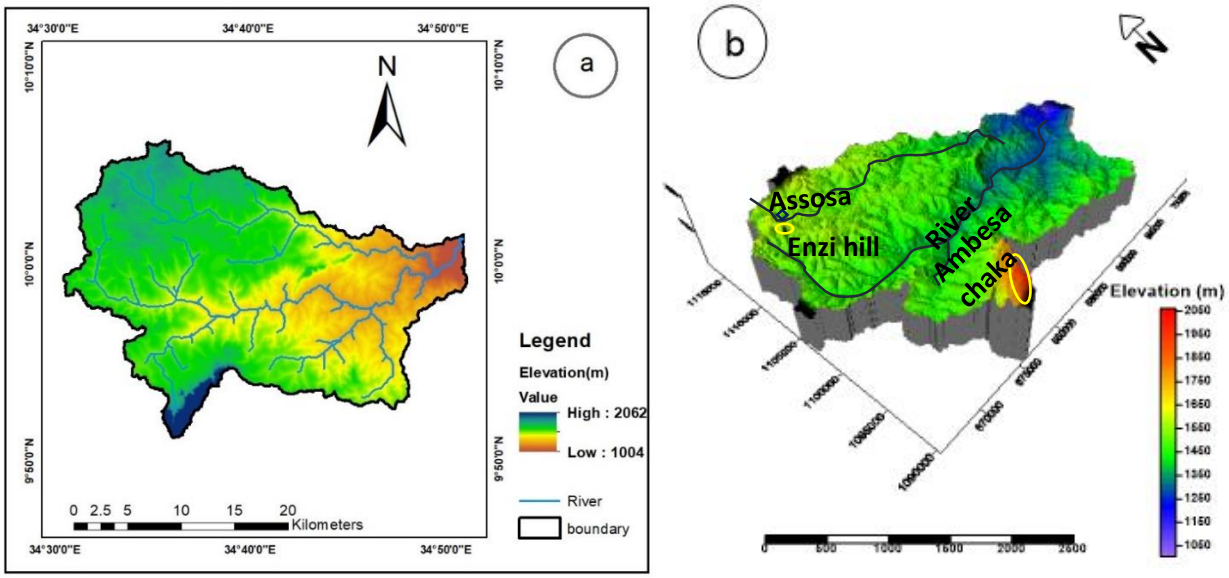

Figure 3.3: (a) Elevation map of Afa-Selga watershed (b) 3D view of Afa-Selga watershed

3.1.4 Hydrology

The area is primarily located in the Dabus sub-catchment of the Abbay River basin, which originates in Begi woreda in the Oromia Region, south of the BGRS, and flows northward into the region. The average flow discharge for Afa stations measured from 2008-2013 by the Ministry of Water Resources is 4.8 m^3/s. There are rivers in the area that are both perennial and/or intermittent. The perennial River Afa and Selga mostly drain the area's central and southern parts from west to east.

The Afa Rivers, which discharge most of the area's runoff, describe the hydrological characteristics of the studied area. The predominant drainage pattern in the watershed is structurally controlled and indicates a rectangular to sub-parallel form. While the major rivers that drain the area's east have a parallel drainage pattern, all the streams that drain the area have a parallel drainage pattern.

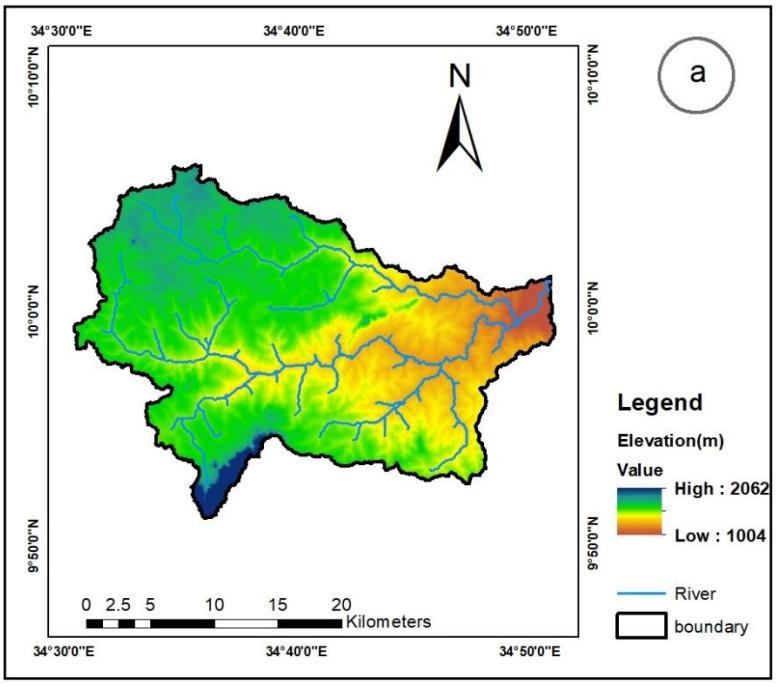

Figure 3.4: Drainage pattern of Afa-Selga Watershed

3.2 Geology

3.2.1 Litho-Stratigraphy

Precambrian rocks, Tertiary age groups of volcanic rocks, and Quaternary age groups of lacustrine and alluvial deposits are among the several lithologic units exposed within the study area. (Tefera, 1991)

3.2.1.1 Precambrian Rocks of the area

Precambrian intrusive rocks and Precambrian stratified rocks are the two categories of Precambrian rocks. Precambrian stratified rocks include a variety of units, including biotite, biotite-hornblende gneiss, meta-ultramafic rocks, amphibolite, amphibolite and quartzofeldspathic schist, metasediments, and metavolcanics. Marble and other Precambrian intrusive rocks include a variety of outcrops of the geological types Metagabbro, Metaquartz diorite, Metatonalite, Metagranite, Granite, and Alkali granite. Few of these two types of Precambrian rock units are known in the watershed, and compared to other outcrops, these units are found at higher altitudes. Some of these rock types are mentioned below. (Tefera, 1991).

It is a particular kind of intrusive Precambrian rock that commonly appears light to pinkish-grey and grows in stream cuttings. It is a granitic rock composed of medium to coarse-grained minerals, including quartz, feldspar, and mica that are frequently visible. Granite and other granitoids are often found together with this rock. Higher altitude landforms are created by the metagranite. Various fracture systems define the rocks.

These fracture systems have been partially filled with quartz veins and pegmatite. Along the Afa and Selga rivers' courses and beds, as well as in their tributaries, granite gneiss rock outcrops are common. The granitic mass north of the Afa-Selga watershed is foliated along the north-south

direction but has an irregular form. The Tertiary basalt terrene in the area of Asosa frequently contains small, impassible granite rocks. The majority of the area beneath the basalt layer appears to be covered by the same metagranite mass. North of the Afa-Selga watershed, there are some relatively significant metagranite masses. Since they display signs of local deformation, some of these plutons were likely deposited during the final stages of regional deformation and are late tectonic.

Early Paleozoic

Quartz-graphite schist (pqqs)

This unit is seen in three distinct locations throughout the domain as irregular outcrops that create little hills and ridges with a SW trend. The rock is foliated, laminated, finely grained, and dark grey the unit is located in the southwest parts of the domain. It creates sharp hills and valleys here. The quartz-graphite schist in the area known as Buda Selga, in the northeastern corner of the domain north of Bambasi

It reaches a width of one kilometer and a length of almost six kilometers. The rock has a high to gentle slope and is heavily layered. There are also tiny areas of quartz-graphite schist in between the aforementioned. In thin sections the quartz-graphite schist is composed of 40-45% graphite, 30-35% quartz, 5-10% sericite and 5% opaque.

Granite (Pgt3)

This unit is relatively homogeneous body made up of medium to coarse grained, massive granitic rocks. They form hills and ridges and outcrops as big rounded blocks.

Late protorozoic

Metasediments (Pcms1)

From one location to another, it differs in composition, texture, structure, degree of weathering, and deformation. Graphite schist, chlorite schist, talc-chlorite schist, amphibole-biotite-feldspar-quartz schist, amphibole-biotite schist, muscovite-feldspar-biotite-amphibole schist, chlorite-biotite schist, quartz-muscovite-sericite schist, and In areas where it has been severely weathered, the unit can range from massive variants that are slightly deformed to schistose and foliated types that are extensively deformed.

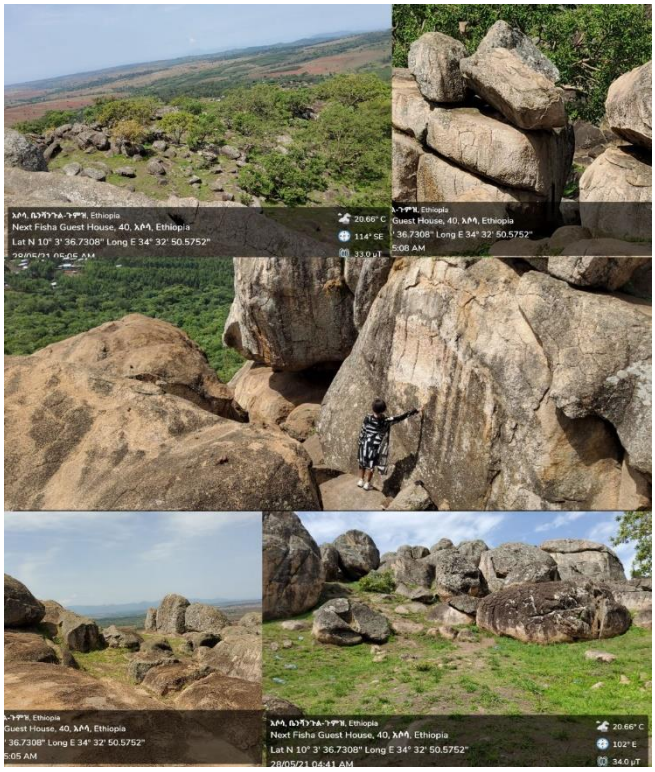

Figure 3.5: some in-field images of the study area Precambrian rock types

There are three main locations where metasediments schists occur, One is in the area's northwest, running from Geissan southward; the second is east of Geissan, reaching southward from Mudul village beyond Menge town; and the third is in the area's south-western corner, extending from Assosa northwest around Kashmangal village, which encompasses the watershed. Granitoids intrusive masses and Tertiary volcanic cover rocks separate these three occurrences from one another.

Granite-granodiorite (Pgt1)

The Syn-tectonic intrusive composed of foliated granite which found at southern part of the area. It forms prominent topography and has moderate reliefs. Typically represented by Anbesa chaka

Granite. The rock is grey to grayish pink, medium grained and foliated and sheared and leucocratic. The rock is composed of 25-34% of quartz, 15-42% plagioclase, 30-46% perthitic k-feldspar, 2-5% of biotite and traces of opaque, hornblende, muscovite, garnet and zircon.it exhibits granular and granoblastic texture.

Granodiorite (gd)

The northwestern and northeastern regions of the map show a larger area covered by granodiorite rock. The grey, massive to foliated, medium-coarse-grained rocks display a well-preserved plutonic texture. In most cases, foliation appears as aligned and pigmented mineral grains. Highly gneisses varieties of granodiorite that have the appearance of banded gneisses are widely north and west and fault parts of Ethiopia. It is founds the northern parts of the study area (Assosa area).

Metaquartzdiorite (dt)

In the mapped region, metaquartzdiorite, metatolinate, and Meta granodiorite are found close to one another. The degree of transformation and deformation within these intrusions varies according to the location. These intrusive features are characterized by consistency and variety in the degree of deformation and metamorphism. Pretectonic and syntectonic incursions are represented in some of these (Mengesha, 1991).

Middle Proterozoic

Granodiorite-tonalite (Pgdt)

This unit is found in the eastern and southeastern regions, specifically in the Bengwa locality and along the Dabus catchment. The unit lies in the Asosa-Krumuk and Gimbi map sheet.but Quaternary sediments and Tertiary volcanics cover it to the southwestern and northeastern. However, given their widespread distribution further south in the Gore map sheet (Mengesha and

Berhe, 1987) and their occasional outcrop in stream cuts and deep gorges, it's possible that these rocks are widely distributed beneath the cover rocks.

The rocks have light to dark grey tones, medium to seldom fine and coarse grains, and varying degrees of deformation and shearing. Rocks in this unit range in texture from dominating quartz diorite, tonalite, and granodiorite, to uncommon diorite/gabbro.

Biotite and biotite-hornblende gneiss (Pcgn2)

Well-foliated, medium-grained, grey to dark grey biotite and Areas north are underlain by biotite-hornblende gneisses with well-developed compositional layering. Additionally, there are quartzofeldspathic gneiss, muscovite-biotite schist, and subordinate Calc-silicate genesis. Grey, medium-grained, well-foliated, granoblastic biotite gneisses with a color index ranging from 5 to 10 are the typical gneisses found close to the settlements of Kashmangal.

The main ingredients are biotite (5–10%), plagioclase (30%), microcline (20%), and quartz (40%). Alteration of placoclase to sericite and epidote, and biotite to chlorite is frequently observed. The most often used accessories are muscovite, sphene, and magnetite. The foliage typically exhibits a steep to moderate north-south trend.

Metasediments and metavolcanics (Pcms2)

Low-grade metamorphic schists that are both volcanic and the western portion of the map sheet is where sedimentary origins are found. One location can be found in the far northwest of the charted regions, one location can be found in the far northwest of the charted which stretches south of Azali village and past Dul village to the Ethiopian-Sudanese border.

The second instance is located in the north eastern part of the mapped region. It is isolated from the previous occurrence by an intrusive plutonic rock mass that is granitoids. The primary rock

types include chlorite, phyllite, and sericite-quartz. Distinct phyllite phases: quartz-albite-calcite-epidote-chlorite, quartz-sericite-quartz-calcite, and epidote-magnetite-chlorite-sericite-quartz-calcite. The typical accessories ere iron oxides and biotite. In several locations within this map unit, layers of grey, fine-grained felsic schist with quartz and feldspar Porphyroblasts, or "eyes," were found. These felsic rocks are calcite-hematite-quartz schist and epidotefeldspar-quartz-mica schist. Haematite, sphene, and magnetite are the most used accessories.

Meta ultramafic rocks (Pumf)

The mapped area contains several varied-sized Meta ultramafic bodies, the most notable of which are found in the Tulu Dimtu belt. These ultramafic intrusives are related to tectonized ultramafic schists because they undergo deformation and metamorphism. The Meta ultramafic rocks in the Tulu Dimtu belt are represented by the Anchore, Daleti, Tulu Dimtu, Jaja Kubsa, and Korka Meti bodies.

The Meta ultramafic, which are characterized by silicified ultramafic (birbirite) and serpentinite, serpentine schist, talc schist, and talc-carbonate schist with subordinate pyroxenite, form notable ridges that are nearly completely devoid of vegetation. Most often, they appear as elongated masses that match the foliation tendency of the nearby rocks.

The Meta ultramafic are characterized by silicified ultramafic (birbirite), serpentinite, serpentine schist, talc schist, and talc-carbonate schist with subordinate pyroxenite. These rocks form notable ridges that are nearly completely barren of vegetation. They typically appear as elongated masses that match the foliation trend of the nearby rocks.

Birbirite (Pbr)

The silicified ultramafic material known as birbirite has a smoothed surface and noticeable ridges. They were primarily observed in the domain of Afa. They are fine-grained, pale to dark brown, and they crop out in a few locations close to the serpentinized ultramafic' edges. The rocks from the Yubdo ultramafic, where birbirite is named, are comparable to those described here (Duparc and Borloz, 1927).

3.2.1.2 Tertiary volcanic rocks

Alkali olivine basalt (Te)

The southwestern and northeastern parts of the watershed are affected by this flow. The Precambrian rocks in the area had a trap series that was unevenly layered on top of them. Lateralization was created as a result of the weathering impact of the warm climate. Basalt has been found at depths of 37 and 30 meters in Selga boreholes, however, it has not been penetrated. Compared to the nearby basement rocks, basalt often occupies an area with lower elevation. Less than 100 meters thick, very worn, and bearing lateritic crust, tertiary volcanic rocks are thin in thickness. There are residual caps of basalt flows made of alkali olivine basalt (Te).

Lower basalt (Tib)

In the Gimbi map sheet, the volcanic rocks that are most exposed are the lower flood basalt (Tib). It restlessly rests on top of crystalline basement rocks such as Metagranodiorite, Metadiorite, and post-tectonic granite. In addition, these basaltic lava flows constitute the region's earliest volcanic products. Paleo-depressions were filled with basaltic lava flows, which produced a broad, level terrain due to their lithology and massive volume.

The fresh rock in some river basins that are tributaries of Dabus has a dark grey to grey color, and depending on the degree of weathering, it has weathered to a grey and reddish brown color. These

parts demonstrate the interaction with underlying basement rocks. It typically has an unusual variety of vesicular kinds and is enormous. It cover the southwestern and northeastern parts of the area

3.2.1.4 Quaternary Sediments

Alluvial Sediments (Qal)

According to (Gadisa, 2017), the watershed's river valleys are where the majority of the alluvial deposits are found. The sediment of this sort is typically found at Afa sites beneath thin flows of basaltic strata. This layer primarily consists of sand and gravel created by the mechanical breakdown of granitoids and gneiss, with some basalt being transported and deposited by rivers as they traveled along their courses. Many of these deposits serve as placer gold sources for underground water supplies.

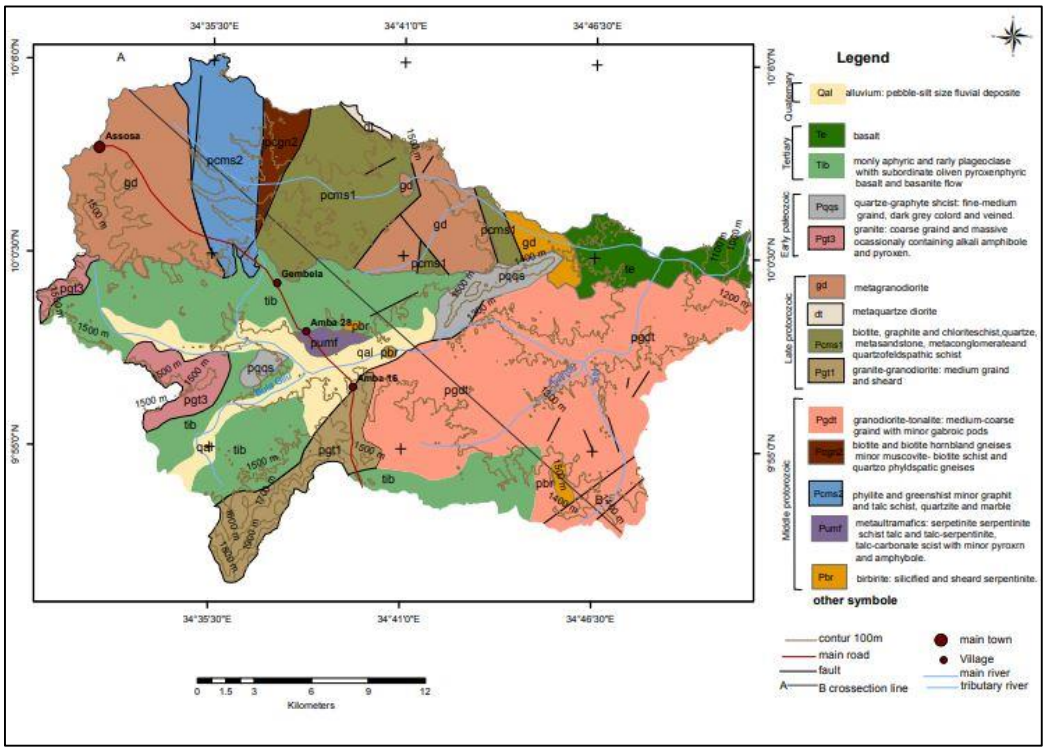

Figure 3.6: Lithologic Map of the area

3.2.2 Geological Structures

The primary planar structures in the crystalline basement rocks of the map area are foliation, schistosity, and gneissosity. In the basement rocks throughout western and southwestern Ethiopia, they typically strike north-south. On the contrary, the western area of the map is dominated by north-easterly strikes. Mineral aggregate lineation and, to a lesser extent, the long axes of lenticels and prismatic minerals like amphiboles serve as the primary representations of linear structures. They generally fall gently north or south across the whole map area, trending parallel or sub-parallel to the foliation strike.

Faults: The map area contains two distinct sets of lineaments. These come in three sets: a northeast-to-north-northeast set, a northwest-to-north-west and E-W set. Ethiopia's western and south-western regions are home to these two groups of lineaments; (Seife and Rothery, 1986 cited by (Gadisa, 2017). Many of them have been located using aerial photographs. During ground traveling, several have been found to have faults with horizontal offsets up to several kilometers. The western portion of the map area is where northerly and north-westerly trending lineaments are most noticeable. Sheared and mylonitic zones on some surfaces demonstrate movement. (Gadisa, 2017).

The Assosa-Kurmuk and Gimbi geologic map shows that there are faults with both dextral and sinistral senses of displacement, with the former appearing to predominate. Both lateral and vertical movements are believed to have occurred along the Kurmuk fault, which separates the Kurmuk plain on the west from the elevated Ethiopian plateau on the east. Additionally, it forms a significant border between the high-grade terrain to the west and the throw-grade terrain to the east. The primary tectonic and structural features in the region trend E-W, NS, N-W, and N-E. (Gadisa, 2017).

The geological section A-B (figure 3.7) selected with the purpose of hydrogeological important Reason (which bisects geological rock units North-East, connects rift floor, escarpment and highlands, crosses geological structures fractures joints and rivers). Geological map with preferred cross section line A-B. Topographic data is obtained from DEM to get elevation profile and 3D view of the study area. GIS, Global mapper and excel are extensively used in preparation of geological and hydrogeological cross sections.

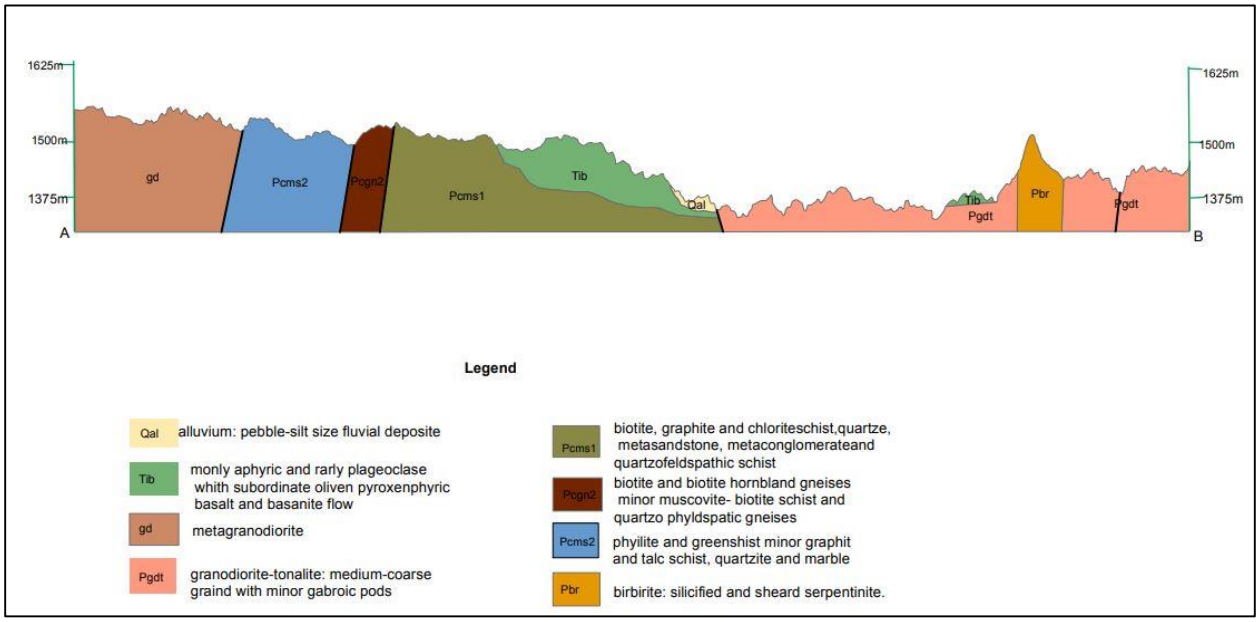

Figure 3.7: Geological cross section (North_ East)

The cross-section in the study area shows geology unit of alluvium, Lower Basalt, Granodiorite, Metaquartzdiorite, Birbirite, Granodiorite-tonalities, Metasediments and metavolcanics, Biotite and biotite-hornblende gneiss. The middle part is the rift floor and the northern part of the study area is the highland. Generally, the cross-section covers 24.6 km North-East, the maximum elevation is 1600 m.a.s.l and the minimum is 1375 m.a.s.l (figure 3.7)

3.3 Hydrogeology

3.3.1 Aquifer Classification

The hydrogeological characterization of several rock types forms the basis for the classification of diverse lithological units. (Gadisa, 2017) To categorize the hydrogeological units into aquifer systems, Alebachew et al, (2003), states that both qualitative and quantitative characteristics are used. According to him, the differences in groundwater storage, transmission, and yield among the different formations are the basis for categorizing aquifers

Qualitative Parameters

The qualitative division of the principal hydrogeological units into pours fissured and/or karst permeability, and permeability rocks of groundwater is based on the groundwater point data and pump test data (Ethiopian Geological Institute , Explanatory notes on hydrogeological and hydro-chemical maps of Asosa-Kurmuk sheet, 2004).

Quantitative Parameters

Based on the hydrogeological properties of different rock types, such as permeability, aquifer depth, and yield achieved, this parameter is used. The following aquifer system classifies various lithological units based on qualitative and quantitative hydrological parameters and geomorphologic settings. (Gadisa, 2017).

Moderately productive fissured aquifers

Alkali Olivine Basalt

In those places, the basalt cover typically takes the shape of flat-topped outcrops and lies irregularly on the crystalline basement. However, in the center of the area, basalt is found at lower elevations than basement rocks. The thickness of the outcrop varies as well, reaching roughly

100m at its thickest point and as low as 15m in some areas. Additionally, the degree of weathering varies from one location to another. It is heavily lateralized in some parts, somewhat laterized in others, and huge in others. Selga River areas are primarily covered by this unit. (Gadisa, 2017)

As a result, the hydrogeological quality of basalt varies locally from location to location. Due to the low clay concentration of these unique soils, if the soil cover is thick and oxidized, its permeability (percolation to depth) will be high. This will improve the ability of the underlying cracked rock to store groundwater. (Gadisa, 2017)

In general Aquifers with a moderate output are typically encountered in basalt (mainly with fracture permeability). These formation's aquifer parameters, according to EGI, are T = 100 - 10 m^2 /d and Q = 5 - 1 l/s.

Low-productive fissured aquifer

This kind of aquifer is made up primarily of basement rock, which covers most of the area. The hydraulic conductivity, groundwater storage, and spring yield of some of the aquifer's outcrops, including Metagranite, a granitoids rock with coarse grains that occurs in combination with granites, vary from location to location. Local groundwater buildup is anticipated in locations with penetrative faulting and related brecciated rock sections. (Gadisa, 2017)

The thickness of the weathered zone varies among places depending on whether the proportion of the basic mineral components is larger or there has been more assimilation with other rocks like diorite. Local groundwater buildup and low-yield springs are anticipated in these areas. Most of the study area is covered in this unit. (Gadisa, 2017)

According to the Geological Survey of Ethiopia and Chernet (1993), the region's low-productive fissured aquifers have transmissivity (T) that ranges from 1 to 10 m^2/d. The results of hydraulic

parameters, which were examined using pumping test data, can also confirm the above-mentioned parameters, being in the range of 2.76 to 9.92 m^2/d.

Aquitards

There are some intrusive rocks in it. Aquitard out crops in the catchment include phonolite and trachyte plugs, which grow in clusters and along fracture lines. Fine-grained igneous rock, or phonolite plugs, is a light-colored volcanic rock that is distinguished by the presence of some intrusive rocks. Aquitard out crops in the catchment include phonolite and trachyte plugs, which grow in clusters and along fracture lines.

Fine-grained igneous rock, or phonolite plugs, is a light-colored volcanic rock that is distinguished by the presence of permeability the trachyte and phonolite plugs are considered as aquitards. Ethiopian Geological institute (EGI) determined that this formation has ranges of aquifer parameters of: (T= 0.01 -1 m^2/d, Q = 0.05– 0.5l/s).

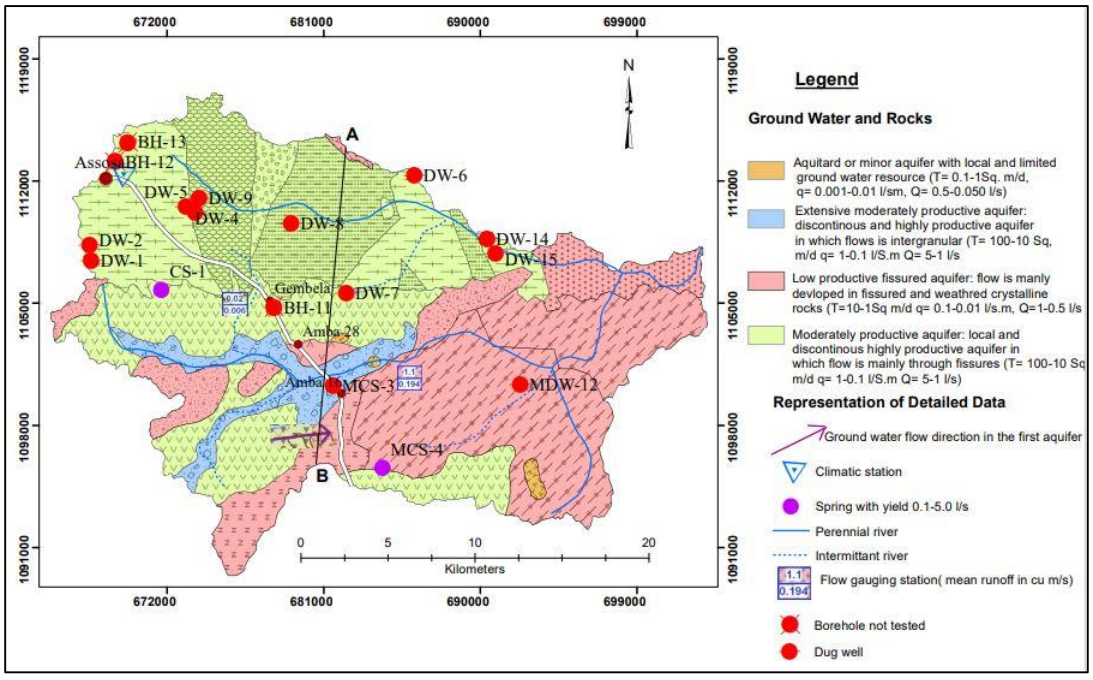

Figure 3.8: Hydrogeological map of the area Borehole of the area

(Figure 3.9) is presented based on the evidences obtained from geomorphological, geological, structural, hydrogeological, hydrological, hydro-chemical, geophysical and Topographical. This multi-proxy approach provided important information to achieve the conceptual circulation model of the groundwater and generalized aquifer system from the upland towards the main rift axis.

Geological Map of Kurmuk and Assosa area 1:250,000 Scale and Geological Map of Gimbi area 1:250,000 scale, Hydrogeological Map of Kurmuk and Assosa and Gimbi 1:250,000 scale (EGI, 2004) and Topographic map (The Digital Elevation Model, DEM) was generated from Alaska web page has been extensively used to create databases and prepare geological and hydrogeological maps.

The first step in the Preparation of the conceptual model was identifying the purpose, then identifying the study area, deciding appropriate boundary moderately conditions, creating a two-dimensional hydrogeological model and estimating sources and sinks. Review of publications (reports) and Data collection from previous studies have been done.

Based on the analysis of the geological formations, it appears that the hard rock's aquifer properties are subpar. However, aquifers ranging from moderately to aquitards can be identified in coarse alluvial silt deposits, such as surface deposits and underground river channels, as well as in lateritic weathering basalt and basement rocks and fractured zones of rocks.

These broken and worn zones of the basement outcrops and basaltic rock potentially recharge the groundwater in this location. Wherever the water table is below the river level and the loose alluvial sediments along the aforementioned river courses are thick enough, it is also anticipated that these rivers will recharged the sediments. The ground water potential is superior in the Area in terms of hand dug wells, drilled deep wells and spring.

Basalts, granites, and other Quaternary age deposits, such as alluvial deposits, are the rock units which makes the watershed and are important aquifers. The primary causes of these rocks' water-bearing characteristics are secondary processes including weathering and fracturing. According to observations the water-bearing layers are the result of these secondary processes, according to the lithological well logs of the study area. Reservoir rocks are not found in the same rock units of the area where such secondary processes do not exist.

Therefore, degree of groundwater productivity in the study area is entirely depends on secondary porosity and permeability that develop as a result of weathering and fracturing. (Gadisa, 2017) Based on this Neumann's curve fitting method, the aquifer types of the study failed beneath unconfined aquifer which is anisotropic. Because, from the result, the ratio of both horizontal and vertical hydraulic conductivity of the aquifer is different from one. (Gadisa, 2017)

According to Alamerew et al, (2003) as cited in Gadisa, (2017), the catchment's hydrogeological units are divided into three categories: the dominating basement unit, which occupies the majority of the research area and is categorized as low productive; the moderately productive fractured aquifers; and the third category, aquicludes units. Also in the study area to classify the aquifer, the depth of the outcrops and aquifer thickness play an important part; the aquifer thickness of the study area ranged from 28.70 to 63.14m and the depth ranged from 57m to 120m and this depth can show us the borehole is a shallow borehole depths. (Gadisa, 2017)

The area's aquifer types are divided into three categories based on these values and the catchment's geologic units: the first is the moderately productive fissured aquifer, which is composed of basalt And is highly to moderately fractured and weathered. Therefore, in the research area, this unit is the most known aquifer units due to its secondary structures and is classified as a moderately

productive fissured aquifer. Low-productive fissured aquifers in the region, which are associated with granite, mica, amphibolite, granite, and metasediments, are the second type of aquifers found there.

These rock units are categorized as basement rocks since there aren't many secondary structures and therefore less groundwater development in them. The third category of aquifers in the research region is aquitards, which also comprise paragneiss (basement), serpentinite, and metodiorite. The majority of the rocks in the study area are Precambrian basement rocks. These units vary from low fissured aquifers to aquitard/aquicludes in the area. However, it is not good water bearing due to the absence of more secondary structure that governs infiltration to make groundwater.

Some basement rock types in the study area are metagranite, granite, and metasediments. The catchment's exposed unit is Tertiary Volcanic Rocks, which comprise Alkaline Olivine Basalt and can be regarded as the primary water-bearing layer of the study region because of secondary structures. These rocks are located next to basement rocks. The research area's moderately productive fissured aquifer types are primarily caused by alkali olivine basalt units.

Table 3.1 Comparison of hydraulic values of the area with that of the Ethiopian Hydrogeological map (Chernet, 1993) & (EGI, 2004)

Reliability of the present study with that the previous work done regional wise which include the study area.		
Aquifer types based on productivity	Hydraulic property values taken from Chernet, (1993) & EGI, (2004)	Hydraulic property values of study area from pumping test data.
Moderately productive aquifer	T=100-10 m^2 /d	T = 44.3 m^2 /d
	K=0.14-62 m/d	K = 1.5434 m/d b = 28.70m depth = 57m

Low productive aquifer	T=10-1 m^2 /d K=0.004-0.14 m/d	T = 9.92-3.0 m^2 /d K = 0.1124 m/d b = 63.14m depth = 102m
Aquitards	T= 0.01 -1 m^2/d	T = $8.64*10^{-8}$ m^2 /d K = $2.13*10^{-4}$ m/d b = 40.65m depth = 120m

In the study area, two methods of groundwater recharge are anticipated. The first and most significant is recharge, which results from precipitation entering into groundwater. The second, which is unique to the region, is recharge from streams and rivers to the fractures and alluvial deposits they pass through. Given its heavy rainfall, the area is said to be blessed with an abundance of excess water that can infiltrate into the ground and recharge groundwater.

In this area, foundation outcrops and fractured and weathered zones of basaltic rock may allow groundwater to recharge. Additionally, wherever their thickness is enough and the water table is below the river level, it is anticipated that the loose alluvial sediments along the previously mentioned river courses will be recharged by these rivers.

Groundwater discharge areas are formed by moderate depressions in highlands, while elevated areas are groundwater recharge areas. Weathered rock recharges inter-mountain depressions. Due to the elevation difference between high cliffs and deep gorges, many springs emerge in the middle or top of cliffs due to thin impermeable layers, variation in rock weathering, lithological variation, and structure penetration. Topographically high areas are generally considered recharge areas, while topographically low areas are discharge areas.

However, topographically high areas can be regarded as recharge areas, and topographically low areas can be regarded as discharge areas. The movement of groundwater in a given area depends

on geomorphology, presence of vegetation and soil cover, drainage density, geological and structural formation of the area, rainfall intensity and duration, sunshine hour and strength etc. Its flow direction is expected to follow the surface water flow direction. Local flow direction deviations due to the impact of bedding of sediments; foliations or some hidden structures can exist.

Variations in the hydraulic conductivity of the different rocks can also cause local deviations in general groundwater flow direction. As shown in the hydrogeological map of the area groundwater flows to the East and West directions. The groundwater divide is NE-SW and Assosa town is close to the surface water divide, and it is the recharge zone of the groundwater system. Generally, the groundwater and surface water flow directions are the same. (Ethiopia Geological Institute, Explanatory notes on hydrogeological and hydro-chemical maps of Asosa-Kurmuk sheet, and 2004).

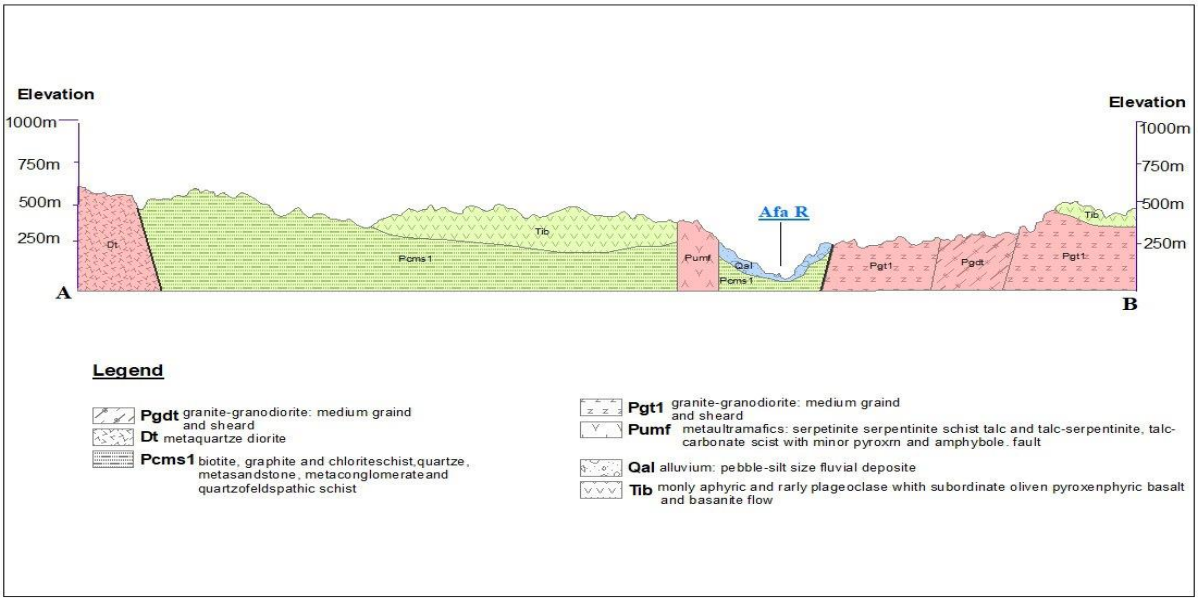

Figure 3.9: Hydrogeological cross section (North_south)

3.5 Method

3.5.1 Data source and collection

Various available data were gathered from different organizations and websites. The other organizations and institutes are the Ethiopian Geological Institute (EGI), the Ethiopian Ministry of Water and Energy (MoWE), and the Ethiopian Geospatial Institute for LULC data.

Meteorological data were collected from Ethiopian Meteorological Institute (EMI), (https://power.larc.nasa.gov, https://www.isdaafrica.com/isdasoil/ and http://asf.alaska.edu) are some of the websites which obtained wind data, soil data and DEM (Digital Elevation Model) respectively and groundwater-related data were collected from Benishangul-Gumuz Regional State Water Works and Construction Enterprise (B/G/R/S WWCE).

3.5.2 Meteorological and hydrological data

Secondary meteorological data inputs for the model including monthly precipitation, potential evapotranspiration, temperatures (minimum and maximum), and wind speed data were acquired from the Ethiopian Meteorological Institute (EMI) from the meteorological stations inside and around the Afa-Selga watershed.

The years 2004 to 2020 are chosen for the processing of meteorological data (precipitation, temperature, and wind speed), with an average value for each seasonal time step, i.e., the winter and summer seasons corresponding to October to May and June to September, respectively. The available meteorological data were used to generate annual and seasonal meteorological characteristics. Five meteorological stations are within or close to the Afa-Selga watershed (Assosa, Amba16, Bambasi, Sherkole, and Abadi).

Daily rainfall recording data are available in all stations, but temperature records have only been recorded in four stations (Assosa, Bambasi, Sherkole, and Abadi) , due to a lack of recent wind speed data from the Ethiopian Meteorological Institute daily wind speed data for five stations downloaded from power access climate data (https://power.larc.nasa.gov).

Average monthly values of rainfall were used to derive average annual rainfall, wet season precipitation (June–September) and dry season precipitation (October–May). Hydrological data was obtained from the Ethiopian Ministry of Water and Energy (MoWE) that available flow data from the years 2004-2014 in and around the watershed (Afa stations).

Due to a data shortage, the PET was calculated using the Hargreaves equation (Hargreaves & Samani, 1982), which is appropriate in areas where only temperature data is available for climatic analysis. The FAO advises using the Hargreaves method (Allen et al., 1998) as a backup method for estimating PET if there are insufficient meteorological data for the Penman-Monteith approach

Meteorological variables are often measured at meteorological stations, and the data is only accurate for the location where it was measured. These variables are needed for applications in hydrology and water resource management. Meteorological variables at different stations can be estimated by spatial interpolation. (Belete, 2018)

Raster interpolation methods include Inverse Distance Weighting (IDW), Spline, and Kriging. The meteorological data input for the model was prepared using the Inverse Distance Weighting IDW approach. It is the most widely utilized strategy because it is simple and typically produces good results (Lu and Wong, 2008).

3.5.3 Land use/Land cover, DEM, and Soil data

Physical data, a 30 m resolution image of land use land cover land cover of the watershed was collected from EGII (Ethiopian Geospatial Information Institute) for the year 2018.

The soil textural type of the study area was downloaded from the first continental-scale soil property map with a resolution of 30 m, iSDAsoil website (https://www.isda-africa.com/isdasoil/) offers soil data with a level of detail that is similar to the actual variability on the ground and 12.5 m resolution DEM was downloaded from the Alaska Satellite Facility /ASF web page/ (http://asf.alaska.edu) and used appropriately as an input for the model to compute the study area's groundwater recharge.

3.5.4 Groundwater level

Depth to groundwater level data is one of the inputs for the WetSpass model is the depth to groundwater, which was collected from the B/G/R/S Water Works and Construction Enterprise and the Assosa town Water Supply and Sewerage Enterprise which provide the well history data and measured the depth to groundwater level using Deep meter.

3.5.5 Parameter tables

The model requires four different types of parameter tables to run and for the effective running of the model, those types of parameter tables were created in a suitable format (dbf). As an input to the model, attribute lookup tables for the runoff coefficient parameter table, soil parameter table, and summer and winter land use parameters table were created (*Appendix I and II, III, and IV*). These various lookup tables for biophysical data were compiled and evaluated from different literature.

3.5.6 Estimation of missed data

Different meteorological and hydrological data were collected, and missing data were checked. The missed data were filled in using XLSTAT (2016) software. Data missing completely at random (MCAR), data missing at random (MAR), and data missing not completely at random (NMAR) are the three types of missing values, according to Allison (2001).

Data missing completely at random (MCAR), if the event that leads to missing data is independent of observable variables and unobservable parameters. It should occur entirely at random. When the data missing completely at random (MCAR), the analysis of the data is unbiased data missing at random (MAR), if the event that leads to missing data is related variables. When data not missing completely at random (NMAR), If the data is missing for a particular reason.

Most XLSTAT functions (ANOVA, PCA, regression, etc.) include options to handle missing data. However, only a few approaches are available. This tool allows you to complete or clean your dataset using advanced missing value treatment methods.

The methods available in this tool correspond to the **MCAR** and **MAR** cases.

Different methods are available depending on your needs and data:

- For **quantitative** data, XLSTAT allows
    - Remove observations with missing values.
    - Use a mean imputation method.
    - Use a nearest-neighbor approach.
    - Replace missing values with a given numeric value.

- Use the NIPALS algorithm.
- Use an MCMC multiple imputation algorithm.
- Use the EM (Expectation Maximization) algorithm for data following a multivariate normal distribution.

- For **qualitative** data, XLSTAT allows
  - Remove the observations with missing value.
  - Use a mode imputation method.
  - Use a nearest neighbor approach.
  - Replace missing values by a given textual value.
  - Use the NIPALS algorithm.

The MCMC imputation method was used in this study to fill in the metrological missed data using the XLSTAT add-in plug-in for Microsoft Excel. This tool's methods fit MCAR and MAR situations. A sophisticated, comprehensive, and user-friendly data analysis and statistical solution was made available to everyone by XLSTAT since it was started in 1995.

3.5.7 Data homogeneity test

The homogeneity of hydro-climatological series data can be assessed using various methods. This study applied parametric (Standard Normal Homogeneity Test, SNHT) and non-parametric (Pettitt) tests to examine homogeneity annual series of precipitation (P) and minimum (T_{min}), maximum (T_{max}) air temperature and wind speed data.

The absolute homogeneity test is widely used to assess the continuous of the time series. Four homogeneity tests namely (SNHT), (BR) test, Pettitt test, and (VNR) test were used. Under the null hypothesis, the annual data records are independent and identically distributed and the series is considered as homogeneous except for VNR test. Meanwhile, under the alternative hypothesis, SNHT, Pettitt test and BR test consider that the series contains a break in the mean and classified as inhomogeneous one.

The main advantages of the three tests is each tastes is capable to exactly the year where break occur. In contrast VNR cannot detect the year break because it assumes that series is not randomly distributed under the alternative hypothesis.

XLSTAT (2016) was used to calculate the empirical significance level (p value). In this case, a significance level of 5% was used for this test and XLSTAT software was used for better presentation of the results.

3.5.7.1 The Standard Normal homogeneity test

According to Alexandersson (1986), this test compares the mean of the first k years of the record with the latest n-k years in order to identify variations in a time series of rainfall data.

$$T(k) = K\bar{Z}^{-2}1 + (n-k)\bar{Z}^{-2}2 \quad \text{k=1,2,3,….n} \qquad 3.1$$

$$\bar{Z}\,1 = \frac{1}{k}\sum_{i=1}^{k}\frac{y-\bar{y}}{s} / \sigma \qquad 3.2$$

$$\bar{Z}\,2 = \frac{1}{n-k}\sum_{i=k+1}^{n}\frac{y-\bar{y}}{s} / \sigma \qquad 3.3$$

$$s = \frac{1}{n}\sum_{i=1}^{n}(y-\bar{y}) \qquad 3.4$$

Similar to the Buishand range test, the null and alternative hypotheses are the same. T(k) gets its highest value close to the year k = K if there is a break in the records at any year K. σ is the standard

deviation, $\bar{y}$ is the average of time series and $\bar{z}_1$ *and* $\bar{z}_2$ are the parameters of T(k) statistic The definition of the test statistic T_0 is:-

$$T_{0=}\ {}_{0\le k\le n}^{max}\, T(k) \qquad 3.5$$

When T_o increases above a certain level, which is based on sample size, the null hypothesis is accepted. Time-series breaks are found close to the starts and ends using the standard Normal Homogeneity test.

3.5.7.2 Buishand test

The Buishand range test is a parametric test with a null hypothesis, meaning that test values are assumed to be independent and identically normally distributed. According to the alternate hypothesis, there should be a jump-like shift (break) in the series. The Buishand test can be applied to variables following any form of distribution. The test statistics are the adjusted partial sum of the first year or cumulative deviations from the mean (Buishand, 1982), and k till n years, which are defined as:

$$s_0^* = 0 \qquad 3.6$$

$$s_k^* = \sum_{i=1}^{k}(Y_i - \bar{Y}) \qquad k=1, 2, 3\ldots n \qquad 3.7$$

Y_i , Is the element of the times-series and $\bar{Y}$ is the mean value of the times-series. When a time-series is homogenous, the values of s_k^* fluctuates around zero because there are no systematic deviations of theY_i values with respect to their mean. If a break is present in year K, then s_k^* reaches a maximum (negative shift) or minimum (positive shift) near the year k = K. the $(\frac{s_k^*/s}{\sqrt{n}})$ depicted in graph representing the results of this test. The significance of the shift can be tested

with the rescaled adjusted range statistics (R), which is the difference between the maximum and the minimum of the s_k^* values scaled by the sample standard deviation:

$$R = \frac{\max_{0<k<n} s_k^* - \min_{0<k<n} s_k^*}{s} \quad 3.8$$

3.5.7.3 Pettitt's test

The Pettitt's test is an adaptation of the rank-based Mann- Whitney test that allows identifying the time at which the break occurs. The test is a non-parametric rank test and requires no assumption about the data distribution. The null hypothesis is the same as in the Buishand range test. The ranks r1... rn of the Yi... Yn are used to calculate the statistics (Pettitt, 1979).

$$X_{k=} \sum_{i=1}^{k} (r_i - k(n+1) \qquad k=1, 2, 3 \ldots n \quad 3.9$$

If a break occurs in year K, then the statistic is the maximal or minimal near the year k = Ki.

$$X_k = \max_{0<k<n} |X_k| \quad 3.10$$

3.5.7.4 Von Neumann ratio tests

The data are assumed to be independent and uniformly distributed random values in the Von Neumann ratio test (Neumann, 1941), a nonparametric test. Here's how to compute the von Neumann ratio (N):

$$N = \sum_{i=1}^{n-1} \frac{(y_i - y_{i+1})^2}{(y-\bar{y})^2} \quad 3.11$$

The value of N is typically less than the critical value if there is a break in the time series under investigation. The value of N may increase over 2 if the sample exhibits abrupt changes in the mean (Bingham and Nelson, 1981). The year of the break is only not detected by this test. Although the von Neumann ratio test is always very effective, it cannot determine when a change occurred.

Based on the number of tests that rejected the null hypothesis, Wijngaard et al, (2003) categorized the test results into three classes: "useful," "doubtful," and "suspect." If the four tests yielded one

or no rejection of the null hypothesis, the results were deemed useful; they were then homogenous and suitable for additional investigation. The series was deemed questionable and was examined prior to additional analysis if it rejects both of the four tests' null hypotheses. If three or more of the four null hypotheses are rejected by a data series, it is deemed questionable and is not further analysis.

3.5.8 Homogeneity tests result

Four tests (i.e., SNHT, Buishand range test, Pettitt test, and the von Neumann ratio test) were used to determine if the seasonal and yearly rainfall time-series at the five rainfall stations in and around the Afa Selga watershed were homogeneous. Every test's outcomes were assessed at the 95% significance level. If the p-values were less than the 5% significance level, the data series was considered to be non-homogeneous. The findings of the homogeneity tests for five stations based on annual rainfall, minimum and maximum temperature and wind speed are displayed in Table 3.6.

Based on the number of tests that rejected the null hypothesis, Wijngaard et al, (2003) categorized the test results into three classes: "useful," "doubtful," and "suspect." If the four tests yielded one or no rejection of the null hypothesis, the results were deemed useful; they were then homogenous and suitable for additional investigation. The series was deemed questionable and was examined prior to additional analysis if it rejected both of the four tests' null hypotheses. If three or more of the four null hypotheses are rejected by a data series, it is deemed questionable and is not subjected to additional analysis.

The annual precipitation result indicates that there are three inhomogeneous stations with p-value lower than the significance level of 0.05. According to the results of the Pettitt test, one (Assosa

station) out of five stations has homogenous records. The VNR test identified inhomogeneity at two (Abadi and Sherkole) stations. As presented in Table 3.2, the Amba 16 and Bambasi stations were homogeneous according to the four absolute homogeneity tests.

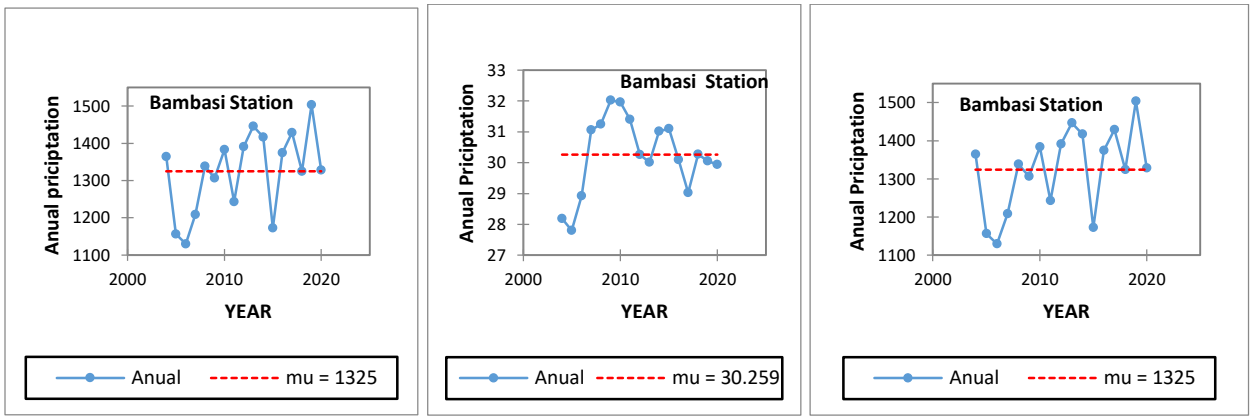

Figure 3.10: Testing of precipitation data homogeneity for Bambasi station by Pettitt, SNHT and by Buishand test respectively (mu is the average of observed data).

Table 3.2 the test result for the annual precipitation for the annual precipitation series. Note: red cell refers to non-homogenous stations at the 5% significant level

Stations	Pettitt's test		SNHT test		BR test		VNR test	
	K	p-value	To	p-value	R/√n	p-value	N	p-value
Assosa	52.000	0.027	5.900	0.850	5.080	0.050	1.694	0.263
Abadi	38.000	0.189	3.715	0.300	3.732	0.250	0.956	0.013
Amba 16	34.000	0.304	3.114	0.472	3.367	0.372	2.329	0.763
Bambasi	46.000	0.070	5.354	0.112	4.428	0.109	1.575	0.185
Sherkole	50.000	0.34	4.551	0.269	4.462	0.058	1.933	0.413

The annual maximum Temperature result indicates that there are two inhomogeneous stations with p-value lower than the significance level of 0.05. According to the results of the SNH test, (Assosa

station) out of four stations have in homogenous records. The VNR test identified in homogeneity at Sherkole stations. As presented in table 3.3, the Abadi, Amba 16 and Bambasi stations were homogeneous according to the four absolute homogeneity tests

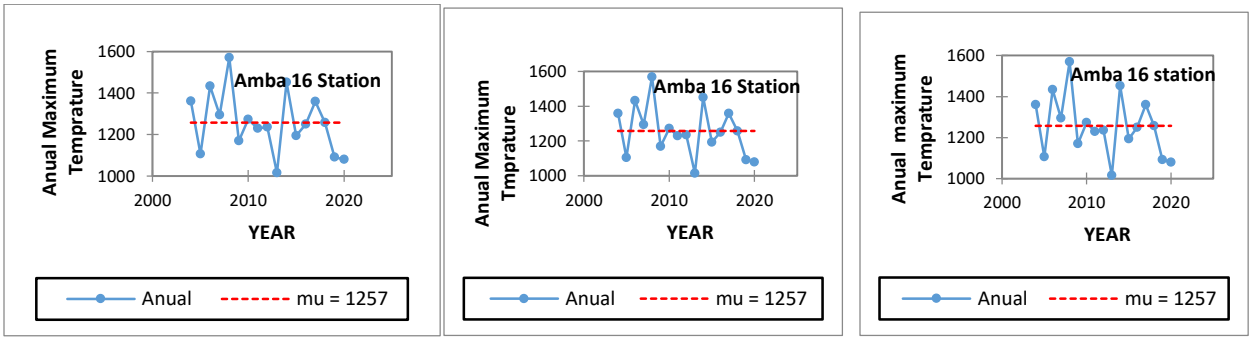

Figure 3.11: Testing of maximum temperature data homogeneity for Bambasi station by Pettitt, SNHT and by Buishand test respectively (mu is the average of observed data).

Table 3.3 The test result for the annual Maximum Temperature for the annual precipitation series. Note: red cell refers to non-homogenous stations at the 5% significant level

Stations	Pettitt's test		SNHT test		BR test		VNR test	
	K	p-value	To	p-value	R/√n	p-value	N	p-value
Assosa	30.000	0.428	13.139	0.007	4.964	0.057	38.000	0.192
Abadi	20.000	0.848	0.795	0.991	1.726	0.961	2.674	0.925
Bambasi	34.000	0.293	2.018	0.628	2.751	0.633	1.837	0.245
Sherkole	42.000	0.118	9.243	0.061	4.926	0.054	0.542	< 0.0001

The annual minimum Temperature result indicates that there are three inhomogeneous stations with p-value lower than the significance level of 0.05. According to the results of the Pettitt test, Assosa station out of four stations have in homogenous records. The VNR test identified in

homogeneity at Abadi and Bambasi stations. As presented in table 3.4, the Sherkole stations were homogeneous according to the four absolute homogeneity tests.

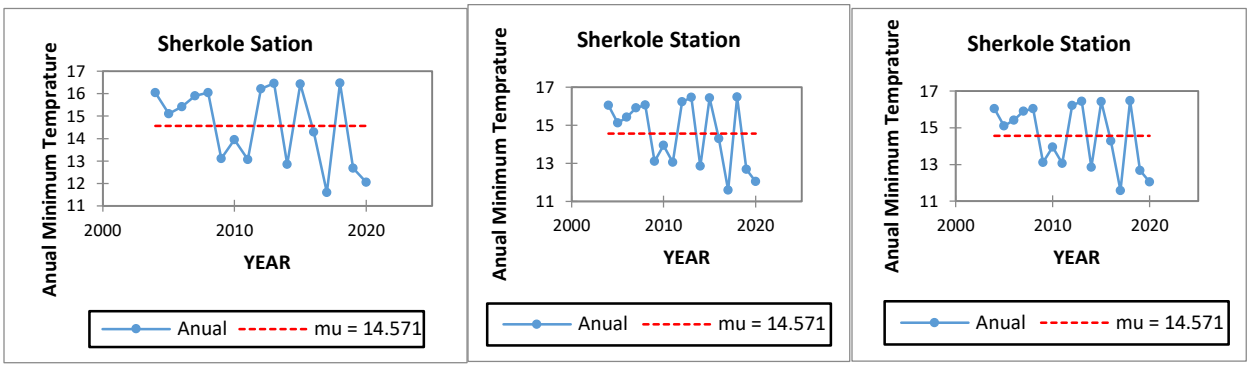

Figure 3.12: Testing of Minimum Temperature data homogeneity for Bambasi station by Pettitt, SNHT and by Buishand test respectively (mu is the average of observed data).

Table 3.4 The test result for the annual Minimum Temperature for the annual precipitation series. Note: red cell refers to non-homogenous stations at the 5% significant level

Stations	Pettitt's test		SNHT test		BR test		VNR test	
	K	p-value	To	p-value	R/√n	p-value	N	p-value
Assosa	50.000	0.042	7.519	0.014	4.853	0.05	1.293	0.052
Abadi	44.000	0.093	4.714	0.181	3.914	0.211	0.717	0.002
Bambasi	38.000	0.195	4.717	0.270	4.206	0.134	1.022	0.009
Sherkole	28.000	0.522	3.731	0.302	3.460	0.343	2.072	0.550

The annual wind speed result indicates four inhomogeneous stations with a p-value lower than the significance level of 0.05. The VNR test identified inhomogeneity at all stations (Abadi, and Assosa, Amba16 and Bambasi stations).

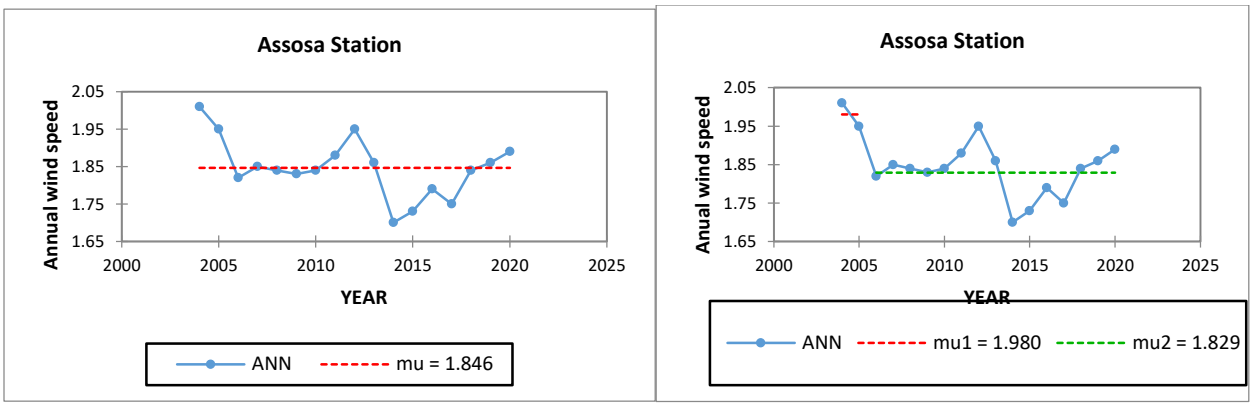

Figure 3.13: Testing of Minimum Temperature data homogeneity for Assosa station by Pettitt, and SNHT test respectively (mu is the average of observed data).

Table 3.5 The test result for the wind speed for the yearly precipitation series. Note: red cell refers to non-homogenous stations at the 5% significant level

Stations	Pettitt's test		SNHT test		BR test		VNR test	
	K	p-value	To	p-value	R/√n	p-value	N	p-value
Assosa	39.000	0.193	6.454	0.052	4.758	0.066	0.773	0.002
Abadi	20.000	0.848	0.795	0.991	1.726	0.961	2.678	0.001
Amba 16	39.000	0.188	6.454	0.051	4.758	0.063	0.573	0.001
Bambasi	38.000	0.165	4.768	0.290	4.232	0.144	1.025	0.009

(Table 3.6) presents the breaking points at inhomogeneous stations and their corresponding classification. The breakpoint years for the annual rainfall, minimum and maximum temperature series at Assosa stations were found in 2013 and 2018. In Assosa station the break year was found in 2013 for precipitation and minimum temperature by Pettitt test, 2018 maximum temperature by SNHT test. Whereas, the von Neumann ratio test did not give information about the break year.

Whereas, the von Neumann ratio test did not give information about the break year. The overall results show that all are 'useful' station series

Table 3.6 The Broken Year non-homogeneous stations and their classification

Stations	Break year																classification
	Pettitt's test				SNH test				BR test				VNR test				
	ppt	Tmax	Tmin	wind	ppt	Tmax	Tmin	wind	ppt	Tmax	Tmin	wind	ppt	Tmax	Tmin	wind	
Assosa	2013		2013	-	-	2018	-	-	-	-	-	-	-	x	-	-	useful
Abadi	-	-	-	-	-	-	-	-	-	-	-	-	x	-	x	-	useful
Amba 16	-	-	-	-	-	-	-	-	-	-	-	-	-	-	-	-	useful
Bambasi	-	-	-	-	-	-	-	-	-	-	-	-	-	-	x	-	useful
Sherkole	-	-	-	-	-	-	-	-	-	-	-	-	x	x	-	-	useful

3.5.9 Model Performance Evaluation

Certain quantitative data are needed to measure model performance. The performance of the model was evaluated in this study using stream flow data collected at the watershed. In this study, the effectiveness of the simulation and the applicability of the WetSpass model were assessed using two statistical criteria, including the Nash-Sutcliffe efficiency (NSE) and such as the goodness of fit coefficient of determination (R^2)

The NSE values can be in the range of - ∞ to 1.0. The model performance can be considered acceptable when the NSE value is between 0.0 and 1.0, whereas the model performance is considered poor when the NSE value is less than 0.0. (Nash and Sutcliffe, 1970; Moriasi et al., 2007). Moreover, NSE values above 0.75 are considered to demonstrate good model efficacy, NSE

between 0.36 and 0.75 indicates satisfactory performance, while values below 0.36 are thought to demonstrate inadequate performance (Moriasi et al., 2007; Van Liew et al., 2007).

$$NSE = 1 - \frac{\sum_{i=1}^{n}(Q_{obs,i} - \overline{Q_{sim}})^2}{\sum_{i=1}^{n}(Q_{obs,i} - \overline{Q_{obs}})^2} \quad (3.12)$$

The percentage of the overall variance in the observed data that the model can explain is indicated by the coefficient of determination (R^2). The degree of agreement between the simulated and observed data increases as R^2 approaches 1. The squared ratio between the covariance and the multiplied standard deviations of the observed and simulated values is known as R^2 (Krausem et al., 2005). And the following equation was considered:

$$R^2 = \left[\frac{\sum_{i=1}^{n}(Q_{obs,i} - \overline{Q_{obs}}) \times (Q_{sim,i} - \overline{Q_{sim}})}{\sqrt{\sum_{i=1}^{n}(Q_{obs,i} - \overline{Q_{obs}})^2 \times (Q_{sim,i} - \overline{Q_{sim}})^2}} \right]^2 \quad (3.13)$$

Where $Q_{obs,\,i}$ is the observed surface runoff value, $Q_{sim,\,i}$ is the simulated surface runoff value $\overline{Q_{obs}}$ is the mean observed surface runoff value $\overline{Q_{sim}}$ is the mean simulated surface runoff value, n is the total number of observation, $Q_{obs,\,i}$ and $Q_{sim,\,i}$ are annual or monthly observed and simulated The base flow separation was performed using the automated Web-Based Hydrograph Analysis Application (WHAT), which has three separate filters: the Eckhardt recursive digital filter method (RDF) (Eckhardt, 2005), the one-parameter digital filter method (OPM) (Lyne and Hollick, 1979; Nathan and McMahon, 1990; Arnold et al., 2000), and the local-minimum method (LMM). (Lim et al., 2005), where the Eckhardt recursive digital filter approach was used in this work. Equation (3.14)

$$b_t = \frac{1 - BFI_{Max} x \alpha b t - 1 + 1 - \alpha x BFI_{Max} x Q_t}{1 - \alpha x BFI_{Max}} \quad (3.14)$$

Where Q_t is the total stream flow at time step t (m^3 /s), *bt* is the base flow at step t-1 (m^3/s), BFI_{max} shows the greatest long-term ratio of base flow/total stream flow, x total stream flow at time step and α is the filter parameter. For ephemeral streams with porous aquifers, Eckhardt, (2005) recommended BFI_{max} values of 0.50, 0.25 for perennial streams with hard rock aquifers, and 0.80 for perennial streams with porous aquifers. In this instance, the suggested values of 0.80 for BFI_{max} and 0.98 for the filter parameter which correspond to the hydrogeological features of the watershed were applied.

3.6 Model input data organization

First, the spatial data required for the recharge modeling was gathered and prepared. Topographic, meteorological, soil, and land use data are all included in the data that were collected. Digital data is manipulated, processed, and analyzed using remote sensing and GIS applications. These data are adjusted and produced raster grid cell ready. Following that, the WetSpass model includes the raster data to generate maps of the study area's annual and seasonal recharge. Finally, the findings are related to the physical characteristics and elements of the water balance that are important for groundwater recharge.

Since Batelaan and De Smedt, (2001, 2007) developed WetSpass modeling for temperate regions, which have different climatic and topographic conditions than the tropics, some input parameter modification was required to apply it in the tropical region. In temperate climates, summer and winter last six months each. However, According to the Ethiopian Meteorology Institute in Ethiopia Benishan-gul Gumuz region is classified as a mono-modal region, summer (the rainy season) ranges five months (MJJAS), while winter (the dry season) consists of Seven months.

Thus, WetSpass was applied to the Afa-Selga watershed using four months of summer and seven months of winter as the input data for the meteorological grid map. Annual and seasonal maps of the topography, slope, land use, soil, potential evapotranspiration, and groundwater level (depth to groundwater) were prepared. Due to a lack of monthly data for groundwater depth, the same map input was used for both seasons.

Meteorological variables are often measured at meteorological stations, and the data is only accurate for the location where it was measured. These variables are needed for applications in hydrology and water resource management. Meteorological variables at different stations can be estimated by spatial interpolation. (Belete, 2018)

Raster interpolation methods include Inverse Distance Weighting (IDW), Spline, and Kriging. The meteorological data input for the model was prepared using the Inverse Distance Weighting IDW approach. It is the most widely utilized strategy because it is simple and produces good results (Lu and Wong, 2008). Therefore, using ArcGIS10.4 the data were interpolated by the Inverse Distance Weighting (IDW) method. The main steps of the method are shown in the Methodological flow chart below.

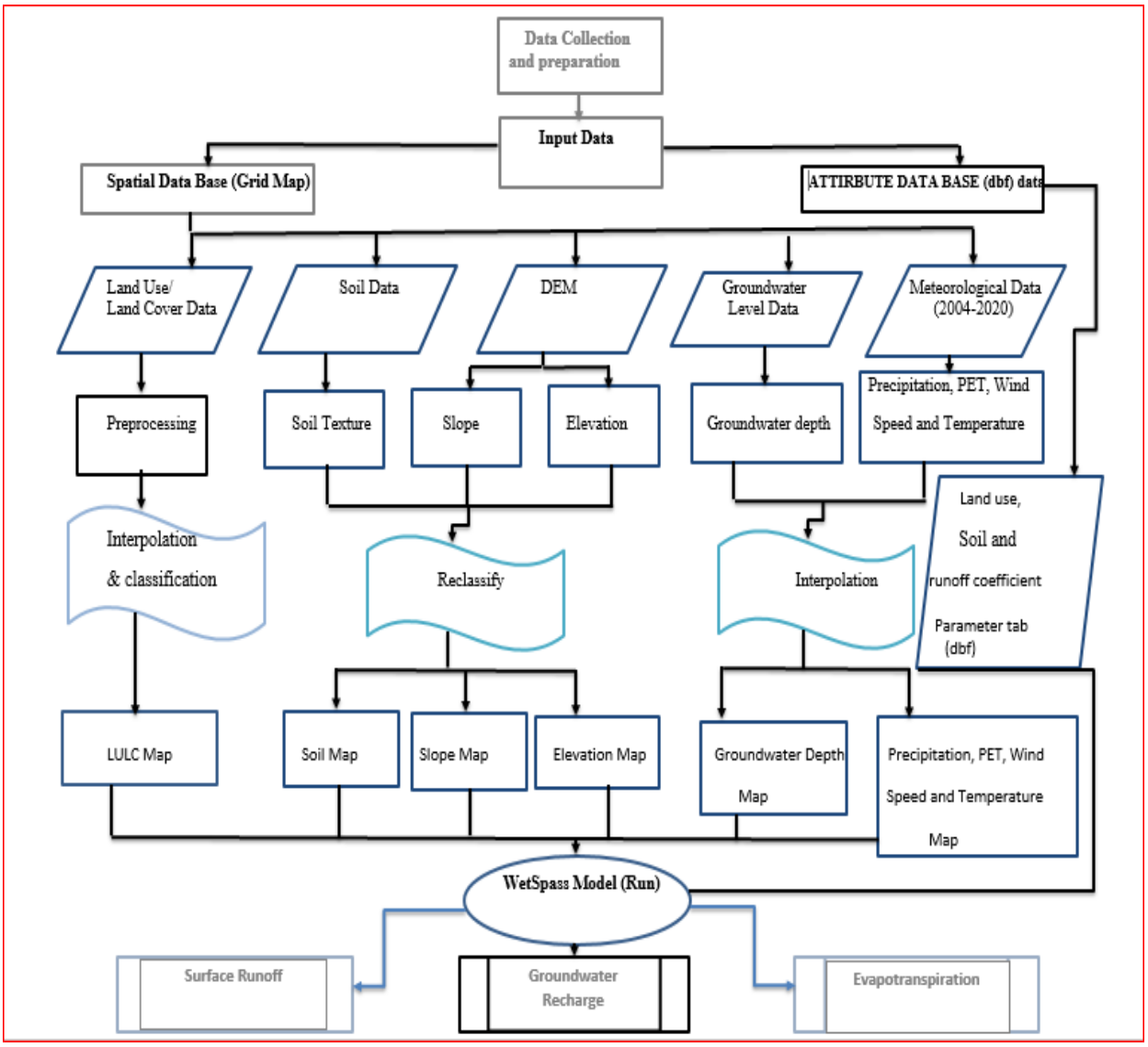

Figure 3.14: Methodological flow chart

3.6.1 Data analysis tool

ArcGIS 10.4, and the WetSpass model were used in this study software combination. ArcGIS10.4 is undoubtedly utilized for map preparation, data format conversion, and interpolation of various data that were gathered in point data format to produce the raster maps. For the preparation of conceptual models, additional software like Surfer 11 for 3D DEM preparation was used. The environment necessary for MS Word and MS Excel is provided by the Microsoft Office Package (2016). XLSTAT (2016) for filling in missed data and data homogeneity test and R-software SPI-package for estimating potential evapotranspiration.

Table 3.7: Materials and software used in this research

No	Software and Material	Functions/ used for
1	GPS	Borehole point collection
2	ArcGIS software 10.4	To create raster maps, different data that are collected in point data format are interpolated, various data formats are converted, and map preparation.
3	R-software software SPI-package	Estimation of potential evapotranspiration
4	Arc View 3.3 and WetSpass Extensions	WetSpass model Running
5	Google Earth	Identifying features and collecting ground truth
6	Surfer 11	3D DEM preparation
7	Microsoft Office Package (2016)	The 2016 version of Microsoft Office Package offers the environment needed for MS Excel,
8	XLSTAT(2016)	Filling missing data and data homogeneity test

3.7 Groundwater recharge calculation using WetSpass Model

The water balance calculation is done at the raster cell level in the distributed WetSpass model. A raster cell's impervious fraction, vegetated fraction, bare soil fraction, and open water fraction

independent water balances are added together to create the individual raster water balance. The total amount of water.

Thus, the water balance of each raster cell is added to determine the balance of a specific area. The water balance for vegetated surfaces, which is dependent on the average seasonal precipitation (P), groundwater recharge, real transpiration (T_v), surface runoff (S_v), and interception fraction (I) and (R_v) is calculated using:

$$P = I + S_V + T_V + R_V \quad (3.15)$$

Where, P is the average seasonal precipitation, I is the vegetation's interception [LT^{-1}], S_v is the runoff over the land surface beneath vegetation [LT^{-1}], T_v is the actual transpiration [LT^{-1}], and R_v is groundwater recharge [LT^{-1}]. Actual evapotranspiration (ET_v) is the term used to describe the total amount of transpiration (T_v) and evaporation from bare soil between vegetation in this context. The actual evapotranspiration, ET_v, is equal to the sum of the evaporation of water intercepted by vegetation, I, and ET_{tot}.

$$ET_{tot} = I + T_V + ES \quad (3.16)$$

Where ES is the evaporation from the bare soil between the plants, ET_{tot} is the total actual evapotranspiration, "I" is the evaporation of water intercepted by vegetation, T_V transpiration of vegetation cover.

The total water balance of a specified area was calculated because of the summation of the water balances of every raster cell (Batelaan and De Smedt, 2007). Every land-cover class was characterized by four sorts such as bare soil, impervious surface, vegetation and open water. This information was stored within the land-use parameter tables. The components of the water balance within the study area going to be estimated using the water balance equations

$$ET_a = avETv + asEs + aoEo + aiEi \quad (3.17)$$

$$S_a = avSv + asSs + aoSo + aiSi \quad (3.18)$$

$$R_a = avRv + asRs + aoRo + aiRi \quad (3.19)$$

Where $\mathbf{ET_a}$, $\mathbf{S_a}$ and $\mathbf{R_a}$ are the total evapotranspiration, surface runoff, and groundwater recharge of a raster cell respectively, each having a vegetated, bare-soil, open water and impervious area component denoted by av, as, ao , and ai, respectively. Precipitation is taken as the starting point for the computation of the water balance of each of the above-mentioned components of a raster cell.

Surface runoff was calculated as precipitation amount, precipitation intensity, interception, and soil infiltration capacity. In considering water losses through evaporation and transpiration, the calculation of seasonal evapotranspiration and a reference value of transpiration are obtained from open-water evaporation and a vegetation coefficient. Recharge is the major and last component to be simulated in the WetSpass model. The groundwater recharge will be calculated as a residual term of the water balance, i.e.

$$Rv = P - Sv - ETv - Es - I \quad (3.20)$$

Here the actual evapotranspiration is given as the sum of transpiration and **Tv** and $\boldsymbol{Es}$ (the evaporation from bare soil found in between the vegetation). The spatially distributed recharge is therefore estimated from the vegetation type, soil type, slope, groundwater depth, and climatic variables of precipitation, potential evapotranspiration, temperature, and wind speed. After all the input data and lookup tables are prepared, the information will be uploaded to the relevant WetSpass model after which the model runs.

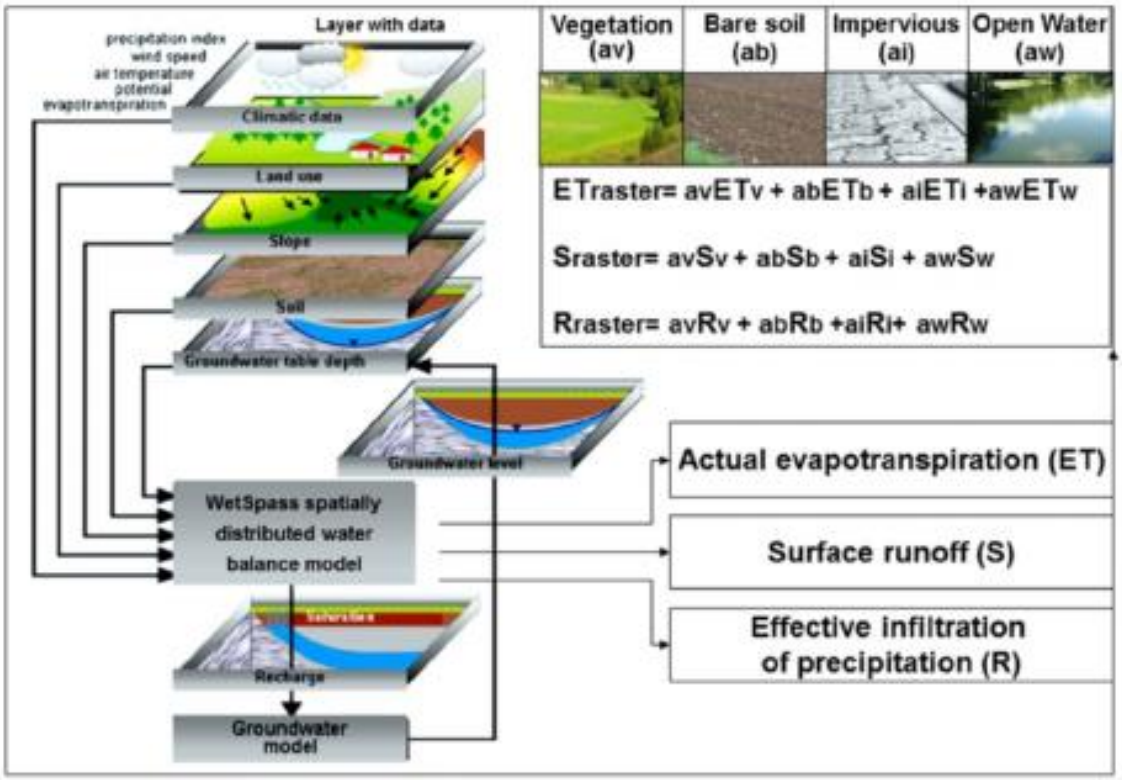

Figure 3.15: WetSpass model conceptual diagram (Batelaan and Smedt 2001)

4. RESULTS AND DISCUSSION

4.1 WetSpass model input data

To run the model correctly, input grid maps must have a similar number of columns and rows with the same cell size. This means that the number of columns, rows, (1258 and 926) respectively and cell sizes (30) across all of the input physical and meteorological grid maps are similar. Grid maps that are prepared on a seasonal basis (winter and summer) and without a seasonal basis are used in the WetSpass model.

As a result, these data were prepared individually for the winter, summer, and yearly seasons to show the watershed's current features as well as future seasonal changes. The inverse Distance Weighting (IDW) method was used to create a grid map from seasonal precipitation, potential evapotranspiration, average temperature and wind speed for the separate seasons of winter and summer. The grid map was produced using the Inverse Distance Weighting (IDW) interpolation method.

4.1.1 Rainfall (Precipitation)

The most climatic factor that affects both the spatial and temporal patterns of water availability is rainfall. The computation of each raster cell water balance starts with the amount of precipitation, and the other processes interception, runoff, evapotranspiration, and recharge follow in a systematic order. Five stations have rainfall records available from 2004 to 2020.

In the watershed, the hydrological year is divided into two seasons: a rainy season (summer), which lasts from May to September, and a dry season (winter), which covers the other months of the year. The average annual rainfall is about 1246.59 with 1201.34 mm and 1287.34 mm as the minimum and maximum annual rainfall respectively, and the average rainfall of summer is 1020.5mm,

whereas the winter is 225.9mm. Table 4.8 displays several instances of how the monthly rainfall varies among various areas within and near the watershed.

Table 4.8: long term mean monthly precipitation in each station

Stations	Jan	Feb	Mar	Apr	May	Jun	Jul	Aug	Sep	Nov	Oct	Dec
Abadi	0.2	1.9	2.4	19.8	75.7	136.0	180.7	187.2	171.8	121.2	11.4	0.0
Sherkole	1.5	0.4	11.7	60.5	130.4	176.1	291.5	394.8	234.3	127.5	8.9	0.2
Assosa	0.8	1.7	9.2	29.7	145.4	189.0	201.0	246.4	194.0	153.3	18.5	12.4
Amba16	1.3	1.8	4.2	60.5	156.5	223.9	226.6	216.6	209.7	145.7	8.0	2.4
Bambase	0.9	0.2	15.7	48.7	183.6	210.1	234.4	243.3	199.5	154.5	28.3	5.3

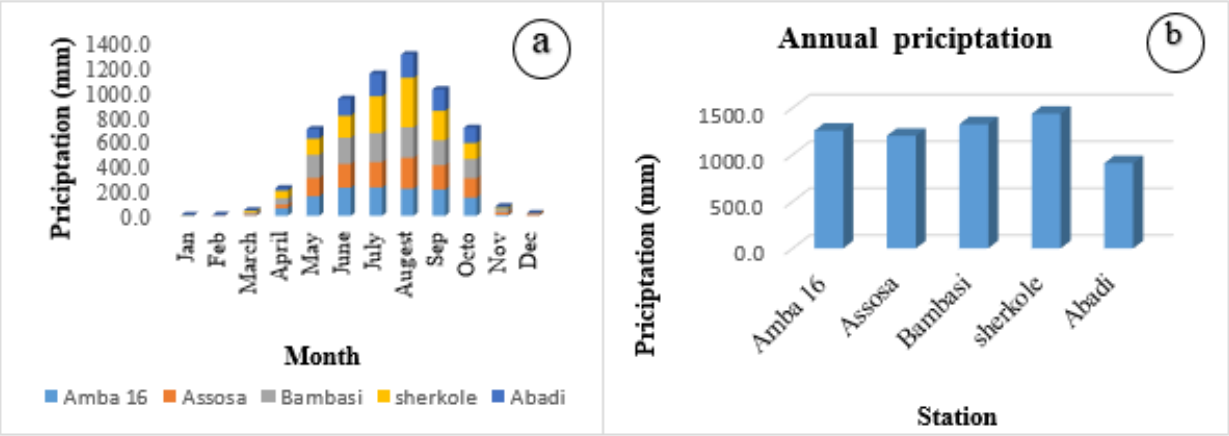

Figure 4.16: (a) Mean monthly precipitation over the long period at each station (b) Annual precipitation for each station

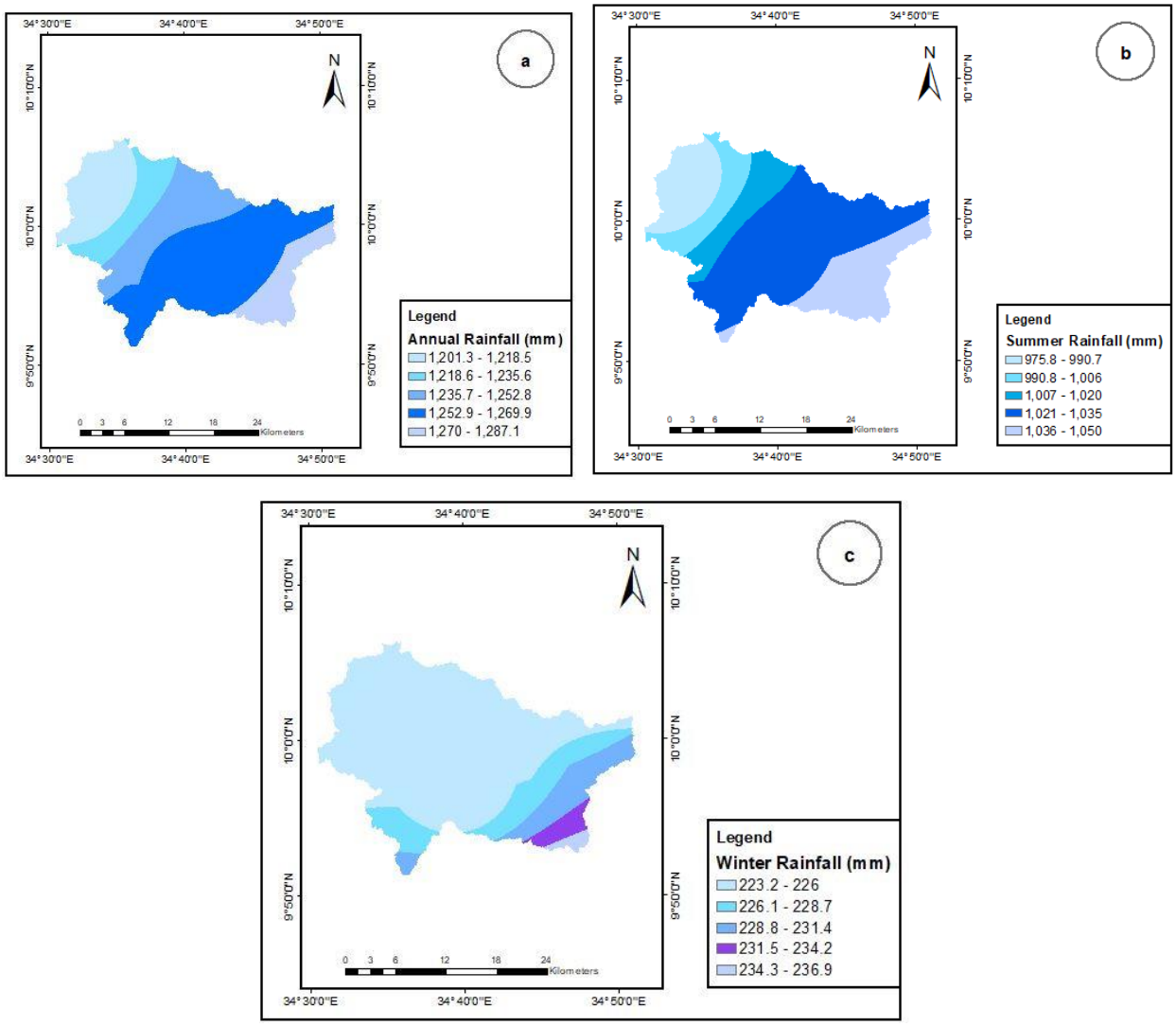

Figure 4.17: Precipitation map of Afa-Selga watershed, (a) annual Precipitation, (b) summer season Precipitation, (c) winter season Precipitation

4.1.2 Temperature

Temperature data are available for all the four weather stations. The winter (dry) season average temperature ranges between 23.20^{o}C and 22.60^{o}C and the mean is 22.88^{o}C, it is between 20.86^{o}C and 20.50^{o}C for the summer (rainy) season the mean is 20.67^{o}C and the annual average temperature ranges between 22.33^{o}C and 21.70^{o}C of the watershed (*Figure 4.18*).

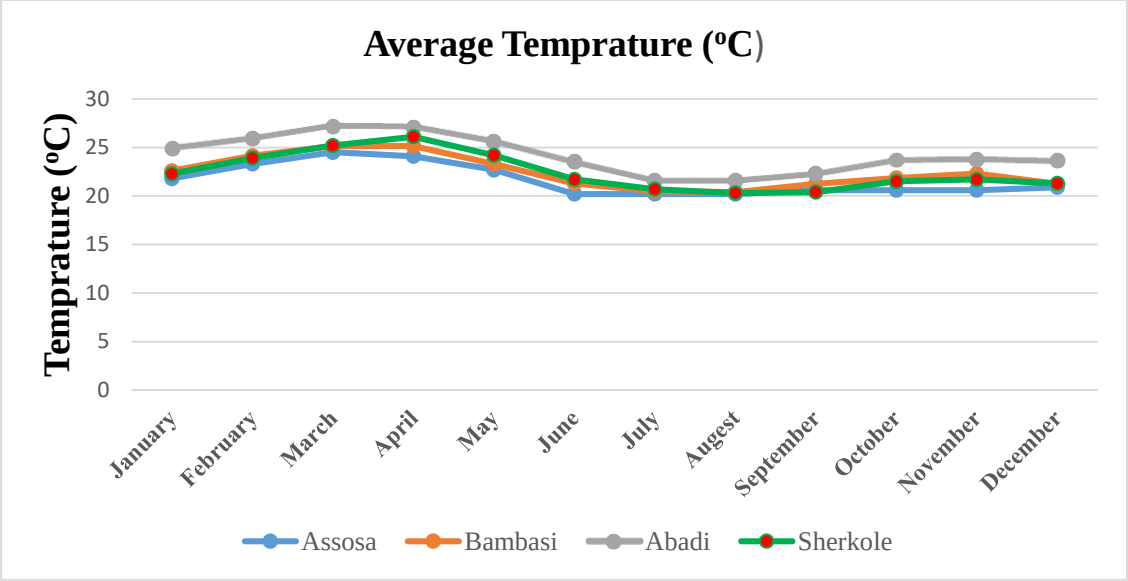

Figure 4.18: Monthly average temperature in different stations (Assosa, Bambansi, and Abadi. Sherkole)

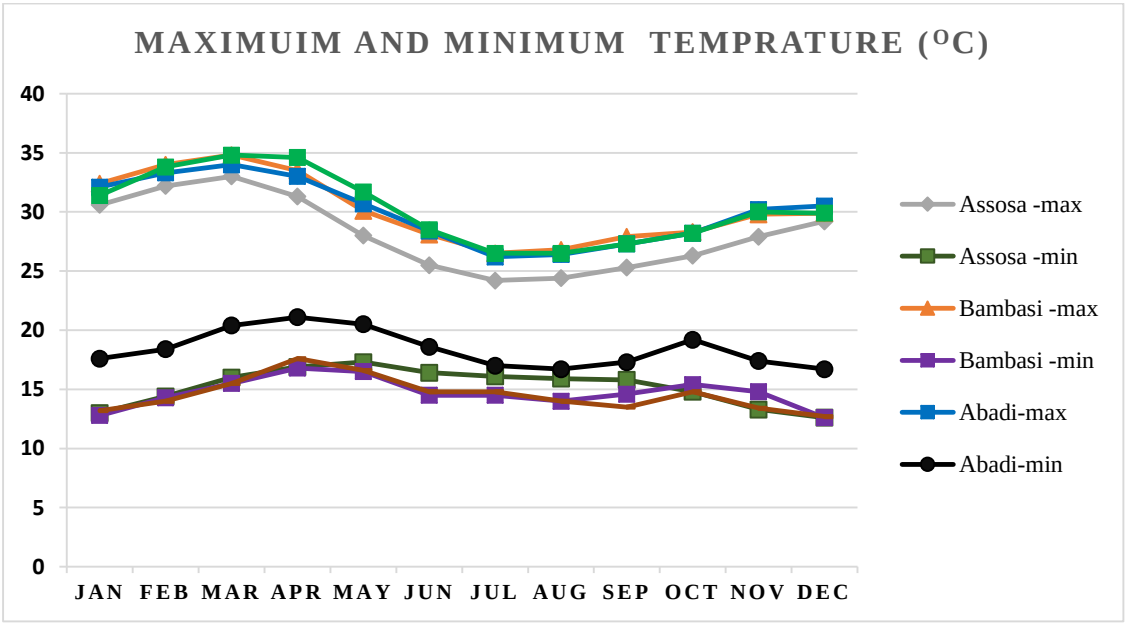

Figure 4.19: Variation in monthly maximum and minimum temperature variation at different stations (Assosa, Bambasi, and Abadi and Sherkole)

The average monthly temperatures are perceived as smaller during July, August, and September. Meanwhile, higher mean monthly temperatures were recorded from March to April. The table below shows the monthly minimum and maximum average temperatures at different stations in and around the watershed.

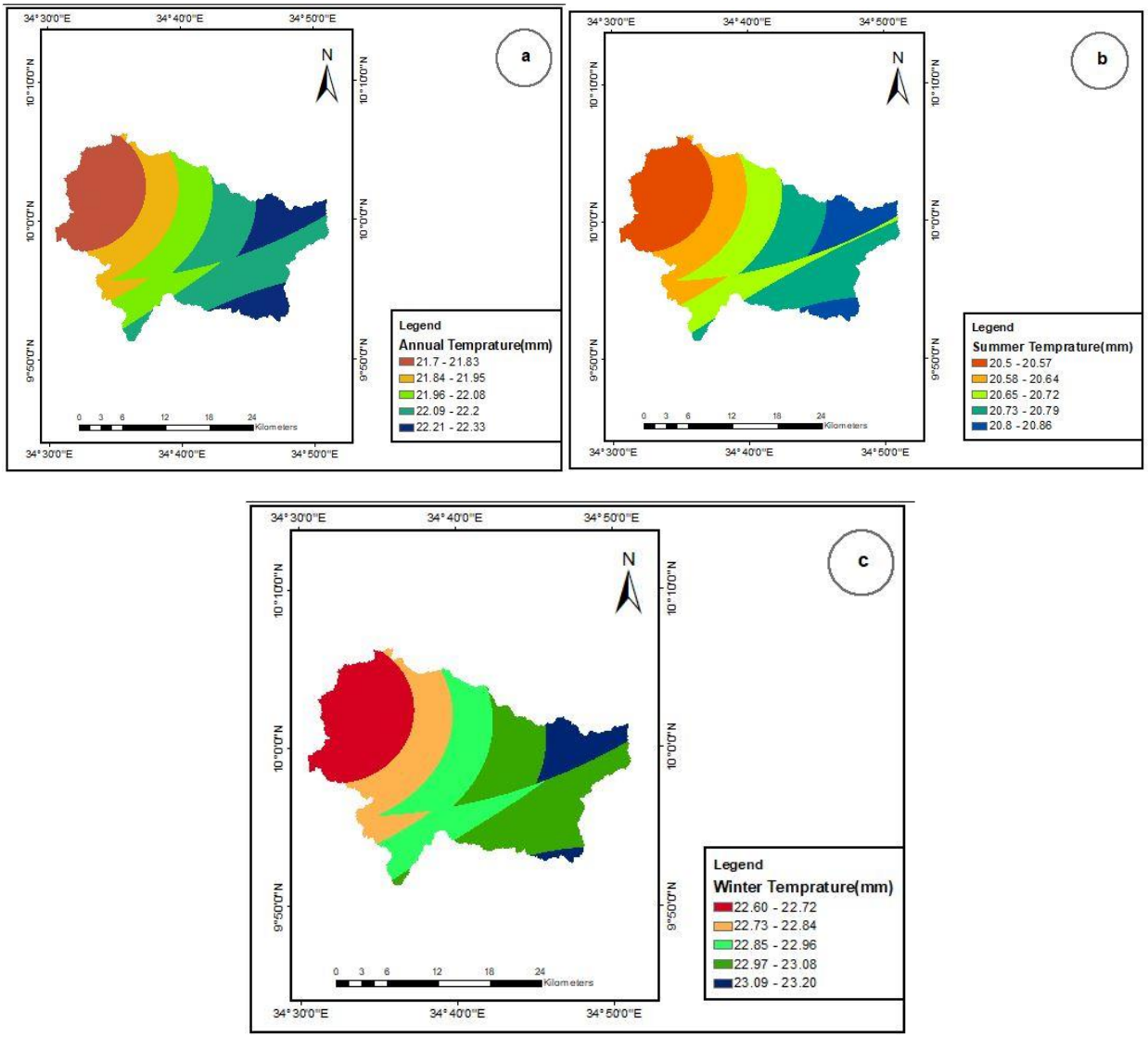

Figure 4.20: Temperature map of Afa-Selga watershed, (a) Annual Temperature, (b) Summer Season Temperature, (c) winter season Temperature.

4.1.3 Potential evapotranspiration

The measured PET in the watershed is needed as an input for the WetSpass model. Similar to (Rainfall) precipitation PET is defined as the amount of water vapor that a plant or soil surface could emit per unit area and unit time under present conditions without a water supply limit. Evapotranspiration is a crucial factor in the water budget because it removes water from the system and regulates the components of a basin's stream flow, soil moisture content, and groundwater recharge (Dereje, 2015).

Due to a lack of data(like humidity, solar radation and sunshine hours data) the PET of the Afa-Selga watershed was estimated using the Hargreaves equation (Hargreaves and Samani, 1982), The FAO suggests the Hargreaves method (Allen et al., 1998) as a backup method for estimating PET if there are insufficient meteorological data for the Penman-Monteith approach.

$$PET = 0.0135 * Rs * conv * (T + 17.8) \quad (4.1)$$

Where: -

PET	Evapotranspiration	[mm day^{-1}]
T	Mean temperature of the day	[°C]
Rs	Solar radiation	[MJ m^{-2} day^{-1}]
Conv	Conversion to ET equivalent conv=4082 .0	[m^2 mm MJ^{-1}]

For four stations (Assosa, Bambasi, Sherkole, and Abadi) from the years 2004 to 2020, the average monthly PET was determined using monthly average temperature data. The average potential evapotranspiration of summer is 290.39 mm (*Figure 4.21 b)*, where the winter is 790.43 mm *(Figure 4.21 c)*, and the average annual potential evapotranspiration is 1080.82 mm with 1090.7 mm and 1150.41 mm as the minimum and maximum annual PET respectively. *(Figure 4.21 a),*

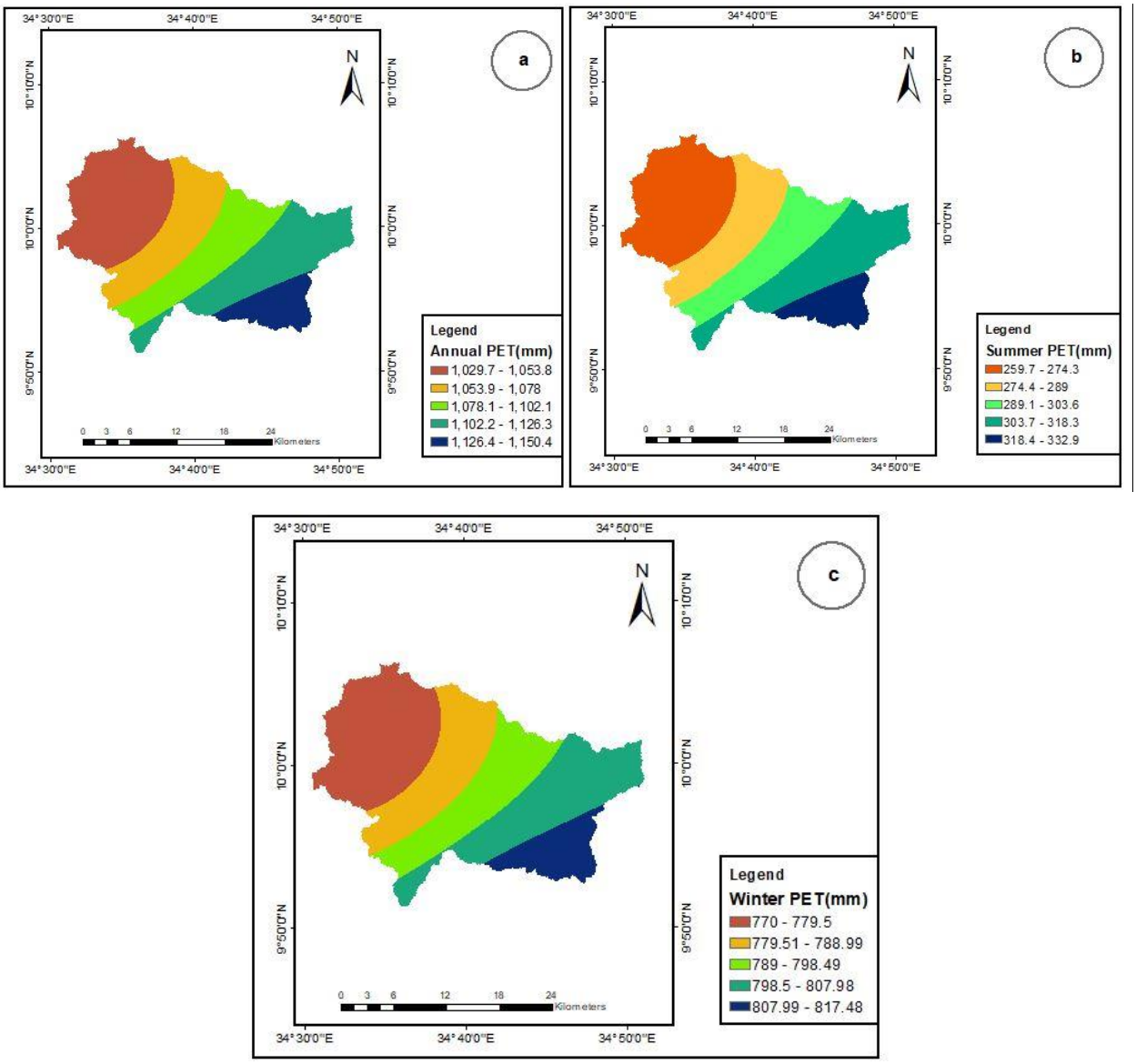

Figure 4.21: (a) PET (Potential evapotranspiration) of Afa-Selga watershed. Annual PET, (b) winter (Dry) season PET, (c) Summer (Rainy) season PET

4.1.4 Wind speed

Wind speed is the primary factor in the removal of water vapor, it has a significant impact on the local rate of evaporation and evapotranspiration. Even though, the rate of evaporation is significantly influenced by wind speed. Five meteorological stations and speed data for the years 2004–2020 were downloaded from power access climate data. These data were uniform

throughout the watershed: the average annual wind speed is 1.84 m/s *(Figure 4.22 a)*, the average summer wind speed is 1.67 m/s *(Figure 4.22 b)*, and the average winter wind speed is almost 1.95 m/s *(Figure 4.22 c)*.

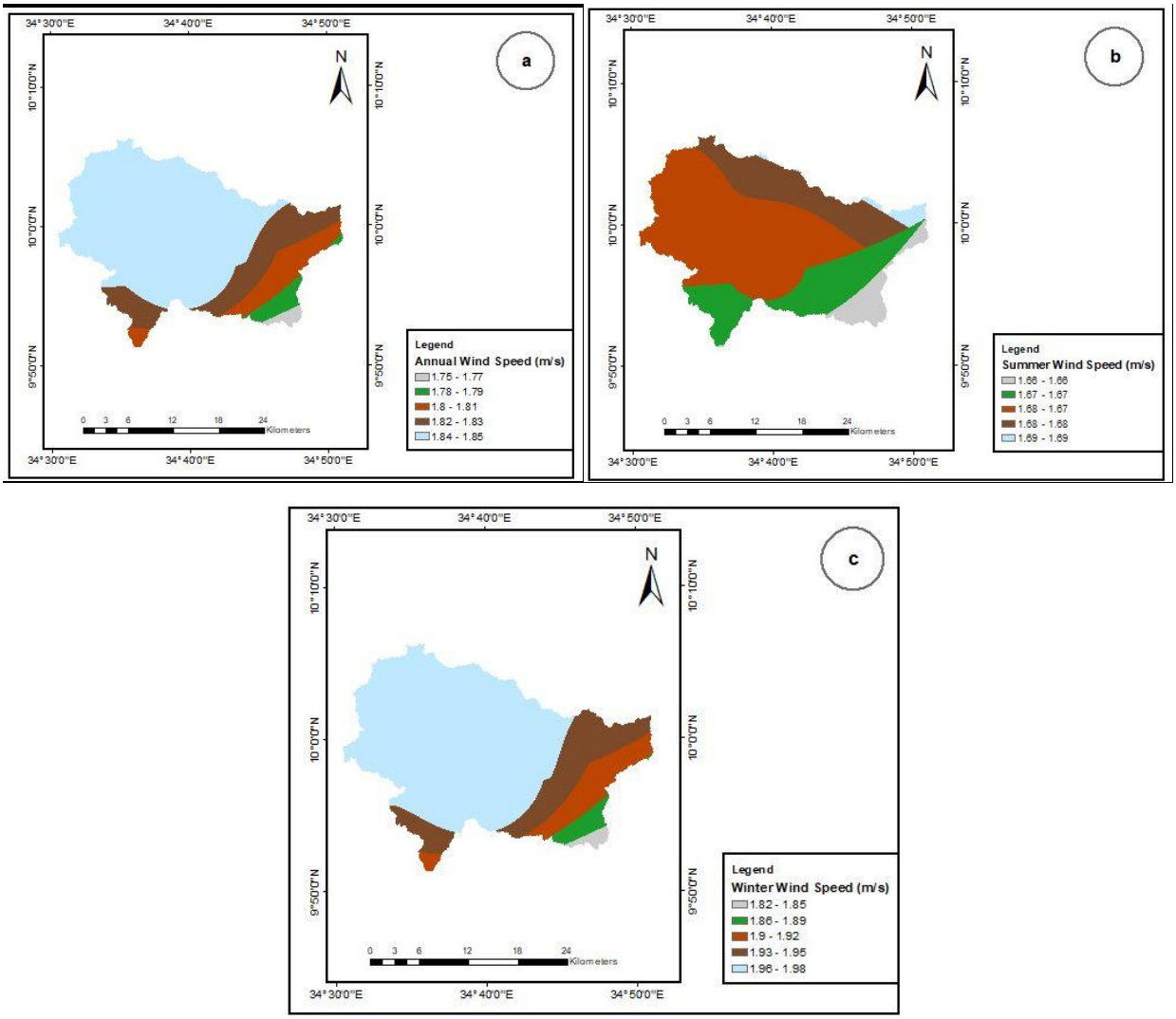

Figure 4.22: Wind speed map of the Afa-Selga watershed. (a) Annual wind speed, (b) rainy (summer) season wind speed, (c) dry (winter) season wind speed

4.1.5 Digital Elevation Model (DEM) and Slope

The DEM was used to extract the elevation, flow direction, flow accumulation, stream network, and stream order of the terrain for each grid cell by Processing DEM. DEM was used to obtain

the topography (elevation) map for the watershed from The Alaska Satellite Facility (ASF) web page(http://asf.alaska.edu).

The watershed mean elevation is 1440.8 m, while the lowest (minimum) elevation point is 1004 m in the downstream section and the highest is 2062 m in the upper stream area *(Figure 4.23 a)*. Using the "slope" module in ArcGIS 10.4, the watershed slope map is generated using the DEM. The slope has a mean value of 5.01^0 and runs from 0^0 to 60^0. (*Figure 4.23 b*)

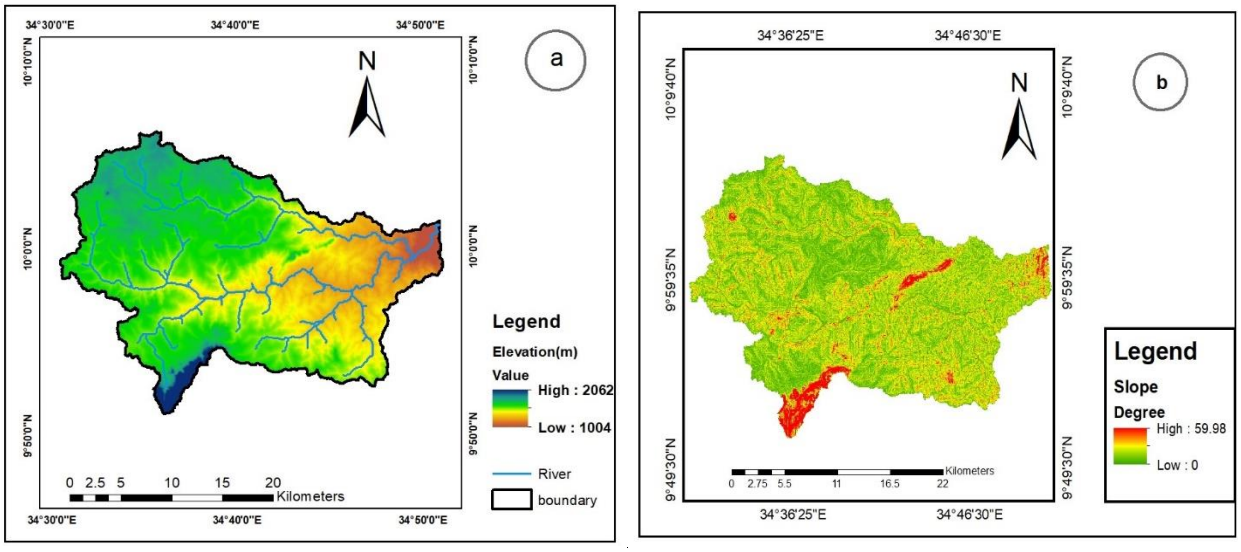

Figure 4.23: (a) DEM (b) Slope map of Afa-Selga watershed

4.1.6 Soil

The soil texture map of the Afa-Selga watershed was downloaded from (https://www.isdaafrica.com/isdasoil/) website, the outcomes indicated that clay, sandy clay, clay loam and sandy clay loam. Clay loam represents the majority of the soil in the watershed which covers 57.88 % of the total area of the area, clay (0.35%), sandy clay (2.52%) and sandy clay loam (39.25%). (*Table 4.9)*

Table 4.9**:** Soil texture type and area coverage.

Soil type	Area (km^2)	Area (%)
Clay	2.04	0.35
Clay loam	335.38	57.88
Sandy Clay	14.63	2.52
Sandy Clay Loam	227.43	39.25
Total	579.5	100

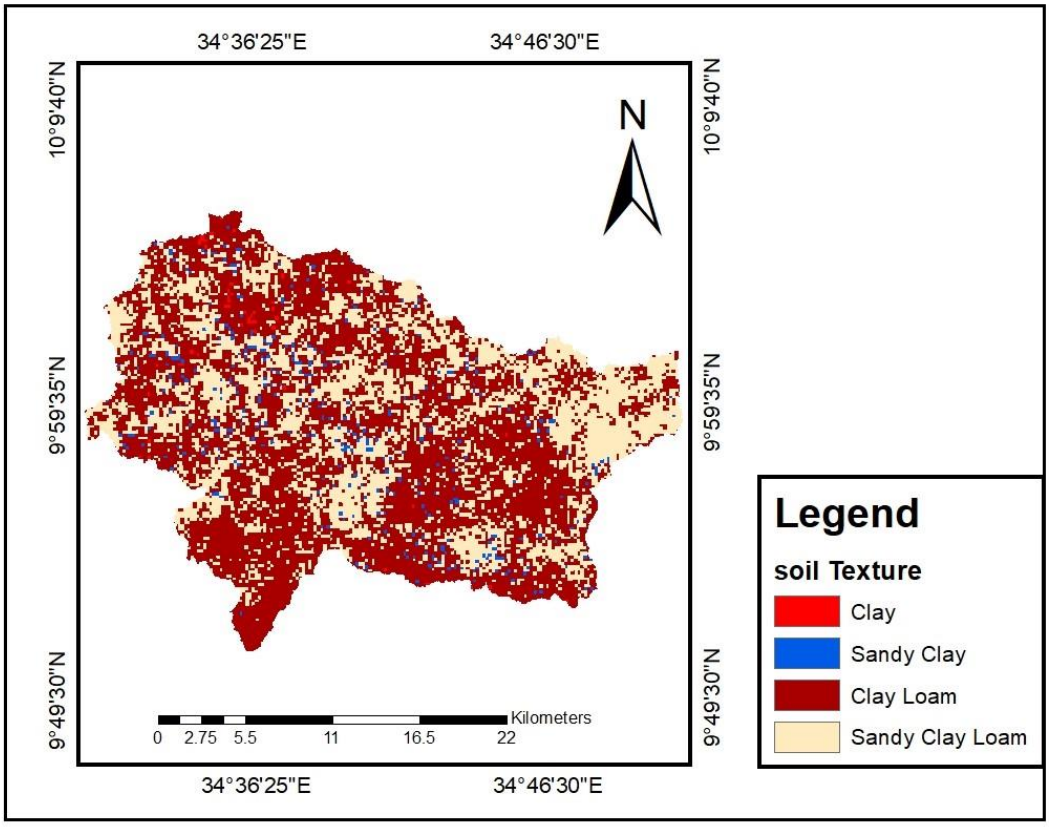

Figure 4.24: Soil texture map of Afa- Selga watershed

4.1.7 Land-use/ Land-cover (LULC)

An essential boundary condition that affects many hydrological processes either directly or indirectly is land use and land cover. The evapotranspiration process is where land use has the most direct impact on the water balance of a catchment. Due to differences in vegetation cover, leaf area indices, and root depth, different land use types have varied evapotranspiration rates (Batelaan and De Smedt, 2001).

Eight land-use/land cover groups, including agricultural land, bare land, woodland, grassland, shrub & and brush land, forests, settlements, and water bodies, were found on the watershed land-use map. Agricultural land, shrub and brush land, woodland, settlement, and grassland comprise the majority of the area's land use and land cover. The dominant land use of the watershed is agricultural land, which consists of 39.43% of the study's total area.

The watershed land-use/land cover map *(Table 4.10 and Figure 4.25)* reveals that agricultural land makes up 52.54% of the watershed, while bare land and shrubs make up about 8.38%, forest and woodland constitute 25.37%, settlements constitute 1.54%, and grassland makes up 12.17%. The remaining 0.01% of the watershed is covered by wetlands.

Table 4.10**:** Land-use/Land cover type and area coverage.

Land use type	Area (km^2)	Area (%)
Agriculture	304.44	52.54
Bare land	0.03	0.01
woodland	110.38	19.05
Forest	36.64	6.32

Grassland	70.54	12.17
Settlement	8.92	1.54
Shrub & brush land	48.50	8.37
Wetland	0.04	0.01
Total	579.5	100

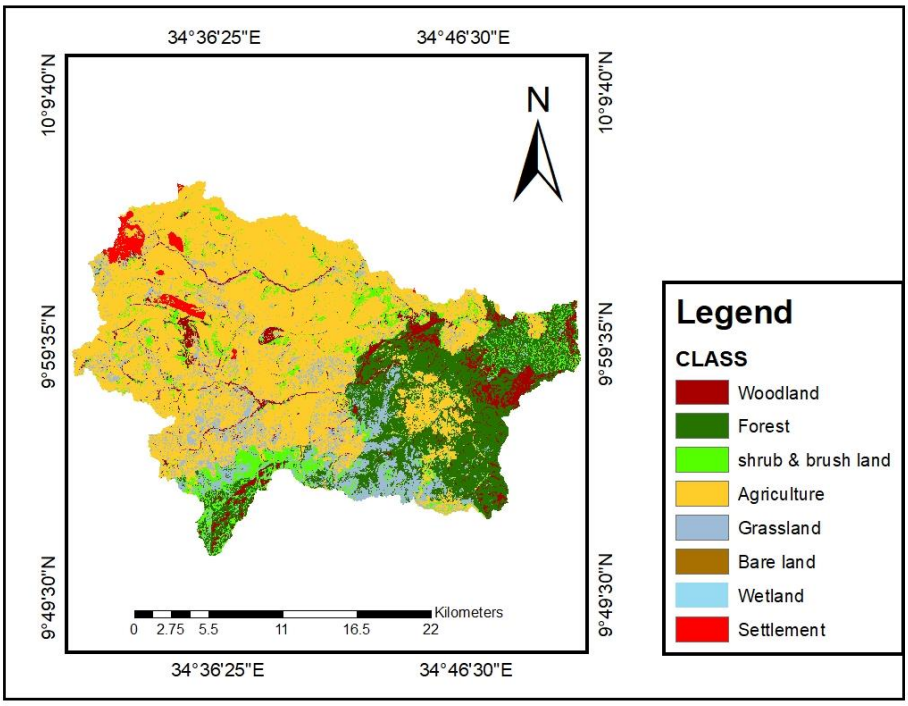

Figure 4.25: Land-use/land cover map of Afa Selga watershed

4.1.8 Groundwater Level

The groundwater level grid map is crucial when using the WetSpass model to calculate groundwater recharge. From the Assosa town Water Supply and Sewerage Enterprise and the B/G/R/S Water Works and Construction Enterprise, 15 borehole data were gathered and depth to ground water was measured using the deep meter. The Inverse Distance Weighing (IDW) spatial interpolation technique in ArcGIS 10 was used to interpolate the groundwater level. After

interpolation, the groundwater level in the Afa-Selga watershed ranges from 0.9 to 25 meters below the surface.

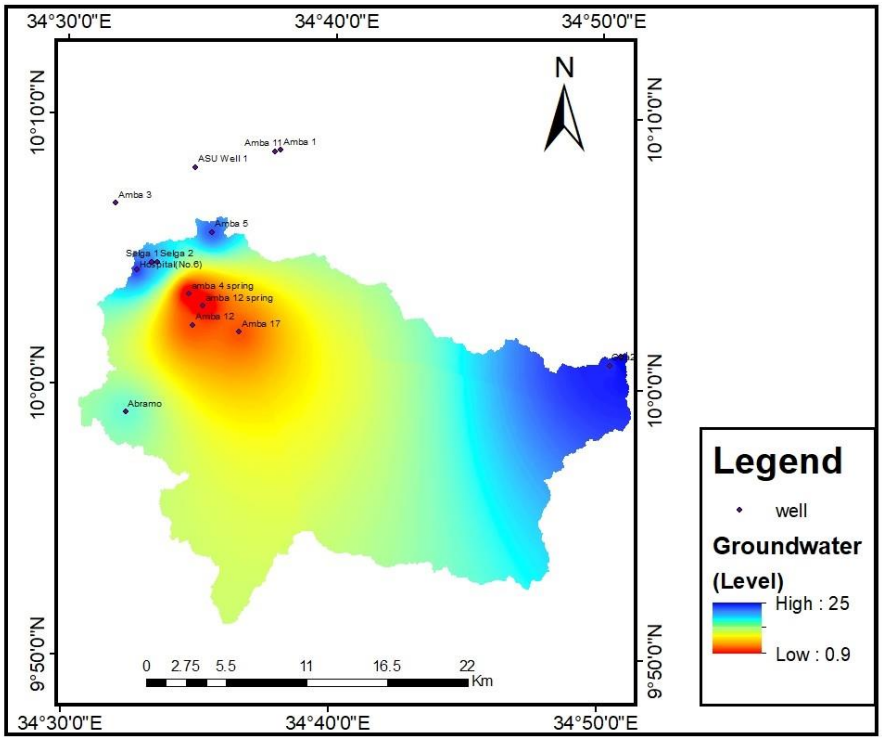

Figure 4.26: Depth to groundwater level Map of Afa-Selga watershed

4.2 Model outputs

4.2.1 Water balance components

After the WetSpass model was run, spatial average grid maps for the Afa-Selga watershed were generated for the winter, summer, and annual seasons. These simulations included the water balance components of surface runoff, actual evapotranspiration (AET), interception, transpiration, soil evaporation, and recharge. the elements of the water cycle that include surface runoff, actual evapotranspiration (AET), interception, transpiration, soil evaporation, and recharge.

4.2.1.1 Actual Evapotranspiration (AET)

The hydrologic cycle is completed by the process of evapotranspiration, which returns water to the atmosphere. Additionally, it includes ground surface, vegetation, and open water evaporation. Additionally, there is transpiration, which is the removal of water from the soil by plant roots, Transportation of the water through the plant into the leaf, and evaporation of the water from the inside of the leaf into the atmosphere (Teklebirhan et al. 2012)

Actual evapotranspiration is the amount of water that evaporates under actual field conditions. Because it is difficult to quantify Actual Evapotranspiration (AET) directly, it is typically inferred from Potential Evapotranspiration (PET). The total Actual Evapotranspiration (AET) is calculated by adding together the water that is intercepted by vegetation, the transpiration of the vegetative cover, and the evaporation from the bare soil in between the vegetation. The watershed average annual evapotranspiration, which accounts for 80.5% of the year's total rainfall, is estimated by WetSpass to be 808.26 mm at the minimum and 1,102.05 mm at the maximum values. Total actual evapotranspiration (ET_{tot}) is expressed in *Equation (3.16)*.

Vegetation partially covers precipitation before it hits the ground. The amount of water that a plant intercepts, or interception, mostly depends on the type of plant. Water that is trapped on a leaf's surface can either fall to the ground or evaporate. A further portion of the waterfalls to the earth. The interception fraction represents a fixed percentage of the annual precipitation value depending on the kind of vegetation. Annual vegetation transpiration ranges from 0 mm to 606..27 mm with an average of 495.31 mm and a standard deviation of 97.7 mm (*Figure 4.27 a*).

The average annual total interception is approximately 67.11 mm, with the minimum and highest interception ranging from 0 mm to 77.2 mm and 13.25 is the standard deviation. (*Figure 4. 27 b*).

The annual average evaporation from bare soil between the vegetation is about 65.11 with a standard deviation of 47.28 mm with a minimum and maximum of 0 mm and 1092.96 mm. (*Figure 4.27 c*).

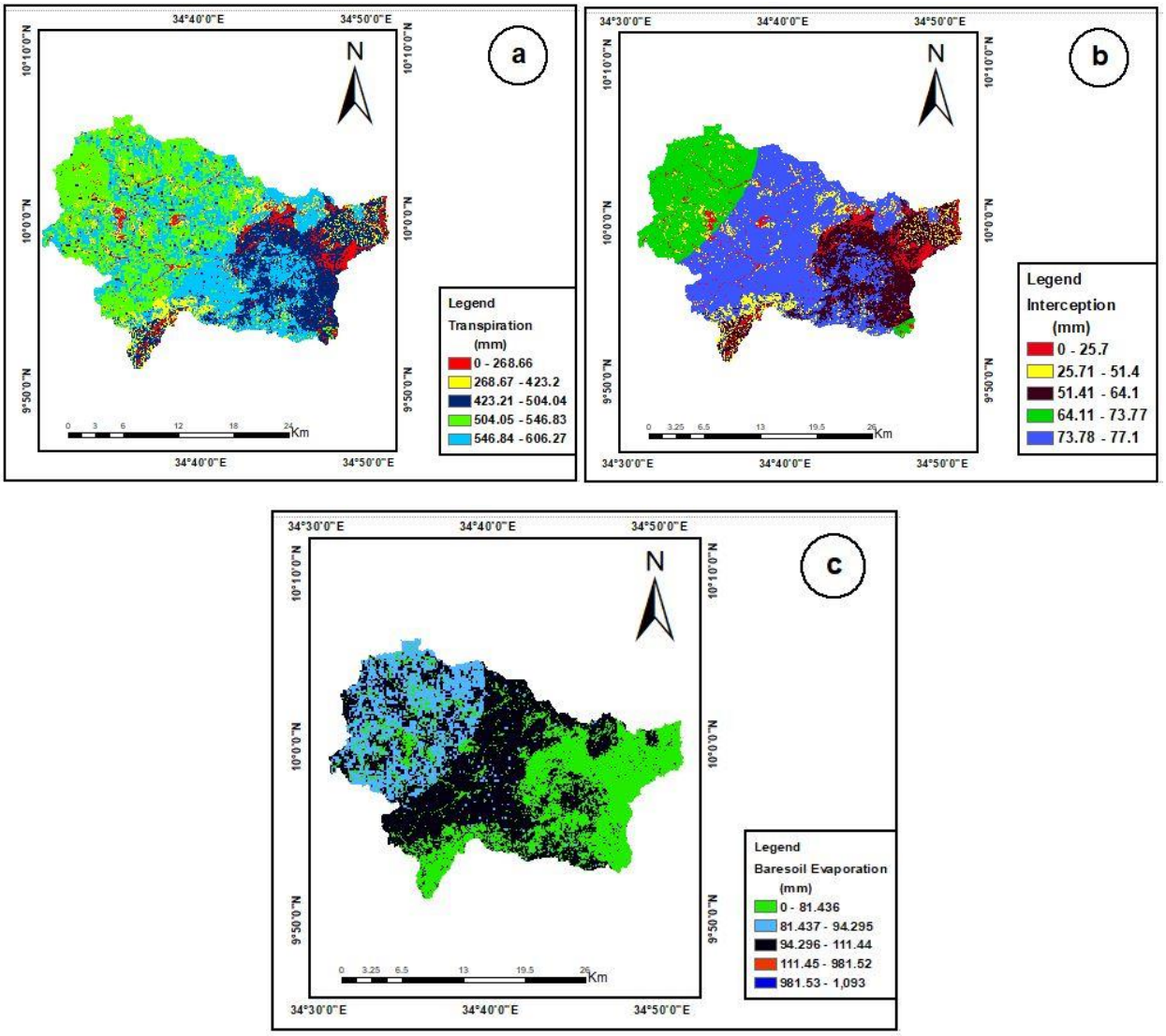

Figure 4.27: (a) Annual transpiration, (b) Annual interception, (c) annual evaporation from bare soil

WetSpass estimates the watershed annual average evapotranspiration (ET_v) to be 1003.33 mm, with minimum and maximum ET_v values of 808.26 mm and 1103.05 mm, respectively *(Figure*

4.28 a), And 36.3 mm is the distribution standard deviation. The watershed mean ET_v during the rainy season is 838.94 mm with a standard deviation of 27.53 and values of 664.86 mm and 903.84 mm for the minimum and maximum values *(Figure 4.28 b),* whereas, during the dry season, the mean ET_v is about 164.83 mm with a standard deviation of 22.73 and values of 65.57 mm and 225.68 mm for the minimum and maximum values *(Figure 4.28 c).* The annual evapotranspiration losses average about 83.6% during the rainy season and 16.4% during the dry season. The difference in precipitation patterns between the two seasons, along with the high watershed temperatures and the vegetation cover are the main causes of this variation between the wet and dry seasons.

Similarly, actual evapotranspiration accounts for 90.7% of the annual precipitation in the Tekeze River Basin, Ethiopia (Gebremeskel and Kebede, 2017), Yenehun et al., (2017) reported 90.7% of the annual precipitation in the Geba basin, Northern Ethiopia, Meresa et al., (2019), obtained 85.5% of the annual precipitation in the Birki Watershed, Eastern Tigray, Northern Ethiopia, According to Belete (2018), the Chemoga Watershed accounts 60% of its annual precipitation, and the upper Bilate river catchment receives 70% (Bitsiet, 2015). As a result, evapotranspiration eliminates the bulk of the precipitation that falls each year (Haile, 2015; Teklebirhan et al., 2012; Tilahun and Merkel, 2009).

The average evapotranspiration accounts for more than 80.5% of the total annual rainfall. This shows that ET is the main process of water loss in the watershed. Due to the watershed high temperatures, one of the causes of ET is the primary process of water loss.

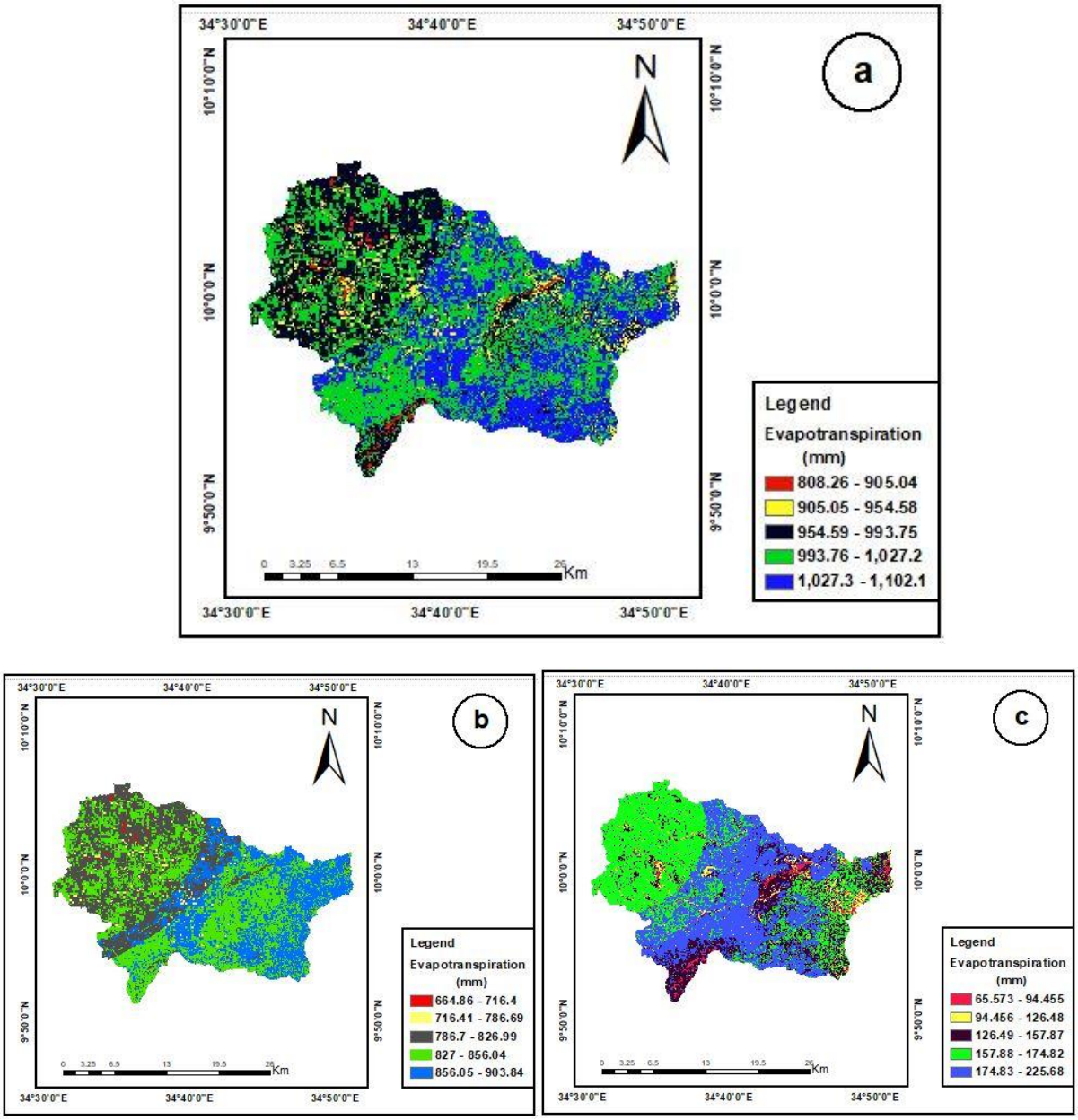

Figure 4.28: (a) Annual actual evapotranspiration, (b) rainy season actual evapotranspiration, (c) dry season actual evapotranspiration

As shown (*Figure 4.28a)* the output annual evapotranspiration grid map that high annual evapotranspiration is observed in the middle and lower parts of the watershed the presence of high

rainfall under woodland, cultivated cropland use land cover ranging from 1027.3-1102.1 mm/year. Low annual evapotranspiration ranging from 808.26-905.04 mm/year is observed in the northeast, middle and southern parts of the watershed this higher value of annual evapotranspiration of Afa-Selga watershed varies with precipitation and land-use/land-cover. Hence, precipitation and land use/land cover are the main controlling factors of evapotranspiration in the watershed.

4.2.1.2 Surface runoff

The surface runoff depends on the soil, land use, and slope and precipitation intensity of the capacity of the soil infiltration. The WetSpass model uses the runoff coefficient method for the estimation of surface runoff (S_v). The surface runoff coefficient is a function of vegetation type, soil texture, and slope. Hence, Sv in the Afa-Selga watershed varies spatially with topography and other catchment characteristics. The amount of surface runoff shows variation during the summer and winter seasons. The simulated annual surface runoff varies from a minimum of 50.36 mm to a maximum of 322.7 mm *(Figure 4.29 a)* with a mean of 125.74 mm and 46.91standard deviation that accounts for about 10.08% from the mean annual rainfall (1246.6 mm).

The mean surface runoff (S_v) of the watershed in the rainy season is 79.27mm (*Figure 4.29b*), while the mean surface runoff (S_v) in the dry is approximately 46.47mm (*Figure 4.29c*). About 63.04% of Sv occurs during the wet seasons (June to September), while the remaining 36.96% occurs in dry months (October to May). This variation comes from rainfall changes in the two seasons.

Similar findings have been reported for different Ethiopian watersheds, including the Upper Bilate Catchment in Southern Ethiopia 20.8% of precipitation (Dereje & Nedaw, 2019), Birki Watershed in Eastern Tigray in Northern Ethiopia, 7.1% of precipitation (Esayas and Gebeyehu, 2019), 6%

of annual precipitation, Tekeze River Basin, Ethiopia (Gebremeskel & Kebede, 2017), Geba basin, Northern Ethiopia 7.2% of annual precipitation, (Yenehun *et al*., 2017) and 7% of precipitation, Illala Catchment, Northern Ethiopia (Teklebirhan *et al*., 2012). In the Chemoga Watershed 31.8% of annual precipitation (Belete, 2018), and 20% of annual precipitation in the upper Bilate River catchment (Bitsiet, 2015).

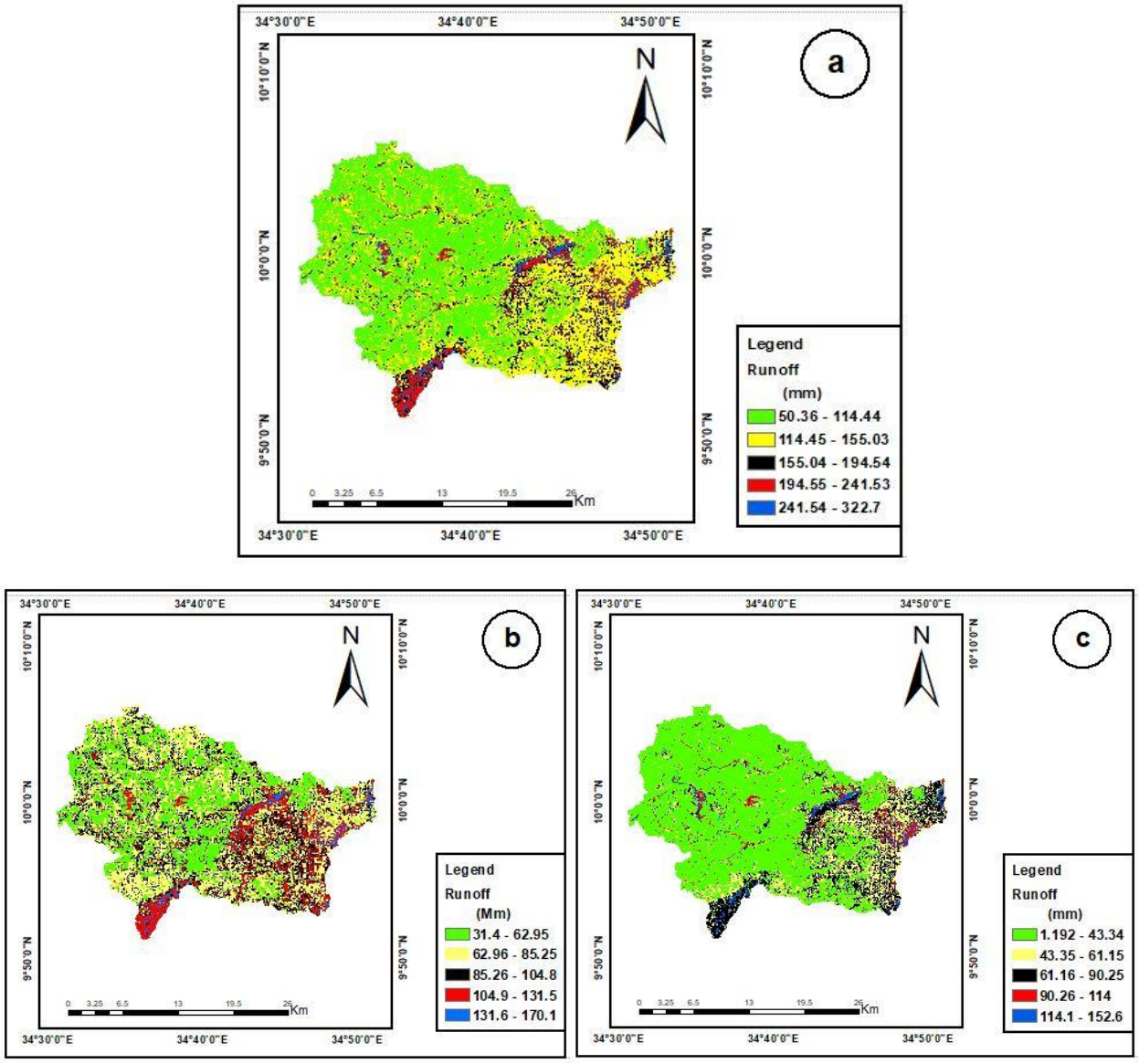

Figure 4.29: (a) annual runoff, (b) rainy season runoff, (c) dry season runoff.

According to the annually simulated surface runoff of the watershed (*Figure 4.29a)*, some northeastern, southern (*Anbesa chaka*), North West part of the watershed has the highest surface runoff ranging from 241.54-322.7 mm/year due to the high clay content of soil which has a low permeability and high slope that enhance for surface runoff. While most of the watershed has low runoff this is because of, clay loam and sandy clay loam and types associated with less slope ranging from 56.36-114.44 mm/year. This shows that the slope and soil types have a great impact on the annual surface runoff of the Afa-Selga watershed in addition to the slope.

4.1.1.3 Groundwater recharge

In general, variables like vegetation cover, slope, soil type, water table depth, etc. affect how much infiltration into groundwater occurs. Natural vegetation cover, level topography, soil permeability, a deep water table, and other factors are more associated with recharge.

Groundwater recharge over a long period of 17 years was simulated by the WetSpass model. The outcome indicates that an average recharge of 117.41 mm, 102.81 mm, and 14.6 mm was simulated for the annual, rainy season, and dry seasons, respectively. About 9.42% of the average annual precipitation (1246.6 mm) contributes to the watershed long-term annual groundwater recharge (*Figure 4.30a*).

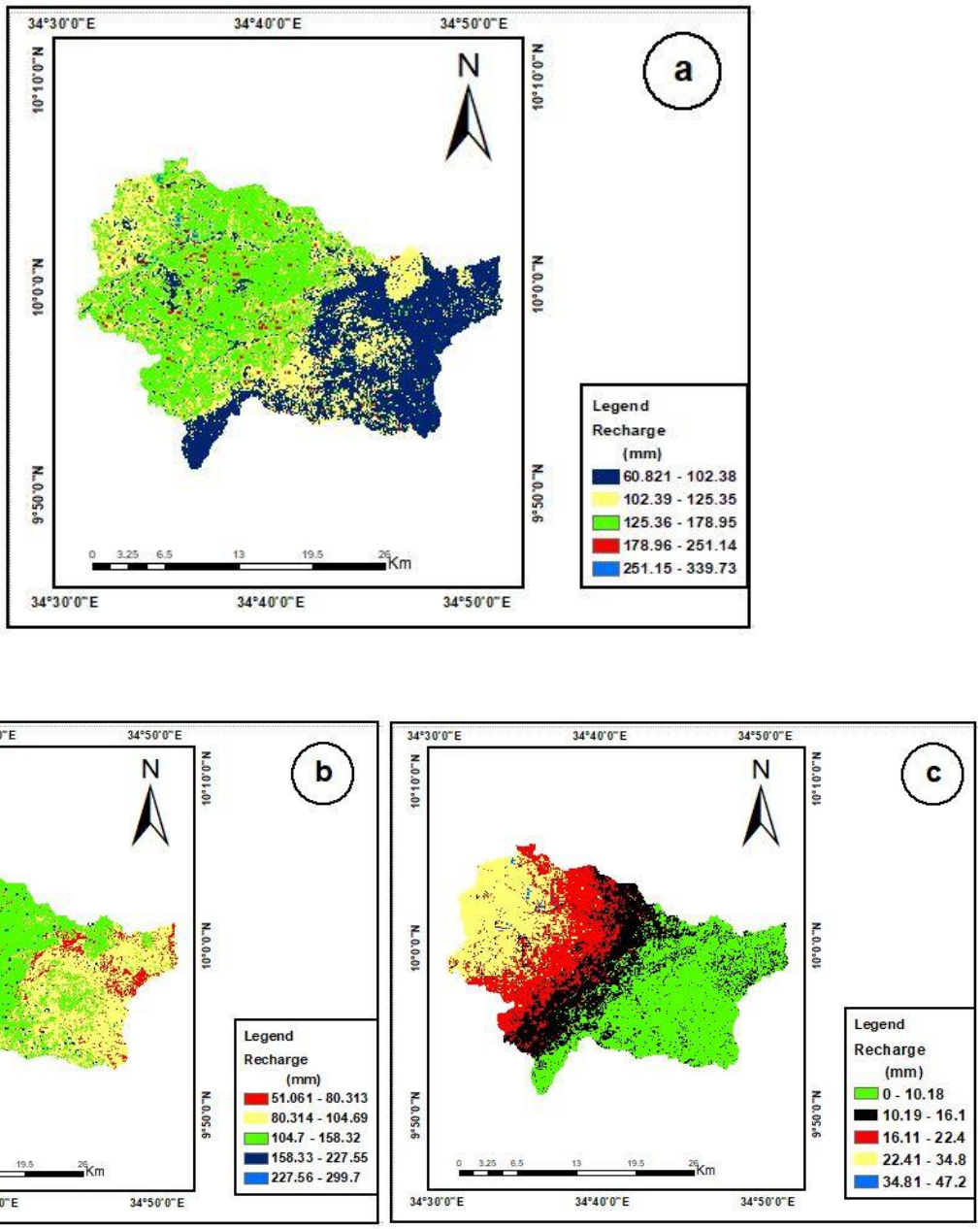

Figure 4.30: (a) Mean annual recharge, (b) Average rainy season recharge, (c) Average dry season recharge

As shown in (*Figure 4.30a)* the middle parts of the watershed generally have high annual groundwater recharge ranges between 251.15-339.73mm/year due to high precipitation and cultivated land's gentle slope topography. Some parts of the northeast and northwest areas of the

watershed have less amounts of recharge ranges between 60.82-102.38 mm/year due to low precipitation, impermeable soils, with forest land. This is due to the release of higher amounts of transpiration through the forest leaf stomata.

Water balance of the watershed, the total precipitation amount goes 80.5 % to evapotranspiration, 10.08% to runoff, and 9.4 % to recharge. Based on that, the groundwater recharge is estimated to be 68,039,095 m^3/yr. (579.5 km^2). About 87.56 % of total annual groundwater recharge in the study area is occurred during the rainy season while the remaining 12.44% occurs in the dry season.

The WetSpass model has been used in related studies by several researchers for their particular study watersheds to estimate average groundwater recharge in various parts of Ethiopia. Accordingly, an average recharge of 37 mm, 6% of precipitation (Tesfamichael et al., 2010); 0.27 mm, 0.5% of mm precipitation (Mustafa and Ali, 2013), 28 mm, 5% of annual precipitation (Tilahun and Merkel, 2009), 9.2% and 9.4 % of the annual precipitation of the in upper Bilate river catchment estimated by (Sinteyehu, 2009, Bitsiet, 2015), 7.4% of the annual precipitation in Birki Watershed (Esayas and Gebeyehu, 2018) , 66 mm, 12% of annual precipitation (Arefaine et al, 2012), 8.2% of the annual precipitation of the in Chemoga watershed (Belete,2018).

Table 4.11: annual and seasonal water balance of the Afa-Selga watershed based on the WetSpass model simulation

Water balance components	**Annual average (mm/yr.)**	**Winter (Dry Season) (mm)**	**Summer(Rainy Season) (mm)**
Precipitation	1246.59	352.4	866.69
Interception	67.11	12.17	54.95
Transpiration	495.31	101.08	394.22
Soil evaporation	65.11	13.62	51.49

Actual evapotranspiration	1003.33	164.83	838.94
Runoff	125.74	46.47	79.27
Groundwater recharge	117.41	14.6	102.81
Difference	**P -ET - SV - R = (1246.6-1003.33-125.74-117.41=0.12)**		

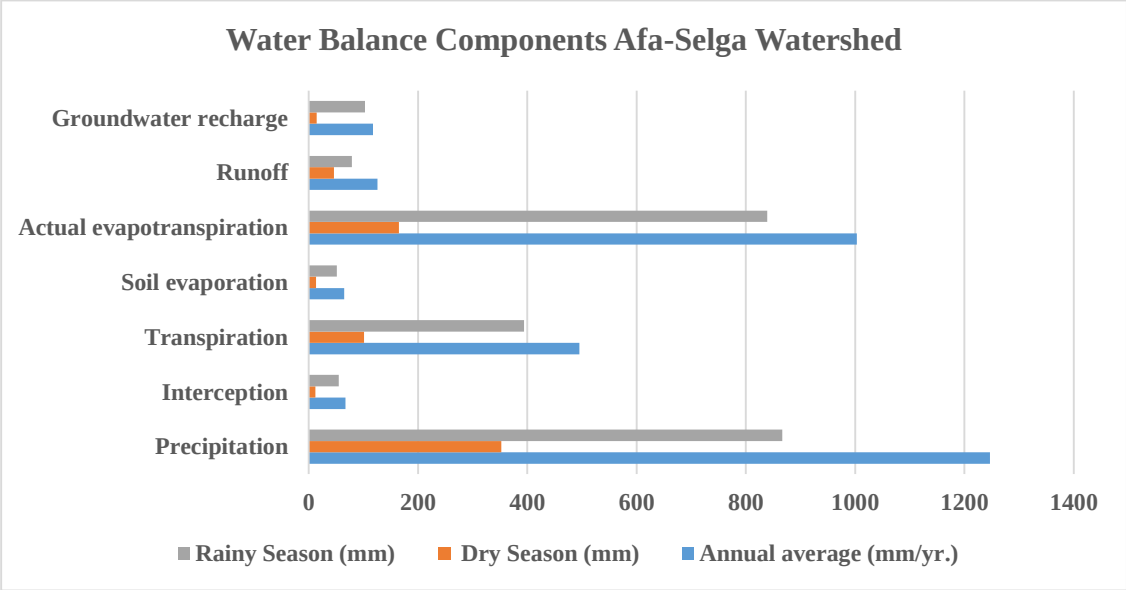

Figure 4.31: Comparison of annual and seasonal precipitation with water balance of the Afa-Selga watershed based on the WetSpass model simulation

The overall summary of the water balance of the Afa-Selga watershed is given in (*Table 4.11* and Figure *4.31*) only a small fraction of the annual precipitation remains to recharge (117.41 mm) the groundwater reservoirs, the rest leaves the watershed mainly through evapotranspiration (1003.33mm) and the rest is by surface runoff (125.74 mm). The mean annual water balance component difference (P-ET-SV-R) is 0.12 mm which shows the simulated result of the watershed by the model is good in estimation of the water balance of the watershed.

4.4 Model Performance Evaluation

To quantify model performance for comparison, specific quantitative data were required by using stream flow data collected at the watershed, the model performance was assessed in this study. In this study, the coefficient of determination (R^2) and Nash-Sutcliffe efficiency (NSE) were used to evaluate the simulation's performance and the applicability of the WetSpass model.

WetSpass models were evaluated using calculated and observed base flows that were obtained from observed discharge recorded at the Afa River station utilizing base flow separation techniques. It was carried out using the automated Web-Based Hydrograph Analysis Application (WHAT), Eckhardt recursive digital filter method. Stream flow data from 2008 to 2013 which were obtained from Ethiopian Ministry of Water and Energy (MoWE) were used to carry out the hydrograph analysis.

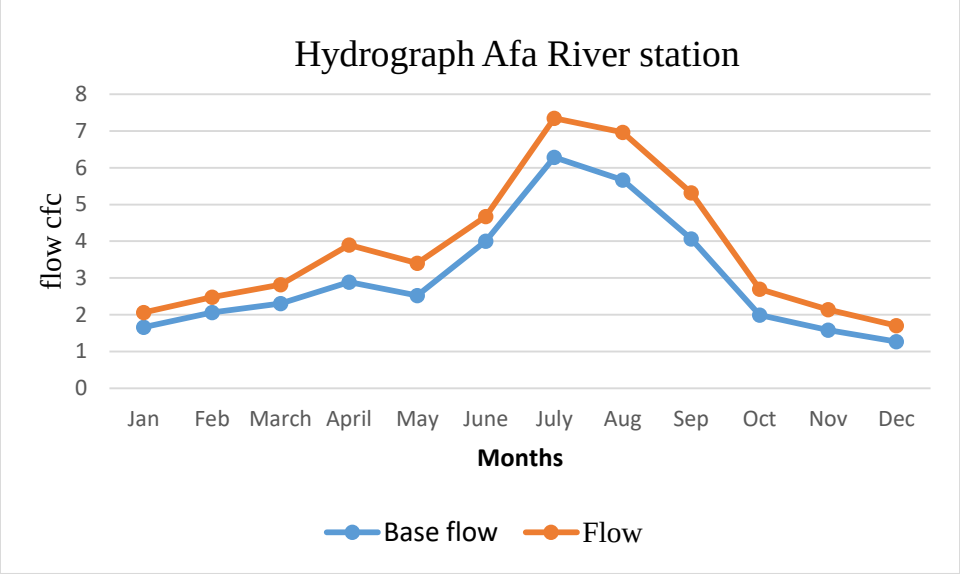

Figure 4.32: monthly base flow separation at Afa River station using Recursive Digital filter, WHAT method

Table 4.12: Summary of annual average total flow, surface runoff and simulated and observed base flow at Afa gauging station.

year	Total Flow (m^3/s)	Direct Runoff (m^3/s)	Simulated Base flow (m^3/s)	Observed Base flow (m^3/s)
2008	5.998	4.476	1.327	1.522
2009	4.862	3.631	1.119	1.231
2010	5.846	4.556	1.31	1.29
2011	4.862	3.631	1.18	1.231
2012	3.963	2.948	1.1	1.015
2013	3.025	2.258	1.452	0.89

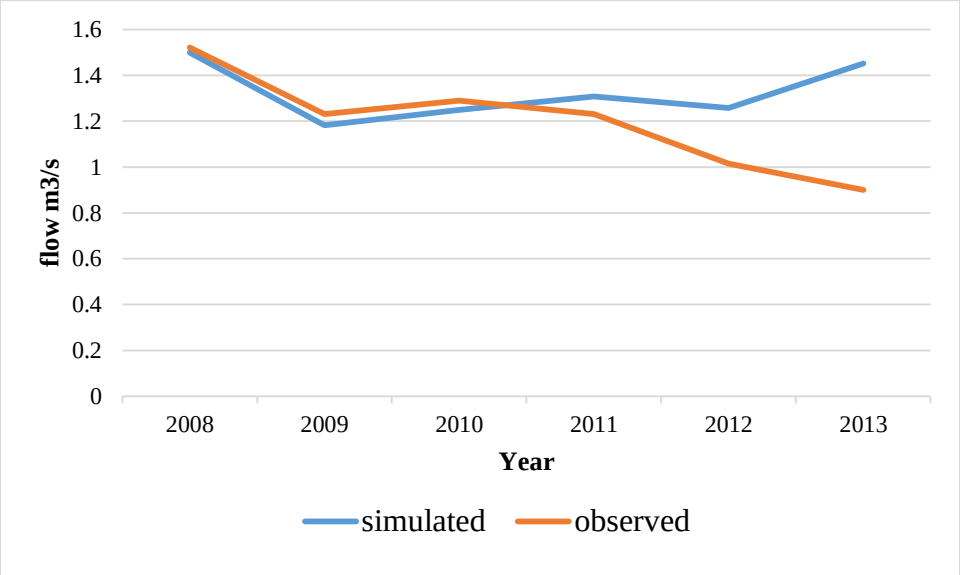

Figure 4.33: Comparison between annual average simulated and observed flow data

(Figure 4.34) shows that the Comparison between base flow from the model and base flow from base flow separation from stream flow by WHAT (R^2=0.89, Nash-Sutcliffe Efficiency (NSE) =0.84) indicates that WetSpass model simulates a representative recharge for the Afa- Selga watershed.

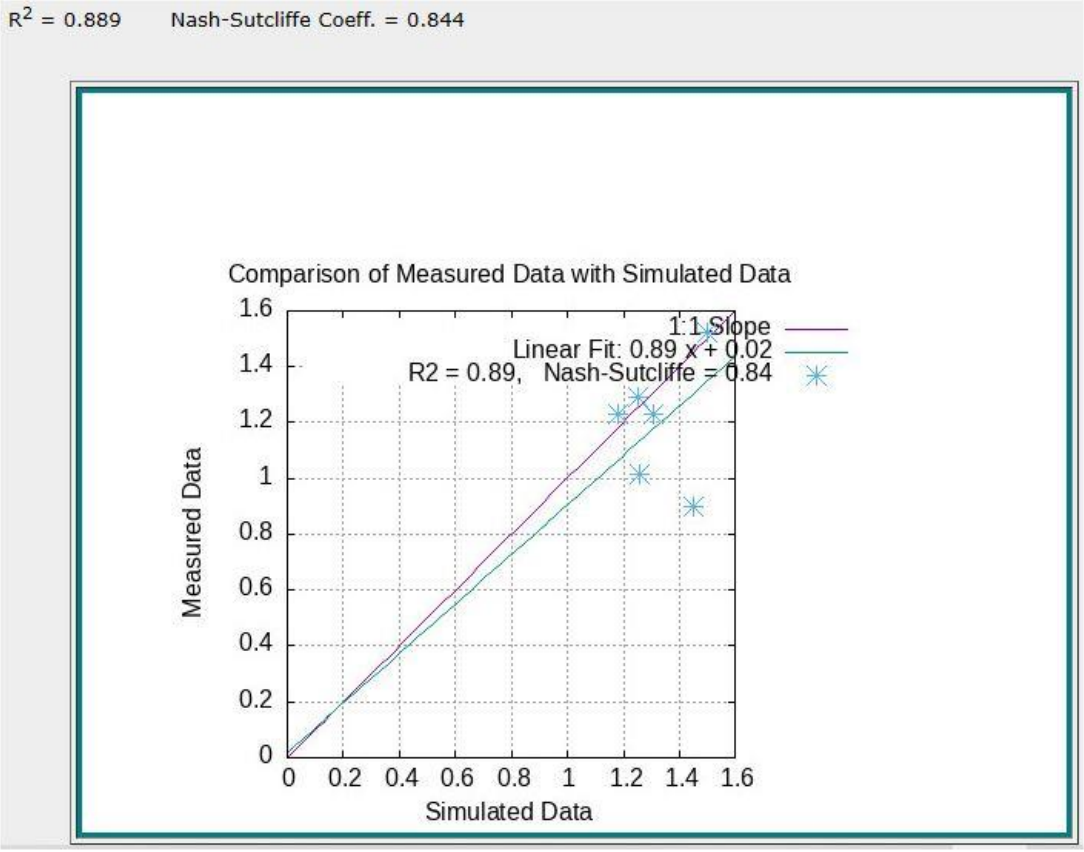

Figure 4.34: Comparison between simulated and observed data

5. CONCLUSION AND RECOMMENDATIONS

5.1 Conclusion

The distributed hydrological WetSpass model has effectively simulated the groundwater recharge estimation in the Afa-Selga watershed under annual and seasonal conditions. Recharge should be estimated taking into account the spatial variance in recharge caused by distributed soil texture, land use/land cover, topography (elevation), groundwater level, slope, and hydro-meteorological variables.

Water balance models The WetSpass model is an important tool for understanding the hydrological processes and for the simulation of spatial and temporal changes in the water resource in the watershed. After the running of the WetSpass model, a spatial simulation of the watershed annual, summer, and winter runoff, evapotranspiration, interception, transpiration, soil evaporation, and finally recharge is obtained.

These model outputs provide annual and seasonal average values for each simulated parameter. Consequently, it is estimated that the average winter and summer groundwater recharge is 14.6 mm and 102.81 mm, respectively, the simulated annual surface runoff varies from a minimum of 50.36 mm to a maximum of 322.7 mm with a mean of 125.74 mm, the annual simulated evapotranspiration 948.9 mm and In the Afa-Selga watershed, the average annual long-term groundwater recharge was determined to be 117.41 mm, or 9.42 % of the watershed average annual precipitation of 1246.56 mm.

According to simulated rainfall amounts, the watershed water balance system consists of 80.5% evapotranspiration, 10.08% runoff, and 9.42 % recharge. Based on the WetSpass model results show that ET is the main process of water loss in the watershed relative to the surface runoff and

the groundwater recharge and high surface runoff relative to groundwater recharge because the catchment is dominated by impermeable soil type.

Indicates that the watershed needs more attention like integrated watershed management, and climate change mitigation measures to increase the rainfall amount. The extremely variable distributions of the climatic factors correlated with changes in land use/land cover, soil type, elevation, and slope are responsible for changes in the water balance component within the watershed.

This study's results show that there is little groundwater recharge compared with other water balance components. The main causes include the high evapotranspiration rate caused by the high temperature, the high surface runoff caused by the impermeable soil, and the impact of changing land use and land cover. There is more groundwater recharge during the rainy season than during the dry. The rates of groundwater recharge are furthermore According to the analysis results, precipitation is the most significant hydrologic process in the study area, and evapotranspiration is significantly high, which decreases recharge rates.

5.2 Recommendation

The Afa-Selga Watershed groundwater recharge has been identified, and the spatial distributions of the water balance component have been quantified. Therefore the following recommendations have been made for future studies:

- It is recommended to conduct a groundwater modeling study to assess groundwater recharge as well as to utilize groundwater resources sustainably. For the resource to be used sustainably and to be protected from pollution and depletion, it is necessary to determine the specific groundwater recharge rates.
- Identifying the structures that govern groundwater flow direction, recharge and discharge conditions and mechanisms should be done in detail through geological and structural analysis.
- The result of a study where natural vegetation has been severely impacted by agricultural practice and deforestation is the presence of a large amount of evapotranspiration relative to groundwater recharge and surface runoff for the watershed. For rehabilitation, a thorough evaluation of land usage and cover should be done.
- Observation wells (groundwater monitoring) should be constructed to manage the area's groundwater fluctuation and to carry out more thorough groundwater flow modeling.

REFERENCES

Abdollahi, K., Bashir, I., Verbeiren, B., Harouna, M., R., Griensve, A., V., Huysmans, M. and Batelaan, O. (2017). A distributed monthly water balance model: formulation and application on Black Volta Basin. *Environ Earth Sc, 17*(198), 1-8.

Abu-Saleem, A., Al-Zubi, Y., Rimawi, O., Al-Zubi, J. and Alouran, N. (2019). Estimation of water balance components in the Hasa basin with GIS based WetSpass model. *J. Agron, 9,* 119–125.

Abu-Saleem, A., Al-Zubi, Y., Rimawi, O., Al-Zubi, J., and Alouran, N. (2010). Estimation of water balance components in the Hasa basin with GIS based WetSpass model. *J. Agron.*, *9*, 119–125.

Aish, A. Batelaan,O. and De Smedt, F. (2010). Distributed Recharge Estimation for Groundwater Modeling Using Wetspass. *Arab. J. Sci. Eng*, *35*(1), 155–163.

Aish, A. M. (2014). Estimation of water balance components in the Gaza Strip with GIS based WetSpass model. *Civ. Environ. Res*, *6*, 77–84.

Al Kuisi M, et al. (2013). Groundwater recharge, evapotranspiration, and surface runoff estimation using WetSpass modeling method in Illala Catchment, Northern Ethiopia. *J. Hydrol*, *1*, 96–110.

Al Kuisi, M. and El-Naqa, A. (2013). GIS-based spatial groundwater recharge estimation in the Jafr basin, Jordan - application of WetSpass models for arid regions. Rev Mex. Ciencias Geol. *30*(1), 96–109.

Al Kuisi, M. and El-Naqa, A. (2017). Spatial estimation of long-term seasonal and annual groundwater resources: Application of WetSpass model in the Werii watershed of the Tekeze River Basin, Ethiopia. *Phys. Geogr*, *38*, 338–359.

Alexandersson, H. (1986). A homogeneity test applied to rainfall data. *Journal of Climatology, 6(6),* 661-675. Retrieved from https://doi.org/10.1002/joc.3370060607

Ali P. Yunus, Takashi Oguchi, Y. S. H. (2015). Morphometric Analysis of Drainage Basins in the Western Arabian Peninsula Using Multivariate Statistics. Advances in Journalism and Communication, 03(01), 19–32. https://doi.org/10.4236/ajc.2015.31003. (2015).

Allen, R. G., Pereira, L. S., Raes, D., & Smith, M. . (1998). Crop evapotranspiration-Guidelines for computing crop water requirements-FAO Irrigation and drainage paper 56. Fao, Rome. *300(9)*.

Allison, P. (2001). missing data. *Sage University Papers Series on Quantitative Applications in the Social Sciences*, 07-136.

Armanuos, A.M., Negm, A., Yoshimura, C. and Saavedra Valeriano, O.C. (2016). Application of WetSpass model to estimate groundwater recharge variability in the Nile Delta aquifer. *Arab. J Geosci, 9*, 553.

Arnold, J.G., Srinivasan, R., Muttiah, R.S. and Allen, P.M. (1999). Continental scale simulation of the hydrologic balance. *J. Am. Water Resour. Assoc, 35*, 1037–1051.

Aster, D. and Seleshi, B. (2009). Characterization and Atlas of the Blue Nile Basin and its Sub basins, International Water Management Institute.

Awulachew, S. B., Yilma, A., Loulseged, D., Loiskandl, W., Ayana, M., & Alamirew, T. (2007). Water resources and irrigation development in Ethiopia. Colombo, Sri Lanka:International Water Management Institute. 78 .

Bate,G., Smailes, P. and Adams J. (2004). A water quality index for use with diatoms in the assessment of rivers. *Water SA, 30*, 493–498.

Batelaan, O., De Smedt, F., Triest, L. (2003). Regional groundwater discharge: phreatophyte mapping, groundwater modeling and impact analysis of land-use change. *Journal of Hydrology, 275 (1–2)*, 86–108.

Batelaan, O., Z., M., Wang, and De Smedt, F. . (1996). An Adaptive GIS Toolbox for Hydrological Modeling, in Application of Geographic Information Systems in Hydrology and Water Resources Management, eds. K.Kovar and H. P. Nachtnebel, IAHS Publ. no. 235.

Batelaan,O. and De Smedt, F. (2001). WetSpass: a flexible, GIS-based, distributed recharge methodology for regional groundwater modeling. *Impact Hum. Act. Ground. Dyn, 269*(269), 11–17.

Batelaan,O. and De Smedt, F. (2007). GIS-based recharge estimation by coupling surface subsurface water balances. *J. Hydrol, 337*(3–4), 337–355.

Belete, B. (2018). Geospatial Approach for Groundwater Recharge Estimation Using WetSpass Model: A Case Study of Chemoga Watershed, Ethiopia. M.Sc thesis, Addis Ababa University, Addis Ababa,Ethiopia.

Beven, K. J. (2001). Rainfall-runoff modeling: the primer, John Wiley & Sons, Ltd.,Chichester, West Sussex, England, U.K.

BGNRS (Benishangual Gumuz National Regional State) . (2013). Regional Climate Change Adaptation Plan of Action, Assosa.

Bhattacharya, A. K. (2010). Artificial Ground Water Recharge With a Special Reference To India. International Journal of Research and Reviews in Applied Sciences - IJRRAS, 4(August), 214–221. (2010).

Bitsiet, D. (2015). Groundwater Recharge estimation using the wetspass model in the upper Bilate river catchment.

BoFED (Bureau of Finance and Economic Development). (2007). Atlas of Benishagul Gumuz National Regional State, Assosa.

Bowden, G. J. (2005). Input determination for neural network models in water resources applications. Part 1-background and methodology. *J. Hydrol, 301*(1), 93-107.

Buishand, T. A. (1982). Some methods for testing the homogeneity of rainfall records. *Journal of Hydrology, 58(1–2)*, 11–27. Retrieved from https://doi.org/10.1016/0022-1694(82)90066-X

Chernet, T. (1993). Hydrogeology of Ethiopia and water resources development. *Ministry of Mines and Energy report*, 157.

Chiang, W.H. and Kinzelbach, W. (2001). 3D – groundwater modeling with PMWIN. A simulation system for modeling groundwater flow and pollution. *Springer*, 346.

CSA. (2007). The Population and Housing Census of Ethiopia; Results at a Country Level," Office of Population and Housing Census Commission, Central Statistical Authority, Addis Ababa, Ethiopia. .

CSA. (2013). Population Projection of Ethiopia for All Regions at Wereda Level from 2014 – 2017, Addis Ababa, Ethiopia, Central Statistical Agency.

Dahan, O., McDonald, E. V., & Young, M. H. . (2003). Flexible Time Domain Reflectometry Probe for Deep Vadose Zone Monitoring. *Vadose Zone Journal, 2(2)*, 270–275. Retrieved from https://doi.org/10.2136/vzj2003.2700

Daniel, N. (2016). Temporal changes in Groundwater Recharge in the Upper Awash Basin with particular emphasis to Becho and Koka areas, Central Ethiopia. Unpublished MSc Thesis, Addis Ababa University,Addis,Ababa, Ethiopia.

De Smedt, F. and Batelaan, O. (2003). Investigation of the human impact on regional groundwater systems. In: Tiezzi, E., Brebbia, C., A., Uso, J.L. (Eds.), Ecosystems and Sustainable Development, Advances in Ecological Sciences, WIT Press. 19:1145– 1153.

Dereje, B. (2015). Groundwater Recharge estimation using wetspass model in upper Bilate river catchment.Unpublished MSc Thesis, Addis Ababa University,Addis,Ababa, Ethiopia.

Dereje, B. and Nedaw, D. . (2019). Groundwater Recharge Estimation Using WetSpass Modeling in Upper Bilate Catchment, Southern Ethiopia. Momona Ethiopian. . *Journal of Science, 11(1)*, 37. doi: https://doi.org/10.4314/mejs.v11i1.3

Dragoni, W., & Sukhija, B. S. (2013). Climate change and groundwater: A short review. *GeologicalSociety, London, Special Publications, 288*, 1–12.

Duparc, L. and Borloz, A. . (1927). Sur la Birbirite une roche nouvelle. Comp. Rend. Soc.Phys.His.Nat. 44, Geneva.

Eckhardt, K. ((2005)). How to construct recursive digital filters for baseflow separation.Hydrological Processes:. *An International jornal, 19(2)*, 507–515.

Eder, G., Fuchs, M., Nachtnebel, H.P. and Loibl, W. (2005). Semi-distributed modeling of the monthly water balance in an alpine catchmen. *Hydrol. Process, 19*, 2339–2360.

El-Rawy, M., Zlotnik, V.A., Al-Raggad, M., Al-Maktoumi, A., Kacimov, A. and Abdalla, O. (2016). Conjunctive use of groundwater and surface water resources with aquifer recharge by treated wastewaterEvaluation ofmanagement scenarios in the Zarqa River basin Jordan. *Environ. Earth Sci., 75*, 1146.

EGI (Ethiopian Geology Institute). (2004). Explanatory Notes to the hydrogeological and hydrochemical maps of the Asosa-Kurmuk Area (NC36-7 West of Asosa and NC36-8 Asosa sheets).

Esayas, M. and Gebeyehu, T. (2018). Estimation of groundwater recharge using GIS-based WetSpass model for Birki watershed, the eastern zone of Tigray, Northern Ethiopia. *Sustain. Water Resour. Manag*. doi:10.1007/s40899-018-0282-0

Fang, G.H., Yang, J., Chen, Y.N., Xu, C.C. and Maeyer, P.D. (2015). Contribution of meteorological input in calibrating a distributed hydrologic model in a watershed in the Tianshan Mountains, China. *Environ. Earth Sci, 74*, 2413–2424.

Freeze. R, Allan and cherry, J., A. (1979). Groundwater prentice-Hall, New Jersy. 616.

Gadisa, B. (2017). Aquifer characterization of Assosa area, BenishanGul Gumuz regional state, western Ethiopia.

Gao, H. H. (2014). Testing the realism of a topography driven model (FLEX-Topo) in the nested catchments of the Upper Heihe, China. *Hydrol. Earth Syst. Sci, 18*, 1895-1915. doi:10.5194/hess-18-1895

Gebremeskel, G. and Kebede, A. (2017). Spatial estimation of long-term seasonal and annual groundwater resources: application of WetSpass model in the Werii watershed of the Tekeze River Basin, Ethiopia. *Physical Geography, 38(4)*, 338–359. doi:https://doi.org/10.1080/02723646.2017.1302791

Gebreyohannes, T., Smedt, F., Walraevens, K. and Gebresilassie, S. (2013). Application of a spatially distributed water balance model for assessing surface water and groundwater resources in the Geba basin, Tigray, Ethiopia. *J. Hydrol, 499*, 110–123.

Gharari, S. H. (2013). Using expert knowledge to increase realism in environmental system models can dramatically reduce the need for calibration. *Hydrol. Earth Syst. Sci*.

Ghouili, N., Horriche, F.J., Zammouri, M., Benabdallah, S. and Farhat, B. (2017). Coupling WetSpass and MODFLOW for groundwater recharge assessment: Case study of the Takelsa multilayer aquifer, northeastern Tunisia. *Geosci. J, 21*, 791–805.

Glavan, M. and Pintar, M. (2012). Strengths, Weaknesses, Opportunities and Threats of Catchment Modelling with Soil and Water Assessment Tool (SWAT). doi:10.5772/34539

Gregory, J.M. and David, M.W. (2013). Temporal and spatial variability of the global water balance. *Clim. Chang, 120*, 375–387.

Gumindoga W, Rientjes T, Haile. A. and Dube, T. . (2014). Predicting stream-flow for land cover changes in the upper Gilgel Abay River basin, Ethiopia: a TOPMODEL based approach. *Phys Chem Earth, 76*, 3-15.

Gunkel, A., Shadeed, S., Hartmann, A., Wagener, T. and Lange, J. (2015). Model signatures and aridity indices enhance the accuracy of water balance estimation in a data-scarce Eastern Mediterranean catchment. *J. Hydrol. Reg. Stud, 4*, 487–501.

Harbaugh, A.W., Banta, E.R., Hill, M.C., and McDonald, M.G. (2000). Modflow-2000, The U.S. Geological Survey Modular Ground-Water Model – User Guide to Modularization Concepts and the Ground Water Flow Process. U.S. Geological Survey, Reston. 120.

Hargreaves, G. H., & Samani, Z. A. (1982). Estimating potential evapotranspiration. *jornals of irrigation and drainage division, 108(3)*, 225-230.

Herrmann, F., Keller, L., Kunkel, R., Vereechen, H. and Wendland, F. (2015). Determination of spatially differentiated water balance components including groundwater recharge on the Federal State level—A case study using the mGROWA model in North Rhine-Westphalia (Germany). *J. Hydrol. Reg. Stud, 4*, 294–312.

Hornero, J. M. (2016). Environment Integrating soil water and tracer balances, numerical modelling and GIS tools to estimate regional groundwater recharge: Application to the Alcadozo Aquifer System (SE Spain). *Sci. Total Environ, 568*(415-432). doi:10.1016/j.scitotenv.2016.06.011

Hurni, H. (1998). Degradation and Conservation of the Resources in the Ethiopian Highlands. *Mountain Research and Development, 8*((2/3)), 123–130.

Husam, B. (2015). Fundamentals of Groundwater Modelling. Groundwater: Modelling, Management and Contamination, January 2011, 113–130.

Ibrahim, J. M. (2020). Streamflow Modeling Under the Impact of Climate Change. (Case Study of Dabus River Sub-Basin, Ethiopia). *Civil and Environmental Research, 12*(7), 19-29. doi:10.7176/CER/12-7-03

IPS (Investment Project Service). (2012). Investment Potential Assessment in the Benishangual-Gumuz National Regional State, Assosa.

Jaturon, K. and Srilert, C. (2013). Distributed Groundwater Recharge Estimation in Phrae Province Using WetSpass. The Second Environment Asia International Conference Chonburi, Thailand.

Jian, S.Q., Zhao, C.Y., Fang, S.M. and Yu, K. (2015). Effects of different vegetation restoration on soil water storage and water balance in the Chinese Loess Plateau. *Agric. For. Meteorol, 206*, 85–96.

Jiang, R., Li, Y., Wang, Q., Kuramochi, K., Hayakawa, A., Woli, K.P. and Hatano, R. (2011). Modeling the water balance processes for understanding the components of river discharge in a Non-conservative Watershed. *Tran. ASABE, 54*, 2171–2180.

Karamouz, M., Szidarovszky, F. and Zahraie, B. (2003). Water resources systems analysis Lewis Publishers, A CRC Press Company, Boca Raton, London, New York, Washington, D.C. 608.

Karimi P. and Bastiaanssen G. M. (2015). Spatial evapotranspiration, rainfall, and land use data in water accounting - Part 1: Review of the accuracy of the remote sensing data. *Hydrology and Earth System Sciences, 19,* 507–532.

Klemes, V. (1983). Conceptualization and Scale in Hydrology. *Journal of Hydrology, 56*(1-3), 1-23.

Kling, H. and Nachtnebel, H.P. (2009). A spatio-temporal comparison of water balance modeling in an Alpine catchment. *Hydrol. Process, 23,* 997–1009.

Lerner, D. N. Issar, A. S. and Simmers, I. (1990). A guide to understanding and estimating natural recharge. International contributions to hydrogeology.Verlag Heinz Heise.

Lim, K.J., Engel, B.A., Tang, Z., Choi, J., Kim, K., Muthukrishnan, S. and Tripathy, D. (2005). Automated web GIS based hydrograph analysis tool, WHAT 1. JAWRA Journal of the American. *Water Resources Association, 41(6),* 1407–1416.

Lu, G. Y., & Wong, D. W. . (2008). An adaptive inverse-distance weighting spatial interpolation technique. Computers & Geosciences. *34(9),* 1044–1055.

Lu, Z.X., Zou, S.B., Xiao, H.L., Zheng, C.M., Yin, Z.L. and Wang, W.H. (2015). Comprehensive hydrologic calibration of SWAT and water balance analysis in mountainous watersheds in northwest China. *Phys. Chem. Earth,* 76–85.

Lyne, V. and Hollic, M. (1979). Stochastic time variable rainfall-runoff modelling. *Institute of Engineers Australia National Conference,, 79(10),* 89–93.

Martin, N. (2005). Development of a Water Balance for the Atankwidi Catchment, West Africa. A Case Study of Groundwater Recharge in a Semi-Arid Climate. Ph.D. Thesis, University of Göttingen, Göttingen,Germany.

Mengesha, T. (1991). Geology of the Kurmuk and Assosa area (Digital Version), Regional Geology Department, GSE, Addis Ababa.

Mengesha, T. (1987). Geological maps of Gore area (1:250,000, Ethiopian Institute of Geological surveys).

Mengesha, T. and Seife, M. B. . (1987). Geology of sheet NC, 36–16, (Gore sheet) Ethiopian Institute of Geological Surveys. Unpublished manuscript.

Meresa, E., Girmay, A. and Gebremedhin, A. (2019). Water Balance Estimation Using Integrated GIS-Based WetSpass Model in the Birki Watershed, Eastern Tigray, Northern Ethiopia. . *Physical Science International Journal*, 1–17. doi:https://doi.org/10.9734/psij/2019

Montanari, L. S. (2006). Investigation of dominant hydrological processes in a tropical catchment in a monsoonal climate via downward approach. *Hydrological Earth System, Sci, 10*, 769-782.

Moon, S., Woo, N.C., and Lee, K.S. (2004). Statistical analysis of hydrograph and water-table fluctuation to estimate groundwater recharge. *Hydrology, 292*, 198–209.

Moriasi D. N., Arnold J. G., Van Liew M. W., Bingner R. L., Harmel R. D., and Veith T. L. (2007). Model evaluation guidelines for systematic quantification of accuracy in watershed simulations. *American Society of Agricultural and Biological Engineers, 50*, 885–900.

Nash, J.E. and Sutcliffe, J. V. (1970). River flow forecasting through conceptual models part-A discussion of principles. *Jornals of Hydrology*, *10*, 282–290.

Nathan, R.J. and McMahon, T.A. (1990). Evaluation of automated techniques for base flow and recession analyses. *Water Resources Research, 26(7)*, 1465–1473.

NMA (Ethiopian National Meteorological Agency). (2001). Initial National Communication of Ethiopia to the United Nations Framework Convention on Climate Change (UNFCCC),

NMSA (National Meteorological Service Agency). (2016). Regional Meteorological Report, Addis Ababa, Ethiopia.NMA, Addis Ababa, Ethiopia.

Nuemann, J. V. (1941). Distribution of the ratio of the mean square successive difference to the variance. {Annals of Mathematical Statistics}. 367--395. Retrieved from https://doi.org/10.1214/aoms/1177731677

Obuobie, E. D. (2012). Groundwater level monitoring and recharge estimation in the White Volta River basin of Ghana. *Afr. Earth Sci*(71–72), 80-86. doi: 10.1016/j.jafrearsci.2012.06.005

Obuobie, E., Diekkrüger, B. & Reichert, B. (2008). Estimation of groundwater recharge in the context of future climate change in the White Volta River Basin, West Africa (Dissertation). Retrieved from Retrieved from http://hss.ulb.uni-bonn.de/diss_online elektronisch

Oki, T. (2005). Encyclopedia of Hydrological Sciences, M.G. Anderson, J. McDonnell, Eds. (Wiley, New York. 1). 13-22.

Pande, C. and Khadri, R. F. S. (2016). Groundwater flow modelling for calibrating steady state using MODFLOW software: acase study of Mahesh River Basin, India. *Erth Syst. Environ.*, 1-17. doi:10.1007/s40808-015-0049-7

Pandian, M., Rajasimman,U, A. & Saravanavel, J. (2014). Identification of Groundwater Potential Recharge Zones using WETSPASS Model in parts of Coimbatore & Tiruppur Districts in Tamil Nadu, India.

Pandian.M., Rajasimman.U. A. & Saravanavel, J. (2014). Identification of Groundwater Potential Recharge Zones using WETSPASS Model in parts of Coimbatore & Tiruppur Districts in Tamil Nadu, India.

Poelmans L, Rompaey A. and Batelaan, O. (2010). Coupling urban expansion models and hydrological models: How important are spatial patterns?

Raghunath, H. M. (2006). Hydrology (Principles, Analysis Design). 2nd Edition, New Age.

Rwanga S. S. and Ndambuki J. M. (2017). Approach to Quantify Groundwater Recharge Approach to Quantify Groundwater Rechargel : A Review. *4*.

Rwanga, S. S. (2013). A Review on Groundwater Recharge Estimation Using Wetspass Model. 156–160.

Rwanga, S. S. (2017). Approach to Quantify Groundwater Recharge Using GIS-Based Water Balance Model A Review," Int. J. Res. Chem. Metall. Civ. Eng., vol. 4, no. 1, doi:10.15242/ijrcmce.ae0317115.

Salem, A., Dezs ″o, J. and El-Rawy, M. (2019). Assessment of Groundwater Recharge, Evaporation,and Runoff in the Drava Basin in Hungary with the WetSpass Model. *Hydrology, 6,* 23. doi:10.3390/hydrology6010023

Salem, A., Dezs″o, J., Lóczy, D., El-Rawy, M. and Słowik, M. (2018). Modeling surface water-groundwater interaction inan oxbow of the Drava floodplain. In Proceedings of the 13th International Conference on Hydroinformatics (HIC 2018), Palermo, Italy. *3*, 1832–1840.

Sanford, W. (2002). Recharge and groundwater models: An overview. Hydrogeology Journal, 10(1), 110–120. https://doi.org/10.1007/s10040-001-0173-5.

Savenije, H. G. (2001). Equifinality a blessing in disguise? . *Hydrological Processes, 15,* 2835-2838. doi:10.1002/hyp.494

Scanlon, B. R. (2002). Theme issue on groundwater recharge. Hydrogeology Journal, 10(1), 3–4. https://doi.org/10.1007/s10040-001-0175-3.

Senanayake, I. P., Dissanayake, D. M., Mayadunna, B. B., and Weerasekera, W. L. (2016). An approach to delineate groundwater recharge potential sites in Ambalantota, Sri Lanka using GIS techniques. Geoscience Frontiers, 7(1), 115–124.

Sentayehu, L. (2009). Integrated hydrogeological investigation of upper Bilate river catchment: Southern rift valley of Ethiopia. Unpublished MSc thesis, Addis Ababa University, Addis Ababa, Ethiopia,111pp.

Singhal, V. and Goyal, R. (2011). Development of conceptual groundwater flow model for Pali Area, India. African Journal of Environmental Science and Technology. . *5(12),* 1085-1092.

Sivapalan, M. (2003). Prediction of ungauged basins: a grand challenge for theoretical hydrology. . *Hydrological Processes, 17*(15), 3163-3170.

Solomatine, D. P. (2011). Hydrological Modelling. Treatise on Water Science. *2,* 435–457.

Srinivasa Rao, Y., and Jugran, D. K. (2003). Delineation of groundwater potential zones and zones of groundwater quality suitable for domestic purposes using remote sensing and GIS.

Hydrological Sciences Journal, 48(5), 821–833. Retrieved from https://doi.org/10.1623/hysj.48.5.821.51452

Tefera, M. and Berhe, S, M. (1987). Geology of sheet NC, 36–16, (Gore sheet) Ethiopian Institute of Geological Surveys. Unpublished manuscript.

Tefera, M. (1991). Geological Map of Kurmuk -Asosa NC 36-7, NC 36-8, Unpublished Map.

Teklebirhan, A., Dessie, N. and Tesfamichael, G. (2012). Groundwater Recharge,Evapotranspiration and Surface Runoff Estimation by Using WetSpass Modeling Method in Illala Catchment, Northern Ethiopia, MEJS. 4(2), pp.96-110. Mekele, Ethiopia.

Tesfamichael, G., De-Smedt, F., Miruts, H., Solomon, G., Kassa, A., Kurkura, K., ... Nurhussen, T. (2010). Large-scale geological mapping of the Geba basin, northern Ethiopia Belgium: VLIR – Mekelle University IUC Program. 46.

Tilahun, K. and Merkel, J.B. (2009). Estimation of groundwater recharge using a GIS-based distributed water balance model in Dire Dawa, Ethiopia. *Hydrogeology Journal, 17*, 1443–1457.

Uniyal, B., Jha, M.K. and Verma, A.K. (2015). Assessing climate change impact on water balance components of a river basin using SWAT mode. *Hydrol. Process, 29*, 4767–4785.

Van Liew, M.W., Veith, T.L., Bosch, D.D. and Arnold, J.G. (2007). Suitability of SWAT for the conservation effects assessment project: Comparison on USDA agricultural research service watersheds. *Journal of Hydrologic Engineering, 12(2)*, 173-189.

Wang, B., Jin, M., Nimmo, J.R., Yang, L., and Wang, W. (2008). Estimating groundwater recharge in Hebei Plain, China under varying land use practices using tritium and bromide tracers. *J. Hydrol, 356*, 209–222.

Wang, W., Peng, S., Yang, T., Shao, Q., Xu, J. and Xing, W. (2011). Spatial and temporal characteristics of reference evapotranspiration trends in the Haihe River Basin, China. *J. Hydrol. Eng, 16*, 239–252.

White, E.D., Easton, Z.M., Fuka, D.R., Collick, A.S., Adgo, E., McCartney, M., Awulachew, S.B. and Selassie, Y.G. (2011). Development and application of a physically based landscape water balance in the SWAT model. *Hydrol. Process, 25*, 915–925.

Wijngaard, J. B. (2003). Homogeneity of 20th century European daily temperature and rainfall series. International Journal of Climatology. *23(6),* 679–692. Retrieved from https://doi.org/10.1002/joc.906

Xu, C. Y. (2002). Modelling in Hydrology. In: Textbook of Hydrologic Models. Uppsala University Department of Earth Sciences Hydrology, Unppsala. 168.

Yazew, E. (2005). Development and management of irrigated lands in Tigray, Ethiopia. PhD thesis, UNESCO-IHE Institute for Water Education, Delft, the Netherlands. 265 .

Yenehun, A., Walraevens, K. and Batelaan, O. (2017). Spatial and temporal variability of groundwater recharge in Geba basin, Northern Ethiopia. *Journal of African Earth Sciences, 134*, 198–212. doi:https://doi.org/10.1016/j.jafrearsci.2017.06.006

Zarei, M., Ghazavi, R., Vali, A. and Abdollahi, K. (2016). Estimating Groundwater Recharge, Evapotranspiration and Surface Runoff using Land-use data: A Case Study in Northeast Iran. *Biol. Forum Int. J, 8*, 196–202.

Zdon, A., Rainville, K., Buckmaster, N., Parmenter, S., and Love, A. H. (2019). Identification of source water mixing in the fish slough spring complex, Mono County, California, USA. Hydrology, 6(1), 1–11. https://doi.org/10.3390/hydrology6010023.

Zektser, I, S. and Everett, L.G. (2006). Groundwater Resources of the World and Their Use National Groundwater Association Press, Westerville, Ohio.346 pp.

Zhang, Y.Y., Zhang, S.F., Xia, J. and Hua, D. (2013). Temporal and spatial variation of the main water balance components in the three rivers source region, China from 1960 to 2000. *Environ. Earth Sci*, *68*, 973–983.

APPENDICES

Appendix I: Soil parameter table of Afa-Selga Watershed

Soil attributes table

Number = Soil type number; Soil = Soil type (texture); Fieldcapac = Field capacity; Wiltingpnt = Wilting Point; PAW = Plant available water content; Residual = Residual water content; A1 = Calibration parameter dependent on the sand content of the soil; Evapodepth = Bare soil evaporation depth; Tensionsh = Tension saturated height; P_frac_sum = Fraction of summer precipitation contributing to Hortonian runoff; P_frac_win = Fraction of winter precipitation contributing to Hortonian runoff

No	SOIL	FIELDCAPAC	WILTINGPNT	PAW	RESIDUALWC	A1	EVAPODE PTH	TENSIONH HT	P_FRAC_S UM	P_FRAC_WIN
9	Clay loam	0.33	0.19	0.14	0.075	0.27	0.05	0.26	0.62	0.41
12	Clay	0.46	0.33	0.13	0.090	0.21	0.05	0.37	0.95	0.85
10	Sandy Clay	0.32	0.23	0.09	0.109	0.25	0.29	0.80	0.05	0.68
7	Sandy Clay loam	0.26	0.16	0.10	0.068	0.32	0.05	0.28	0.54	0.30

Land-use table attributes

Luse_type = Land Use Type; Runoff_veg = Runoff Vegetation; Num_veg_Ro = Runoff class for vegetation type; Num_imp_Ro = Impervious Runoff class for impervious area types; Veg_area = Vegetated Area; Bare_area = Bare Area; Imp_area = Impervious Area; Openw_area = Open water Area; Root_depth = Root depth; LAI = Leaf Area Index; Min_stom= Minimum Stomatal Opening; Interc_per = Interception Percentage; Veg_height = Vegetation Height

Appendix II: Summer land use parameter table of Afa-Selga watershed.

NUMBER	LUSE_TYPE	RUNOFF_VEG	NUM_VEG_RO	NUM_IMP_RO	VEG_AREA	BARE_AREA	IMP_AREA	OPENW_AREA	ROOT_DEPTH	LAI	MIN_STOM	INTERC_PRE	VEG_HEIGHT
21	Agriculture	crop	1	0	0.80	0.20	0.00	0.00	0.40	4.00	180.00	15.00	0.6000
7	Bare land	bare soil	4	0	0.00	1.00	0.00	0.00	0.05	0.00	110.00	0.00	0.0010
31	woodland	forest	3	0	1.00	0.00	0.00	0.00	2.00	5.00	250.00	25.00	18.0000
33	Forest	forest	3	0	1.00	0.00	0.00	0.00	2.00	5.00	375.00	35.00	16.0000
23	Grass land	grass	2	0	1.00	0.00	0.00	0.00	0.30	2.00	100.00	10.00	0.2000

1	Settlement	grass	2	1	0.20	0.00	0.80	0.00	0.30	2.00	100.00	10.00	0.1200
36	Shrubs-bush land	grass	2	0	1.00	0.00	0.00	0.00	0.60	0.60	110.00	15.00	2.0000
44	Water body	open water	5	0	0.40	0.20	0.00	0.40	0.30	2.00	110.00	10.00	0.5000

Appendix III: Winter land use parameter table of Afa-Selga watershed.

NUMBER	LUSE_TYPE	RUNOFF_VEG	NUM_VEG_RO	NUM_IMP_RO	VEG_AREA	BARE_AREA	IMP_AREA	OPENW_AREA	ROOT_DEPTH	LAI	MIN_STOM	INTERC_PRE	VEG_HEIGHT
21	Agriculture	crop	1	0	0.00	1.00	0.00	0.00	0.35	0.00	180.00	0.00	0.6000
7	Bare land	bare soil	4	0	0.00	1.00	0.00	0.00	0.05	0.00	110.00	0.00	0.0010
33	woodland	forest	3	0	0.50	0.50	0.00	0.00	2.00	4.50	500.00	38.00	15.0000
31	Forest	forest	3	0	1	0	0	0	2	5.00	250.00	.00	18.0000
23	Grass land	grass	2	0	1.00	0.00	0.00	0.00	0.30	2.00	100.00	10.00	0.2000

1	Settlement	grass	2	1	0.20	0.00	0.80	0.00	0.30	2.00	100.00	10.00	0.1200
36	Shrubs-bush land	grass	2	0	0.20	0.80	0.00	0.00	0.60	0.00	110.00	5.00	2.0000
44	Wetland	open water	5	0	0.40	0.20	0.00	0.40	0.30	2.00	110.00	10.00	0.5000

Appendix IV: Runoff coefficient parameters for vegetated, bare soil and open water raster cells

LAND USE	LAND USE NUM	SLOPE [%]	SLOPE NUM	SOIL TYPE	SOIL NUM	RUNOFF COEF	UNIQUE_ _NUM	BARE ROCOEF	UNIQUE IMP
Crop	1	<0.5	1	clay loam	9	0.4800	911		0.00
Crop	1	0.5-5	2	clay loam	9	0.5300	912		0.00
Crop	1	5-10	3	clay loam	9	0.5800	913		0.00
Crop	1	>10	4	clay loam	9	0.6300	914		0.00
Grass	2	<0.5	1	clay loam	9	0.2800	921		0.00
Grass	2	0.5-5	2	clay loam	9	0.3300	922		0.00
Grass	2	5-10	3	clay loam	9	0.3800	923		0.00
Grass	2	>10	4	clay loam	9	0.4300	924		0.00
Forest	3	<0.5	1	clay loam	9	0.1800	931		0.00
Forest	3	0.5-5	2	clay loam	9	0.2300	934		0.00
Forest	3	5-10	3	clay loam	9	0.2800	933		0.00

Forest	3	>10	4	clay loam	9	0.3300	934		0.00
bare soil	4	<0.5	1	clay loam	9	0.5800	941		0.00
bare soil	4	0.5-5	2	clay loam	9	0.6300	942		0.00
bare soil	4	5-10	3	clay loam	9	0.6800	943		0.00
bare soil	4	>10	4	clay loam	9	0.7300	944		0.00
open water	5	<0.5	1	clay loam	9	1.0000	951		0.00
open water	5	0.5-5	2	clay loam	9	1.0000	952		0.00
open water	5	5-10	3	clay loam	9	1.0000	953		0.00
open water	5	>10	4	clay loam	9	1.0000	954		0.00
Crop	1	<0.5	1	clay	12	0.5500	1211		0.00
Crop	1	0.5-5	2	clay	12	0.6000	1212		0.00
Crop	1	5-10	3	clay	12	0.6500	1213		0.00
Crop	1	>10	4	clay	12	0.7000	1214		0.00
Grass	2	<0.5	1	clay	12	0.3500	1221		0.00
Grass	2	0.5-5	2	clay	12	0.4000	1222		0.00
Grass	2	5-10	3	clay	12	0.4500	1223		0.00

Grass	2	>10	4	clay	12	0.5000	1224		0.00
Forest	3	<0.5	1	clay	12	0.2500	1231		0.00
Forest	3	0.5-5	2	clay	12	0.3000	1232		0.00
Forest	3	5-10	3	clay	12	0.3500	1233		0.00
Forest	3	>10	4	clay	12	0.4000	1234		0.00
bare soil	4	<0.5	1	clay	12	0.6500	1241		0.00
bare soil	4	0.5-5	2	clay	12	0.7000	1242		0.00
bare soil	4	5-10	3	clay	12	0.7500	1243		0.00
bare soil	4	>10	4	clay	12	0.8000	1244		0.00
open water	5	<0.5	1	clay	12	1.0000	1251		0.00
open water	5	0.5-5	2	clay	12	1.0000	1252		0.00
open water	5	5-10	3	clay	12	1.0000	1253		0.00
open water	5	>10	4	clay	12	1.0000	1254		0.00

Appendix V: Mean monthly annual rainfall for the last 17years of the Assosa station (2004 −2020)

YEAR	Jan	Feb	Mar	Apr	May	Jun	Jul	Aug	Sep	Oct	Nov	Dec
2004	1.2	2.0	0.0	30.0	143.3	102.0	325.2	347.9	262.8	145.4	0.0	0.0
2005	0.0	0.0	0.0	41.7	61.3	245.2	212.5	190.7	197.5	156.9	0.0	0.0
2006	0.0	0.0	0.0	0.0	263.2	320.9	294.1	185.6	187.1	178.6	3.5	0.0
2007	8.2	0.0	4.3	72.6	162.1	317.8	180.6	225.3	244.0	41.6	38.5	0.0
2008	8.5	0.0	2.2	132.2	297.7	250.1	237.7	216.6	250.6	170.9	3.0	0.0
2009	0.0	0.0	6.3	108.3	50.4	350.8	173.7	227.5	172.0	80.5	0.1	0.1
2010	0.0	2.1	0.0	0.0	125.1	251.5	192.7	217.2	220.9	223.5	16.4	23.8
2011	0.0	0.0	3.4	60.5	142.7	122.3	226.6	336.5	189.7	145.7	0.0	2.4
2012	0.0	0.0	0.0	60.5	172.6	202.4	283.5	187.5	181.2	143.6	4.3	0.0
2013	0.0	0.0	0.0	60.5	160.0	100.1	121.7	199.9	231.5	141.6	0.0	0.0
2014	0.0	20.5	33.0	126.7	264.0	223.9	219.7	311.9	197.7	54.6	0.0	0.0
2015	0.0	0.0	4.2	0.0	156.5	223.9	226.6	216.6	209.7	145.7	8.0	2.4
2016	0.0	0.0	0.0	51.2	178.1	207.6	275.6	166.8	214.4	145.7	8.0	2.4
2017	1.3	1.8	4.2	163.1	156.5	223.9	226.6	216.6	209.7	145.7	8.0	2.4

2018	1.3	1.8	4.2	60.5	156.5	223.9	226.6	216.6	209.7	145.7	8.0	2.4
2019	0.0	1.8	0.0	60.5	58.5	354.3	188.3	74.4	176.6	144.5	30.1	2.4
2020	1.3	0.0	9.1	0.0	112.3	85.8	239.9	144.9	209.7	266.4	8.0	2.4
Average	0.8	1.7	9.2	29.7	145.4	189.0	201.0	246.4	194.0	153.3	18.5	12.4

Appendix VI: Mean monthly annual rainfall for the last 17years of the Amba 16 station (2004 −2020).

YEAR	Jan	Feb	Mar	Apr	May	Jun	Jul	Aug	Sep	Oct	Nov	Dec
2004	1.2	2.0	0.0	30.0	143.3	102.0	325.2	347.9	262.8	145.4	0.0	0.0
2005	0.0	0.0	0.0	41.7	61.3	245.2	212.5	190.7	197.5	156.9	0.0	0.0
2006	0.0	0.0	0.0	0.0	263.2	320.9	294.1	185.6	187.1	178.6	3.5	0.0
2007	8.2	0.0	4.3	72.6	162.1	317.8	180.6	225.3	244.0	41.6	38.5	0.0
2008	8.5	0.0	2.2	132.2	297.7	250.1	237.7	216.6	250.6	170.9	3.0	0.0
2009	0.0	0.0	6.3	108.3	50.4	350.8	173.7	227.5	172.0	80.5	0.1	0.1
2010	0.0	2.1	0.0	0.0	125.1	251.5	192.7	217.2	220.9	223.5	16.4	23.8
2011	0.0	0.0	3.4	60.5	142.7	122.3	226.6	336.5	189.7	145.7	0.0	2.4
2012	0.0	0.0	0.0	60.5	172.6	202.4	283.5	187.5	181.2	143.6	4.3	0.0

2013	0.0	0.0	0.0	60.5	160.0	100.1	121.7	199.9	231.5	141.6	0.0	0.0
2014	0.0	20.5	33.0	126.7	264.0	223.9	219.7	311.9	197.7	54.6	0.0	0.0
2015	0.0	0.0	4.2	0.0	156.5	223.9	226.6	216.6	209.7	145.7	8.0	2.4
2016	0.0	0.0	0.0	51.2	178.1	207.6	275.6	166.8	214.4	145.7	8.0	2.4
2017	1.3	1.8	4.2	163.1	156.5	223.9	226.6	216.6	209.7	145.7	8.0	2.4
2018	1.3	1.8	4.2	60.5	156.5	223.9	226.6	216.6	209.7	145.7	8.0	2.4
2019	0.0	1.8	0.0	60.5	58.5	354.3	188.3	74.4	176.6	144.5	30.1	2.4
2020	1.3	0.0	9.1	0.0	112.3	85.8	239.9	144.9	209.7	266.4	8.0	2.4
Average	1.3	1.8	4.2	60.5	156.5	223.9	226.6	216.6	209.7	145.7	8.0	2.4

Appendix VII: Mean monthly annual rainfall for the last 17years of the Bambase station (2004 −2020).

YEAR	Jan	Feb	Mar	Apr	May	Jun	Jul	Aug	Sep	Oct	Nov	Dec
2004	0.9	0.2	15.7	48.7	183.6	210.1	234.4	283.4	199.5	154.5	28.3	5.3
2005	0.9	0.2	15.7	61.7	121.8	165.2	224.2	273.1	107.3	154.5	26.4	5.3
2006	0.9	0.2	15.7	48.7	183.6	166.4	193.2	200.6	157.0	157.6	0.5	5.3
2007	0.5	0.0	22.6	81.0	145.8	180.3	162.9	255.7	157.3	134.3	68.4	0.0

2008	9.9	0.0	3.5	96.5	220.2	225.1	230.1	275.7	172.2	90.8	9.0	5.3
2009	0.0	0.0	3.4	56.2	183.6	309.9	264.2	265.2	122.3	90.9	0.0	11.1
2010	0.0	0.0	0.0	7.5	147.6	245.3	256.5	243.2	222.3	188.5	68.1	4.3
2011	0.0	0.0	16.2	17.4	211.5	122.5	202.3	241.3	243.7	154.5	28.3	5.3
2012	0.0	0.2	0.0	36.6	183.6	210.1	211.8	335.0	251.7	120.3	36.7	5.3
2013	0.0	0.0	7.4	0.0	209.9	237.8	218.1	240.9	317.4	186.6	28.3	0.0
2014	0.0	2.3	27.2	150.9	212.9	165.7	263.6	156.4	184.0	241.8	12.3	0.0
2015	0.0	0.0	75.8	2.3	239.6	130.8	234.4	194.1	131.3	147.1	1.3	16.1
2016	0.0	0.0	12.6	32.8	210.0	249.7	210.9	243.3	277.2	80.0	52.7	5.3
2017	0.9	0.2	15.7	48.7	183.6	290.4	258.7	243.3	199.5	154.5	28.3	5.3
2018	0.9	0.2	15.7	48.7	183.6	210.1	234.4	243.3	199.5	154.5	28.3	5.3
2019	0.0	0.0	0.0	41.7	116.9	337.4	301.9	198.2	203.5	262.4	36.1	5.3
2020	0.0	0.2	20.0	48.7	183.6	114.8	283.6	243.3	246.3	154.0	28.3	5.3
Average	0.9	0.2	15.7	48.7	183.6	210.1	234.4	243.3	199.5	154.5	28.3	5.3

Appendix VIII: Mean monthly rainfall of stations in and around Afa-Selga watershed

Stations	Jan	Feb	Mar	Apr	May	Jun	Jul	Aug	Sep	Nov	Oct	Dec	Annual
Abadi	0.2	1.9	2.4	19.8	75.7	136.0	180.7	187.2	171.8	121.2	11.4	0.0	908.3
Sherkole	1.5	0.4	11.7	60.5	130.4	176.1	291.5	394.8	234.3	127.5	8.9	0.2	1437.8
Assosa	0.8	1.7	9.2	29.7	145.4	189.0	201.0	246.4	194.0	153.3	18.5	12.4	1201.4
Amba16	1.3	1.8	4.2	60.5	156.5	223.9	226.6	216.6	209.7	145.7	8.0	2.4	1257.2
Bambase	0.9	0.2	15.7	48.7	183.6	210.1	234.4	243.3	199.5	154.5	28.3	5.3	1324.5

Appendix IX: Mean annual and seasonal rainfall of stations in and around Afa-Selga watershed

Name	Easting	Northing	Annual Rainfall	Summer Rainfall	Winter Rainfall
Amba 16	682286.2	1100096	1257.04	876.78	380.26
Assosa	669411.8	1110848	1201.34	830.42	370.92
Bambasi	689648.3	1078379	1324.59	887.35	437.24
Sherkole	674282.5	1148263	1437.73	1096.73	341.00

Appendix X: mean annual and seasonal temperature in and around Afa-Selga watershed

Name	Easting	Northing	Annual Temperature	Summer Temperature	Winter Temperature
Abadi	669889.5	1163235	24.2	22.9	25.2
Assosa	669411.8	1110848	21.7	20.8	22.3
Bambase	689648.3	1078379	22.4	21.34	23.2
Sherkole	674282.5	1148263	22.4	21.5	23.1

Appendix XI: Mean annual and seasonal PET of stations in and around the Afa-Selga watershed

Name	Easting	Northing	Annual PET	Winter PET	Summer PET
Abadi	669889.5	1163235	1105.648	793.4	312.3
Assosa	669411.8	1110848	1029.7	770	259.7
Bambase	689648.3	1078379	1176.7	827.2	349.5
Sherkole	674282.5	1148263	1165.4	832.8	332.6

Appendix XII: Mean annual and seasonal wind speed of stations in and around the Afa-Selga watershed

NAME	Easting	Northing	Annual Wind Speed	Summer Wind Speed	Winter Wind Speed
Assosa	669411.8	1110848	1.85	1.674	1.975714
abadi	669889.5	1163235	2.25619	2.070405	2.39432
amba16	682286.2	1100096	1.85	1.674	1.975714
bambasi	689648.3	1078379	1.64	1.639	1.643929

Appendix XIII: depth to ground water table of Afa-Selga Watershed

No	Name	E	N	Elevation	Depth to groundwater Level (m)	Head
1	Amba 1	678870	1121970	1427	22	1405
2	Amba 12	673025	1109917	1515	5	1510
3	Amba 5	674286	1116288	1564	22	1542
4	Hospital(No.6)	669179.8	1113640	1540.5	23	1517.5
5	ASU Well 1	673069	1120704	1528	21	1507
6	Selga 1	670178	1114182	1555	21.5	1533.5
7	Selga 2	670561	1114186	1526	18	1508
8	Amba 11	678470	1121850	1337	23	1314
9	Abramo	668597.1	1103918	1448	16	1432
10	Amba 17	676221	1109499	1486	5	1481
11	Amba 3	667630	1118160	1502	18	1484
12	amba 12 spring	673734.3	1111228	1503	0.9	1502.1
13	amba 4 spring	672771.2	1112041	1514	1.6	1512.4
14	Oda 1	702380.4	1108275	1013	24	989
15	Oda2	701639.6	1107666	1127	23.5	1103.5

Appendix XIV: AAU 1 Well as built profile

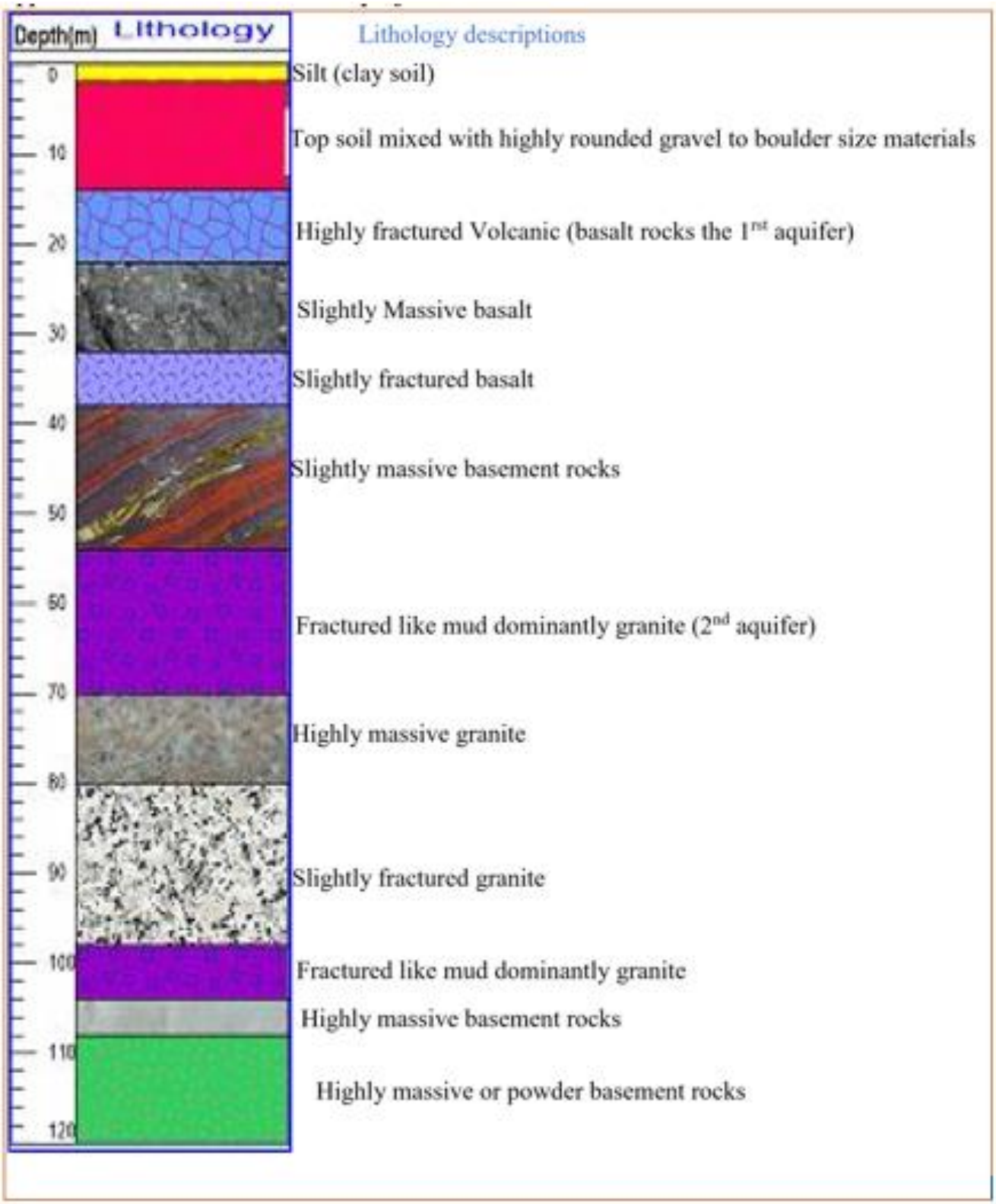

Appendix XV: Selga Well 1 as built profile

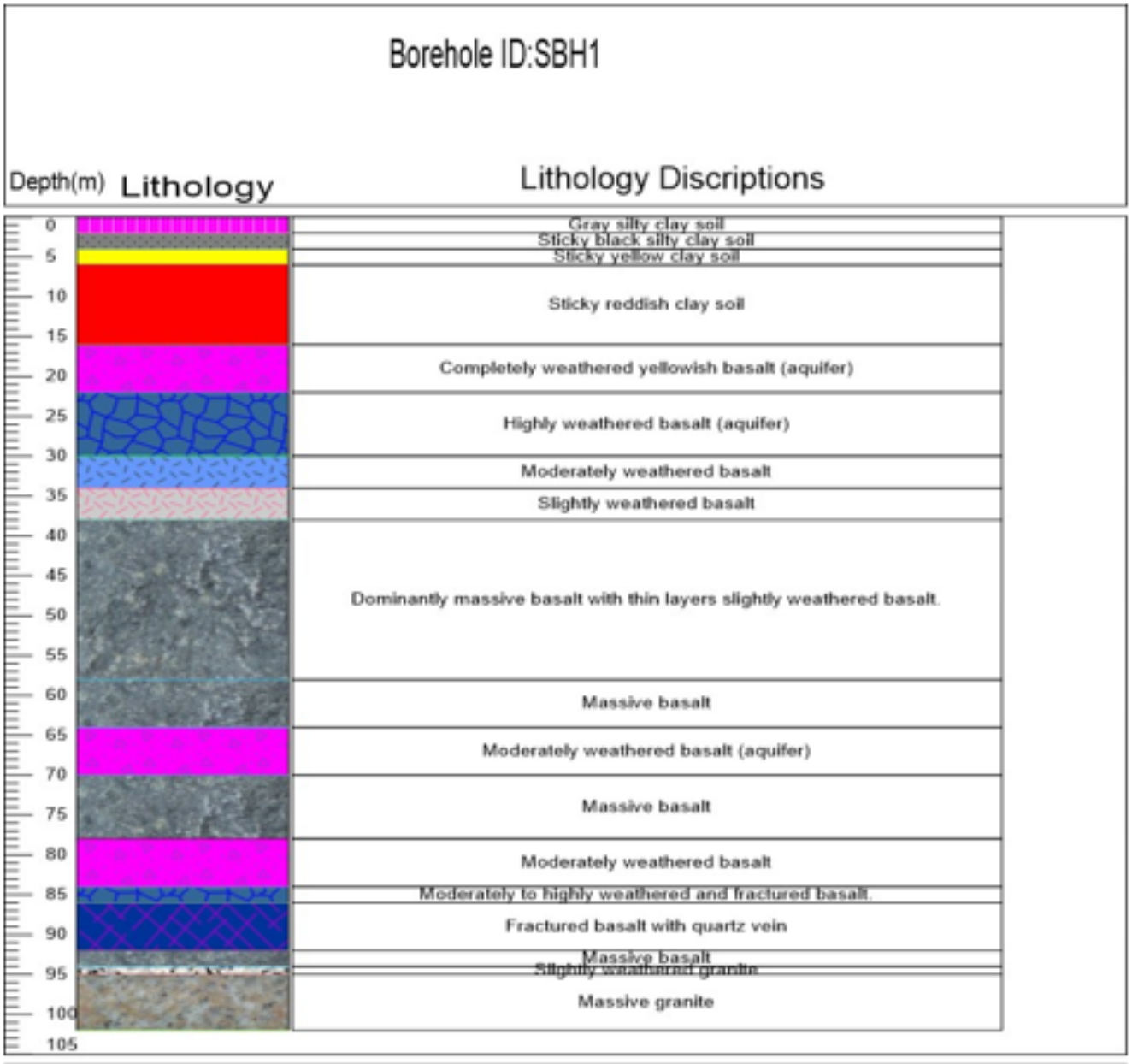

Appendix XVI: Selga Well 2 as built profile

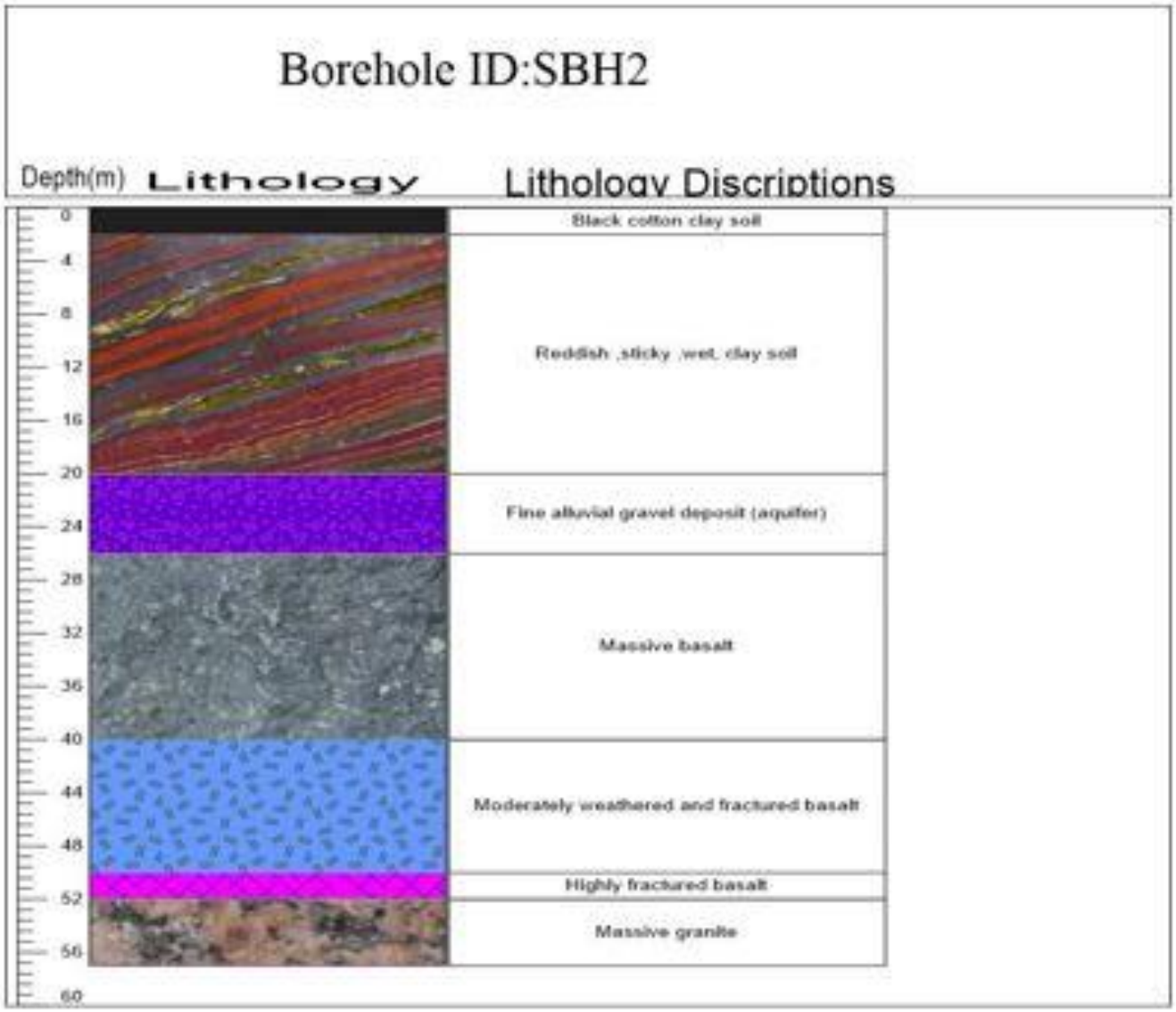

Appendix XVII: some rock type found in Afa-Selga watershed

Appendix XVIII: some rivers found in Afa-Selga watershed

Appendix XIX: (a) depth to groundwater measurement using deep meter (b) some springs found in the watershed